Electrophysiological properties of striatal neurons in the dopamine-intact and Parkinsonian brain

Federica Vinciati

St. Peter's College

Thesis submitted for the degree of Doctor of Philosophy at the University of Oxford

Hilary Term 2015

Abstract

Electrophysiological properties of striatal neurons in the dopamine-intact and Parkinsonian brain

Federica Vinciati, St. Peter's College
Thesis submitted for the degree of Doctor of Philosophy, Hilary Term 2015

The striatum is the major input structure of the basal ganglia, and is composed of two major populations of spiny projection neurons (MSNs), which give rise to the so-called direct and indirect pathways, and several types of interneuron. Dopaminergic inputs to striatum are critical for its proper function. Indeed, loss of dopaminergic neurons in Parkinsonism leads to motor disturbances, grossly disturbs striatal activity, and is associated with the emergence of excessively-synchronized network oscillations at beta frequencies (15-30 Hz) throughout the basal ganglia. How the distinct structural, neurochemical and other properties of striatal neurons are reflected in their firing rates and patterns *in vivo* is poorly defined, as are their possible cell-type-selective contributions to the aberrant oscillations arising in the Parkinsonian brain.

To address these issues, I first used multi-electrode arrays to record the spontaneous firing of ensembles of neurons in dorsal striatum in both anaesthetised dopamine-intact and Parkinsonian (6-hydroxydopamine-lesioned) rats during two well-defined brain states, slow-wave activity (SWA) and spontaneous activation. The chronic loss of dopamine led to an overall increase in the average firing rates of striatal neurons, irrespective of brain state. However, many neurons in the Parkinsonian striatum still exhibited the low firing rates and irregular firing patterns typical of neurons in the dopamine-intact striatum. During SWA in Parkinsonian rats, the firing of striatal neurons was more strongly synchronized at low frequencies, in time with cortical slow (~1 Hz) oscillations. During spontaneous cortical activation in Parkinsonian rats, more striatal neurons engaged in synchronized firing in time with cortical beta oscillations.

Under the same experimental conditions, I then recorded the spontaneous firing of individual striatal neurons and juxtacellularly labelled the same neurons to verify their cell types, and locations; indirect pathway and direct pathway MSNs were distinguished by the expression (and lack of expression respectively), of the neuropeptide precursor preproenkephalin (PPE). After chronic dopamine loss, and on average, only indirect pathway (PPE+) MSNs significantly increased their firing rates during both brain states, and engaged in widespread, synchronized firing in the beta-frequency range. This did not hold true for *all* PPE+ MSNs; the

Parkinsonian striatum contained many MSNs that were virtually quiescent, which were just as likely to belong to the indirect pathway as the direct pathway. Direct pathway (PPE-) MSNs increased their firing only during SWA after chronic dopamine loss and rarely engaged in aberrant beta oscillations.

Taken together, these data suggest that (1) the firing patterns, as well as the firing rates of many striatal neurons are grossly disturbed by chronic loss of dopamine and (2) that the pathological synchronization of the rhythmic firing of a subpopulation of indirect pathway MSNs could contribute to the propagation of aberrant beta-frequency oscillations to downstream basal ganglia nuclei in Parkinsonism.

Acknowledgements

I would like to express my immense gratitude to Professor Peter Magill for teaching me *in vivo* electrophysiology with constant support, patience and advice throughout my studentship. It has been a wonderful experience and I cannot thank him enough.
I would like to thank my co-supervisor Professor Paul Bolam for his support, Dr. Andrew Sharott for his help and training, and Professor Peter Somogyi for the excellent facilities and resources.
Thanks to all the members of the lab for sharing thoughts and laughs.
Thanks to all the great friends I made during my time in Oxford.

To M.

For being there.

Contents

List of figures

List of tables

List of abbreviation

6-OHDA, 6-hydroxydopamine

A, anterior

A2AR, adenosine A2a receptor

ACT, cortical activation

BAC, bacterial artificial chromosome

BG, basal ganglia

cAMP, adenylate cyclase

CC, corpus callosum

ChAT, choline acetyltransferase

CHH, cross-correlation histogram

Chmr4, M4 muscarinic acetylcholine receptor

Chr2, channelrhodopsin 2

CPP, conditioned place preference

CR, calretinin

D, dorsal

D1R, dopamine D1 receptor

D2R, dopamine D2 receptor

DAT, dopamine transporter

DBS, deep brain stimulation

DiI, dye, 1, 1-dioctadecyl-3, 3, 3, 3-tetramethylindocarbocyanine perchlorate

ECoG, electrocorticogram

EEG, electroencephalogram

Enk, enkephalin

EPN, entopeduncular nucleus

FFT, Fourier transform

FS, fast-spiking

GFP, green fluorescent protein

GP, globus pallidus

GPe, external segment of the globus pallidus

GPi, internal segment of the globus pallidus

HBN, lateral habenular nucleus

Hz, Hertz

IAs, slowly-inactivating voltage-dependent potassium current

IKir, inwardly rectifying potassium selective current

ISI, interspike interval

LFPs, local field potentials

LTS, low-threshold calcium spike

MFB, medial forebrain bundle

MOR, μ-opioid receptor

MSN, medium-sized densely-spiny projection neuron

MTg, mesopontine tegmentum

MUA, multi-unit activity

NOS, nitric oxide synthase

NPY, neuropeptide Y

PBS, phosphate buffered saline

PD, Parkinson's disease

PLTS, persistent and low-threshold spike

PPE, preproenkephalin

PPN, pedunulopontine nucleus

PPTA, preprotakykinin A

PV, parvalbumin

RF, reticular formation

SC, superior colliculus

SEM, standard error of mean

LTS, low-threshold spiking

SN, substantia nigra

SNc, substantia nigra pars compacta

SNr, substantia nigra pars reticulata

SP, substance P

SS, somatostatin

STN, subthalamic nucleus

SWA, slow-wave activity

TAN, tonically active neurons

TH, tyrosine hydroxylase

VS, ventral striatum

VTA, ventral tegmental area

CHAPTER 1

Introduction

1.1 Basal ganglia general overview

The basal ganglia (BG) are a collection of five highly interconnected subcortical nuclei that have been implicated in several key roles, including: reward-based learning, exploratory behaviour, goal-oriented behaviour, working memory and timing (Chakravarthy *et al.*, 2010). Neural circuits of the BG are also critical for voluntary movement, including motor planning and action selection (Chakravarthy *et al.*, 2010). The functional significance of the basal ganglia for behaviour is also illustrated in neurological disorders associated with dysfunction in these circuits, such as the motor deficits that arise in Parkinson's disease.

The anatomical arrangement of BG nuclei is generally considered to have a dorsal/ventral division. The dorsal division consists of the striatum (or caudate – putamen), the globus pallidus (GP) and its equivalent in primates, the external segment of the globus pallidus (GPe), the entopeduncular nucleus (EPN) and it

homologue in primates, the internal segment of the globus pallidus (GPi), the subthalamic nucleus (STN) and the substantia nigra (SN). The latter structure is divided into two main parts, the dorsal *pars compacta* (SNc) enriched of dopaminergic neurons, and the more ventral *pars reticulata* (SNr) (Bolam *et al.*, 2000). These structures have a role in processing motor-sensory and associative information. The ventral division of the BG (ventral striatum or nucleus accumbens; ventral pallidum and ventral tegmental area) is more associated with limbic functions (Morgane *et al.*, 2005). The architecture of the BG is strongly suggestive that these structures function as part of a recurrent circuit, where the striatum is the first integration structure of cortical inputs and the branch point where processed information are further conveyed (Figure 1.1). Topographically organized information from the cerebral cortex, various nuclei of the thalamus, and dopaminergic input from SNc, are integrated within the striatum which, in turn, conveys information to the output nuclei of the BG, the GPi and SNr. Information is then sent back, via thalamus, to the cortex, but also to brainstem structures including the superior colliculus, and the reticular formation (Bolam *et al.*, 2000).

1.2 Striatal cellular components and functional organization

The striatum is the main input structure of the BG. It is mainly (~95%) composed of GABAergic medium-sized densely-spiny projection neurons (MSNs). There are also at least four main types of aspiny interneuron, including cholinergic interneurons and GABAergic interneurons that express parvalbumin (PV), nitric oxide synthase (NOS) or calretinin (CR), that play key roles in shaping MSN activity and thus, striatal

output (Kawaguchi, 1993; Kubota *et al.*, 1993; Tepper & Bolam, 2004). MSNs can be broadly segregated in two sub-classes according to their projection sites, neurochemical properties and receptor expression, as shown in Figure 1.1 (Graybiel, 2000). The so called *direct pathway* MSNs, monosynaptically innervate the basal ganglia output nuclei (SNr and GPi) and also send minor collaterals to GPe. They are enriched in the neuropeptide substance P and dynorphin and they express type 1 dopamine receptor (D1R) and M4 muscarinic acetylcholine receptor (Chmr4)(Gerfen & Surmeier, 2011). In contrast, a second MSN population called *indirect pathway* MSNs, exclusively innervates the GPe and express the neuropeptide enkephalin as well as type 2 dopamine receptors (D2Rs) and adenosine A2A receptors (Gerfen & Surmeier, 2011). Direct and indirect pathway MSNs provide the sole striatal output to other basal ganglia nuclei.

This dichotomous organization of striatal MSNs and their outputs is a core component of the highly influential “direct/indirect pathways model” that provides a useful conceptual framework for interpreting the functional organization of the basal ganglia. In the 90s, Albin et al (1989) and DeLong (1990) proposed a model of the basal ganglia in which direct and indirect pathway MSNs act as a synergistic duo with opposing but balanced effects in the control of motor behaviour. In this model, the key assumption is that both MSNs neurons are differentially modulated by dopaminergic neurons of SNc. The activation of D1Rs on direct pathway MSNs increases their output, thus inhibiting GABAergic basal ganglia output neurons and, thence, disinhibiting basal ganglia targets in thalamus, midbrain and brainstem. In contrast, activation of D2Rs on indirect pathway MSNs decreases their output, ultimately counteracting to increase inhibition of basal ganglia targets (Albin *et al.*, 1989; DeLong, 1990). Thus, based on this anatomy and neurochemistry, the

activation of the direct pathway facilitates movements, whereas the activation of indirect pathway inhibits motor output.

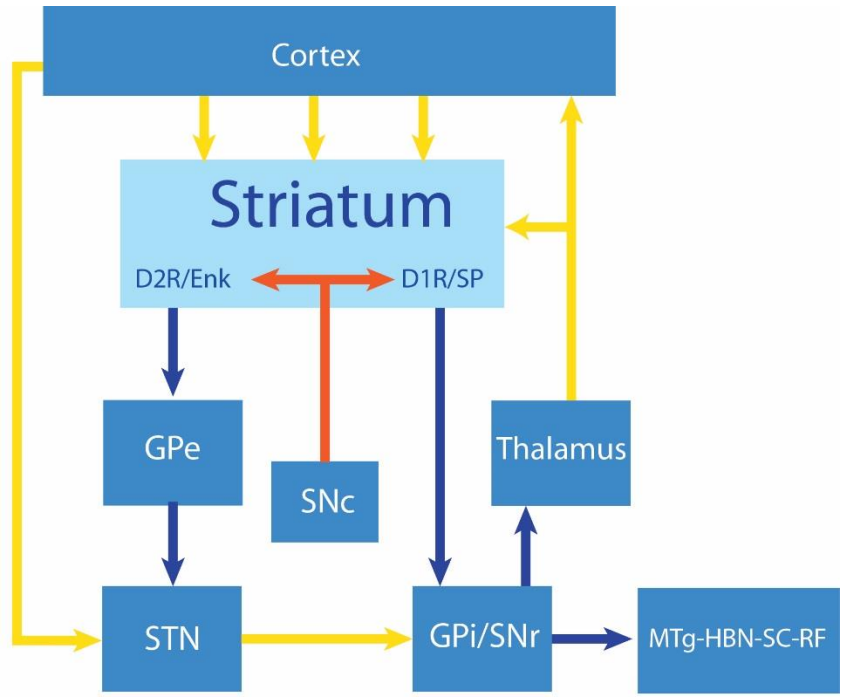

Figure 1.1 **Simplified representation of the main cellular constituents of the striatum with respect to key connections and other basal ganglia nuclei.** The striatum is the main input structure of the basal ganglia, receiving massive glutamatergic inputs from cortex and thalamus. Information reaching striatum is processed by at least two main types of medium-sized densely-spiny projection neuron (MSNs), which are distinguished by their expression of either substance P (SP) or enkephalin (ENK) or different dopaminergic receptors. SP-expressing MSNs constitute the “direct pathway” and preferentially innervate basal ganglia output nuclei (substantia nigra pars reticulata [SNr] and internal globus pallidus [GPi]) and express type 1 dopamine receptors (D1R), whereas ENK-expressing MSNs constitute the “indirect pathway” and only innervate the external globus pallidus (GPe) and express type 2 dopamine receptors (D2R). This connectivity is only partially upheld when taking into account the patch/striosome and matrix compartments of striatum (not shown). The basal ganglia govern behaviour through their GABAergic outputs to the thalamus or to various brain stem structures. The GPi projects to the peduncolopontine nucleus of the mesopontine tegmentum (MTg) and the lateral habenular nucleus (HBN), whereas the SNpr innervates the MTg, the superior colliculus (SC) and the reticular formation (RF). Note that, for simplicity, this scheme omits many important connections,

including inputs to all basal ganglia nuclei from dopaminergic neurons of the substantia nigra pars compacta (SNc), and several connections of the subthalamic nucleus (STN) and GPe. Adapted from DeLong, 1990.

1.2.1 Functional roles of striatum

Direct and indirect pathway MSNs preferentially express different dopamine receptors and are therefore likely to be differentially modulated by dopamine release in striatum. Because of this dual effect of dopaminergic inputs, early investigations found it difficult to determine the relation between movement and striatum. For instance, bilateral lesion of striatum in cats and dogs has been proven to drastically impair motor movement causing animals to run forwards without regard to obstacle or walls in their paths (Mettler & Mettler, 1940). The same authors, two years later, together with other independent groups reported instead a reduction of movement following striatal lesion across multiple species (Mettler & Mettler, 1942; Kennard, 1944; Gybels *et al.,* 1967). Later, the technique of electrical microstimulation of striatum helped to better define the critical involvement of this area in motor behaviour. The most widely cited effect is the contralateral head turning or circling (Kitsikis & Rougel, 1968; Arushanyan & Dutov 1977; Cools, 1973) and contraversive limb rotation (Cools, 1973; Chandler & Crosby, 1975; Alexander & DeLong, 1985a). However these techniques did not unambiguously clarify the role of the striatum because numerous other investigators, also observed suppression, arrest and freezing of movement during striatal stimulation (Kwak *et al.*, 1979; Murer & Pazo, 1993; Klemm, 2001). Furthermore, electrophysiological recordings have shown that individual neurons of the striatum increase their firing during different phases of movement, with some neurons responding during movement initiation, others during

waiting period and others near the termination of movement (Aldridge *et al.*, 1980; Rolls *et al.*, 1983; Crutcher & DeLong, 1984; Hikosaka *et al.*, 1989; Gardiner & Nelson, 1992; Kimura *et al.*, 1992; Romo *et al.*, 1992; Lebedev & Nelson, 1999; Lee & Assad, 2003; Kimchi & Laubach, 2009). Hence, the above studies could not distinguish between different types of striatal neurons. However, with the advent of sophisticated molecular tools for selective manipulation of one of more types of MSNs, new evidence became available and helped to clarify the functional distinction of MSNs. Durieux and colleagues (2009) for instance assessed the role of indirect pathway MSNs by unilateral or bilateral ablation of striatum in adult transgenic mice (*Adora2a*Cre-mouse crossed with an inducible Cre-dependent diphtheria toxin receptor mouse line). They show that, following bilateral injection of diphtheria toxin, transgenic mice were much more active than controls, thereby demonstrating the inhibitory or suppressive role of indirect pathway MSNs on motor activity (Durieux *et al.*, 2009). Kravitz and colleagues (2010) confirmed and extended this result using optogenetic control of direct and indirect pathway MSNs. In this approach, adenovirus-associated viruses containing 'floxed' channelrhodopsin 2 (ChR2) were injected in the motor striatum of BAC transgenic mice expressing Cre recombinase in either direct or indirect MSNs (Drd1–Cre and Drd2–Cre respectively). During bilateral excitation of the indirect pathway MSNs, bradykinesia and decreased locomotion initiation were observed. In contrast, activation of the direct pathway reduced freezing and increased locomotion (Kravitz *et al.*, 2010). The above findings give good evidence that the direct pathway promotes and stimulates movement, whereas the indirect pathway suppresses motor behaviours. However, although the majority of studies have implicated striatum in movement control, there is further evidence that the striatum is involved

in hedonic reward. Ferguson and colleagues (2011) were able to selectively silence either direct or indirect pathway MSNs by membrane hyperpolarization induced by a specific ligand (CNO). In this “chemogenetic” approach, administration of CNO in modified ‘direct pathway rats’ or ‘indirect pathway rats’, resulted in an increase and decrease of amphetamine-induced sensitization, respectively (Ferguson *et al.*, 2011). Similarly, other groups with different approaches reached the same conclusion: by using optogenetic control to activate either pathway, rats show a decrease of the rewarding effect of cocaine when the indirect pathway was activated; the opposite effect was observed when the direct pathway was stimulated (Lobo *et al.*, 2010). Again, the blockade of the direct pathway by specific expression of transmission-blocking tetanus toxin in a doxycycline-dependent manner, resulted in a decrease in cocaine-induced conditioned place preference (CPP) whereas, in contrast to the studies reported above, no difference in CPP was found when transmission along the indirect pathway was blocked (Hikida *et al.*, 2010). In conclusion, these studies collectively suggest that direct pathway MSNs may mediate movement, reinforcement and rewards, whereas indirect pathway MSNs inhibit movement and mediate punishment and aversion (Kravitz & Kreitzer, 2012).

1.2.2 Dorso-ventral division of striatum and ‘patch’ and ‘matrix’ compartments

The striatum is subdivided into sectors along a ventromedial-dorsolateral continuum, largely on the basis of connectivity with extrinsic structures. The dorsal striatum is primarily involved in sensori-motor function, with the dorsomedial

striatum receiving glutamatergic inputs primarily from association cortices (Goldman & Nauta, 1977; Ragsdale & Graybiel, 1981; McGeorge & Faull, 1989), and with the dorsolateral striatum from sensory-motor areas of cortex (Kunzle, 1975; Liles & Updyke, 1985; McGeorge & Faull, 1989). The dorsal striatum is also the major target area of dopaminergic afferents from SNc that modulate MSN function (Bolam *et al.*, 2000). Thalamic projections to the dorsal striatum, including those from ventrolateral and ventroanterior nuclei, target the dorsal striatum in a topographical orientation (Gimenez-Amaya *et al.*, 1995). The dorsal striatum transmits information back to the cerebral cortex other BG nuclei and thalamus (Bolam *et al.*, 2000). The ventral striatum (VS; or nucleus accumbens) is more closely associated with limbic functions (Morgane *et al.*, 2005) and receives glutamatergic input primarily from frontal cortex and limbic regions (Brog *et al.*, 1993) as well as dopaminergic input from the ventral tegmental area (VTA), a separate midbrain nucleus medial to the SNc (Fields *et al.*, 2007). The VS also receives dense projections from midline and medial intralaminar thalamic nuclei, which are topographically organized (Gimenez-Amaya *et al.*, 1995). Efferent projections from the VS project primarily to the substantia innominata and SNr/ VTA (Haber *et al.*, 1990).

The striatum is also further divided into regions of 'patch'/'striosomes' and 'matrix', on the basis of differential connectivity and distribution of neurochemical markers as shown in Figure 1.2 (Crittenden & Graybiel, 2011). Patches compartments are embedded in the surrounding 'matrix' region. Striosomes represent ~10% of striatal volume and are easily distinguished by dense μ-opioid receptor (MOR) binding-expression (Herkenham & Pert, 1981), substance P expression (Bolam & Izzo, 1988) and relatively weak expression of cholinergic markers (Graybiel & Ragsdale, 1978). In contrast, the matrix is characterized by

relatively high expression of acetylcholinesterase and choline acetyltransferase (ChAT) (Graybiel *et al.*, 1986), somatostatin (Gerfen, 1984) and calbindin (Gerfen, 1985). These compartments are distinguished by their differential expression of more than 60 genes (Crittenden & Graybiel, 2011) and by their input-output organization. Striatal neurons located in patches receive input primarily from limbic, prefrontal and temporal cortical regions as well as from orbitofrontal and insular areas (Ragsdale & Graybiel, 1988; Kincaid & Wilson, 1996; Masterman & Cummings, 1997) and from a distinct set of 'ventral tier' SNc neurons (Gerfen, 1985; Gerfen *et al.*, 1987a; Gerfen *et al.*, 1987b). Thalamic inputs from the paraventricular and rhomboid nuclei terminate quite selectively within patches (Gerfen, 1984). Because of these connections, striosome are considered, together with the VS, the limbic areas of striatum. Striatal neurons located in the matrix receive inputs from somatosensory cortex, parietal-temporal occipital association cortex, cingulate gyrus and from most thalamic nuclei (Herkenham & Pert, 1981; Masterman & Cummings, 1997; Fujiyama *et al.*, 2006) and innervate the SNr and GPi (Gerfen, 1992). Both compartments MSNs that project to the GPe, but in same documented case also to separate sub regions (Gerfen, 1984; Jimenez-Castellanos & Graybiel, 1989; Tokuno *et al.*, 2002; Fujiyama *et al.*, 2011). Recently, Fujiyama and colleagues (2011) using a viral vector encoding membrane-targeted green fluorescent protein in rats, found that only direct pathway MSNs in the patch compartment project directly to the SNc in addition to GPe, GPi and SNr, whereas indirect pathway MSN in patches project exclusively to the GPe.

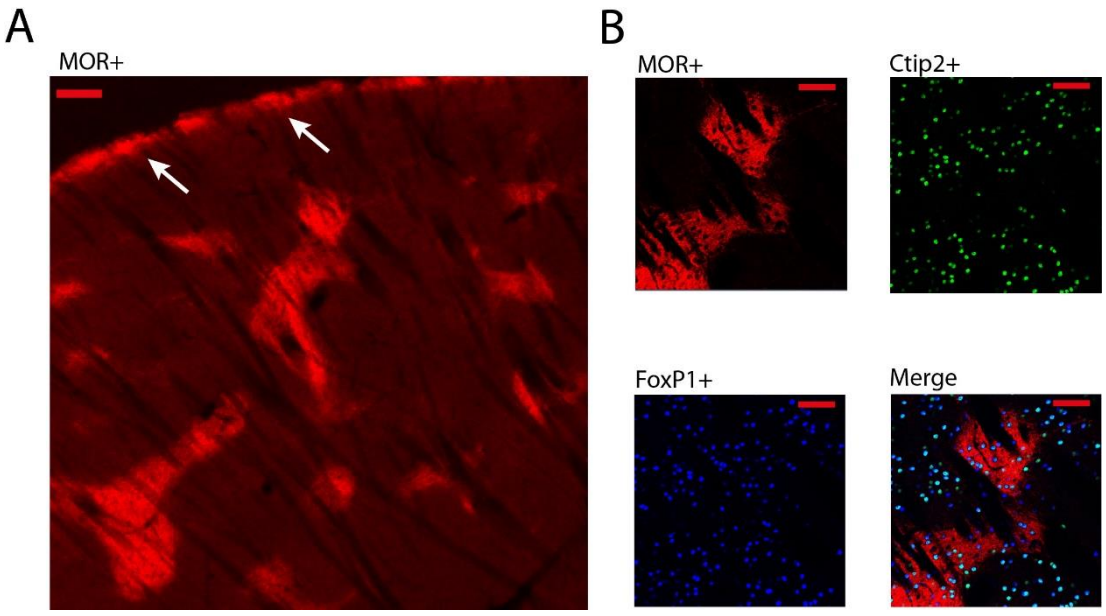

Figure 1.2 **Distribution of MOR in the 'patch/striosome-matrix' system of the rat striatum.** ***A,*** Representative single immunofluorescence image showing MOR distribution within the rat striatum. These and others patch were identified by intense expression of immunoreactivity for mu opioid receptors (MOR). At the edge with the corpus callosum, the subcallosal streak (as indicated by white arrows) is also positive for MOR. Scale bar, 100 µm. ***B,*** Another representation of the distribution of MOR within the striatum also showing the presence of Ctip2 and FoxP1 (selective nuclear markers for striatal projection neurons), and their distribution in the patch/striosome and matrix compartments. Scale bar, 50 µm. (Micrograph of the author of the thesis).

1.2.3 Electrophysiological properties of striatal neurons

Despite the dichotomies in the axonal projections, synaptic connectivity and receptor expression profiles of direct and indirect pathway neurons, MSNs have long been thought as homogeneous in their somatodendritic structure and intrinsic physiological properties. Indeed early anatomical studies have described direct and indirect MSNs as a generic homogeneous population characterized by densely

spiny dendrites (Kawaguchi *et al.*, 1989). Similarly, because MSNs share several electrophysiological properties, they were described almost equivalent, making them indistinguishable (Venance & Glowinski, 2003). Indeed the distinction of MSNs while recording has been technically difficult and time consuming, requiring post hoc tracing of axons (Kawaguchi *et al.*, 1990) or confirmation of identity by single-cell gene profiling (Surmeier *et al.*, 1996). With the advent of bacterial artificial chromosome (BAC) transgenic mice expressing fluorescent protein and other similarly sophisticated approaches, the idea that direct and indirect pathway MSNs have similar somatodentritic structure and physiological properties has been successfully challenged. For instance, it has been shown that direct pathway MSNs have significantly more branch points and tips, and overall more primary dendrites, occupying significantly more striatal volume than indirect pathway MSNs (Gertler *et al.*, 2008). The same authors showed, by computer stimulation, that the more extensive dendritic arbor of direct pathway MSNs underlies their lower intrinsic excitability (as compared to indirect pathway MSNs). Although these results suggest that is the dentritic structure that shapes MSN excitability, other factors, including intrinsic conductances should be taken into consideration for further studies. For instance, the membrane properties of both direct and indirect pathway MSNs are shaped by similar potassium conductances. The powerful inwardly-rectifying potassium selective current (I_{Kir}), accounts for most of the resting conductance of striatal MSNs and for their relatively hyperpolarized resting membrane potential (~-80mV) (Kita *et al.*, 1984; Nisenbaum & Wilson, 1995). When the membrane potential approaches the spike threshold, the activation of a slowly-inactivating voltage-dependent potassium current (I_{As}) influences the firing pattern by delaying the excitation of the membrane. Indeed, when the MSN is depolarized, the activation of

I_{As}, induces a slowing of the rate of depolarization that leads to a long latency of action potential firing (Nisenbaum *et al.*, 1994). The properties of these currents imply that only input of sufficient strength and duration would be able to depolarize striatal membrane induce firing. Also, during depolarization and firing, calcium inflow can activate both small and large conductance calcium-activated potassium channels, limiting MSN output. For these reasons, MSNs seldom fire (Bargas *et al.*, 1999). Recently a few studies were able to discriminate direct and indirect pathway on the basis of differences in current properties. Using whole-cell patch-clamp and single-cell RT-PCR techniques to characterize the inwardly rectifying K^+ currents of nucleus accumbens MSNs, it has been shown that indirect pathway neurons display I_{Kir} currents that inactivate quicker at hyperpolarized potential compared to direct pathway MSNs (Mermelstein *et al.*, 1998). Consistent with this finding, another group examined whether the intrinsic membrane excitability of direct pathway and indirect pathway MSNs differed. Using a BAC transgenic mice to confer cell-type specific expression of green fluorescent protein in direct (targeting M4R) and indirect (targeting D2R) pathway MSNs, Kreitzer and Malenka (2007) show that indirect pathway MSNs fired at nearly twice the rate of direct pathway neurons in response to a given depolarizing current injection. Finally the spontaneous activity of striatal neurons is also characterized by sustained shifts of the membrane potential between ‘Up states’, which describe the membrane potential when it is close to the firing threshold, and ‘Down states’, close to the potassium equilibrium, both *in vivo* and *in vitro* (Wilson & Kawaguchi, 1996; Stern *et al.*, 1997; Stern *et al.*, 1998; Reynolds & Wickens, 2000; Goto & O'Donnell, 2001; Tseng *et al.*, 2001; Sharott *et al.*, 2012). While the Down state is mainly due to an inwardly rectifying potassium conductance, which dominates the membrane conductance of striatal neurons at

rest, the Up state results from complex interactions between cortical excitatory input mainly, and voltage-dependent outward potassium conductances activated at membrane potentials close to the spike threshold (Nisenbaum & Wilson, 1995; Wilson & Kawaguchi, 1996). These transitions between hyperpolarized and depolarized states are necessary for stimulating and shaping action potential firing in MSNs, and so they are in a position to control basal ganglia function by influencing striatal output (Mahon *et al.*, 2006). In summary, MSNs are hyperpolarized at rest due to potassium currents that clamp their membrane at around –80 mV. When they receive excitatory inputs that lack spatial or temporal convergence, the membrane is depolarized but still clamped slightly below the spike threshold. However, when excitatory inputs are of sufficient strength over time, they promote the closure of some potassium channels, bringing the membrane to a depolarized state that lasts for hundreds of milliseconds (Up state), during which MSNs can fire spikes. In awake or freely moving animals at rest, the firing rate of putative MSNs is between 1-3 spike/s (Haracz *et al.*, 1993; Kish *et al.*, 1999); these neurons thus display extended periods of silence *in vivo* (Kiyatkin & Rebec, 1999b; a; Berke *et al.*, 2004). Similar results have been observed in anaesthetized rats where intracellular recordings show that MSNs, during large amplitude slow wave activity, undergo spontaneous fluctuations between hyperpolarized and depolarized states (Mahon *et al.*, 2006). Typically MSNs seldom fire during slow wave activity, but on average, direct pathway MSNs tend to be less active than indirect pathway neurons (Mallet *et al.*, 2005). During ‘cortical activation’, a state dominated by faster low-amplitude oscillations, intracellular activity of MSNs is still triggered and correlated by cortical field potentials, but in contrast to slow wave activity, it is not stereotyped in up and

down transition. Wakefulness tends to be associated with disorganized depolarizing synaptic events of variable amplitude (Mahon *et al.*, 2006).

1.2.4 Neuromodulation of striatal MSNs

The striatum is a convergence-point of several neurochemically-distinct afferents. Excitatory glutamatergic inputs from the cortex and thalamus make synapses with direct and indirect pathways MSNs (Bolam *et al.*, 2000; Doig *et al.*, 2010; Huerta-Ocampo *et al.*, 2014), where the flow of information is then modulated by local GABAergic interneurons, GABAergic GPe neurons and by two main neuromodulators, dopamine and acetylcholine. The striatum receives the richest dopaminergic innervation of all the nuclei in the basal ganglia. Dopamine fibres ascending from the SNc target the dorsal striatum (those from VTA preferentially target ventral striatum) and regulate MSNs output through the activation of type 1 and type 2 dopamine receptors, distributed along their dendrites and axon terminals. By means of several types of dopamine receptors, dopamine influences the excitability of direct and indirect pathway MSNs by altering both voltage-dependent conductances and synaptic transmission (Nicola *et al.*, 2000). Activation of D1Rs promotes the firing of direct pathway MSNs, whereas the activation of D2Rs leads to the opposite physiological effect on indirect pathway MSNs (Surmeier *et al.*, 2007). In addition to D1Rs and D2Rs, several other types of dopaminergic receptors are distributed throughout the striatum, exerting potent and often opposing effects. Briefly, dopamine type 1 and type 5 receptors are Gs-coupled; activation of these receptors produces stimulation of the enzyme adenylate cyclase (cAMP) and thus promoting an overall excitatory effect, whereas activation of type 2, 3 and 4 (Gi-

coupled) receptors results in a decrease in cAMP and so producing inhibitory effects (Kreitzer, 2009). The expression and role of D3Rs, D4Rs and D5Rs receptors in MSNs is still under investigation as well as the ~1% MSNs that co-express D1Rs and D2 receptors (Ince *et al.*, 1997). Dopamine receptor-expressing striatal interneurons also play an important role in regulating both types of MSNs, leading to indirect responses to a “global” dopamine signal. For instance ChAT interneurons co-express D2Rs and D5Rs (Yan & Surmeier, 1997) and modulate both MSNs through muscarinic receptors (Yan & Surmeier, 1997). Two other prominent classes of GABAergic interneurons (NOS+ and PV+) express D5Rs (Centonze *et al.*, 2003a).

Acetylcholine represents a second important neuromodulator in striatum. It arises from brainstem areas (e.g. the pedunulopontine nucleus, PPN and laterodorsal tegmental area) (Dautan *et al.*, 2014) and from local cholinergic interneurons (Mena-Segovia *et al.*, 2008). This neurotransmitter exerts its influence by acting through muscarinic receptors expressed by both direct and indirect pathway MSNs (Yan *et al.*, 2001). The muscarinic receptors have diverse effects, and are expressed by different striatal neurons. Muscarinic receptors M1, M3 and M5 are Gq-coupled; activation of these receptors results in activation of phospholipase C, and the inositol trisphosphate (IP3) signal transduction pathway and thus exerts an overall excitatory effect. In contrast, the activation of Gi-coupled M2 and M5 receptors exerts an inhibitory effect. In striatum, all MSNs express the M1 receptor, but only MSNs of the direct pathway express the M4 muscarinic receptor subtype (Kreitzer, 2009). Cholinergic interneurons express the M2 receptor which can work as an auto-receptor regulating the release of acetylcholine (Kreitzer, 2009).

The striatum also receives modulatory afferents from the histaminergic neurons in the hypothalamus that suppress the excitatory drive to MSNs (Ellender *et al.*, 2011) and from serotoninergic neurons of the midbrain raphe nucleus that exert a multitude of effects by means of several distinct serotoninergic receptors (Parent *et al.*, 2011). Lastly, noradrenaline has been shown to have a role in regulating the physiology of striatal MSNs (Aston-Jones & Bloom, 1981).

1.3 Interneurons

The activity of MSNs is not only dependent upon dopaminergic and cholinergic modulation, but also on other factors, including interactions with striatal interneurons that, despite their relative small population sizes (~5-10%), act by shaping MSN output and thus contribute to basal ganglia-mediated behaviours (Tepper & Bolam, 2004). Four major classes of interneurons in the striatum have been identified using cytochemical, physiological and morphological methods: cholinergic interneurons identifiable by the presence of choline acetyltransferase (ChAT); GABAergic interneurons that contain the calcium-binding protein parvalbumin (PV); GABAergic interneurons that contain the calcium-binding protein calretinin (CR), and a class of GABAergic interneurons that express somatostatin, neuropeptide Y and nitric oxide synthase (NOS) (Kubota et al., 1993). Cholecystokinin-positive aspiny interneurons (Giachetti *et al.*, 1977; Zaborszky *et al.*, 1985), tyrosine hydroxylase-(TH) expressing neurons and NPY-expressing interneurons (Ibanez-Sandoval *et al.*, 2011) have been also identified in mice (Unal *et al.*, 2013).

1.3.1 Cholinergic interneurons

Cholinergic interneurons represent ~1% of the entire striatal neuron population (Oorschot, 1996). They have large somata (~20 to 50 µm in diameter) and are distributed in both matrix and patches although their dendrites often cross the boundaries between compartments (Kawaguchi, 1993). The release of striatal acetylcholine from intrinsic cholinergic interneurons is modulated by dopamine via activation of different types of dopamine receptors (Di Chiara et al., 1994) and by cortical (Kemp & Powell, 1970; Hassler *et al.*, 1978; Frotscher *et al.*, 1981; Somogyi *et al.*, 1981; Dube *et al.*, 1988; Wictorin *et al.*, 1989; Xu *et al.*, 1989; Lapper & Bolam, 1992) and thalamic inputs (Chung *et al.*, 1977; Dube *et al.*, 1988; Xu *et al.*, 1991; Sadikot *et al.*, 1992; Di Chiara *et al.*, 1994; Doig *et al.*, 2010). In turn, cholinergic interneurons modulate neuronal excitability and synaptic transmission in striatum by muscarinic and nicotinic receptors, some of which are expressed by both classes of MSNs, on the axons and synaptic terminals of corticostriatal axons (Akins *et al.*, 1990; Calabresi *et al.*, 1998; Gabel & Nisenbaum, 1999; Zhou *et al.*, 2001; Centonze *et al.*, 2003b; Shen *et al.*, 2005; Threlfell *et al.*, 2012). Cholinergic interneurons are autonomously active and can fire in the absence of synaptic input; they can exhibit at least three distinct firing patterns without the intercession of external signals (Bennett & Wilson, 1998; 1999; Bennett, 2000; Wilson, 2005; Sharott *et al.*, 2012). In awake, behaving primates, striatal units with similar firing properties are referred to as ‘tonically active neurons’ (TAN) and are characterized by a prominent pause on presentation of sensory stimuli (Kimura *et al.*, 1984; Aosaki *et al.*, 1995).

1.3.2 Parvalbumin-expressing interneurons

GABAergic parvalbumin-expressing interneurons constitute ~0.6% of striatal cells (Rymar *et al.*, 2004) and are present in both patch and matrix compartments (Cowan *et al.*, 1990). These interneurons receive direct, convergent glutamatergic inputs from multiple cortical regions (Ramanathan *et al.*, 2002) and are more responsive to cortical inputs than MSNs (Parthasarathy & Graybiel, 1997; Mallet *et al.*, 2005). In turn, these interneurons give rise to GABAergic input to a wide range of nearby MSNs (Koos & Tepper, 1999) via synapses on cell bodies or proximal dendrites (Kita *et al.*, 1990; Bennett & Bolam, 1994). Parvalbumin-expressing interneurons are sometimes referred to as 'fast-spiking' (FS) interneurons due to their peculiar electrophysiological properties (Kawaguchi *et al.*, 1995). Indeed, *in vivo* recording experiments under general anaesthesia have shown that PV+ expressing interneurons display a characteristically short action potential (< 1ms), which is quicker than those of all other striatal neurons and therefore aids their identification by electrophysiology making them easily distinguishable from other neurons (Mallet *et al.*, 2005; Sharott *et al.*, 2012). Similarly, in awake behaving rats, FS interneurons display a distinctive short spike waveform and exhibit a firing pattern dependent on brain state. However, in contrast to *in vivo* studies under general anaesthesia, in awake/behaving animals their firing rates reach a tonic frequency of ~ 15Hz (Berke *et al.*, 2004). Finally, PV+ interneurons respond to cortical input more rapidly, compared to MSNs, and thus their feed-forward inhibition has been suggested to act as a critical filter of cortical information transmitted to striatal MSNs (Parthasarathy & Graybiel, 1997; Mallet *et al.*, 2005; Sharott *et al.*, 2012). Indeed it is possible that, through this specific synaptic transmission, they may assist the

basal ganglia in selecting one action while suppressing incompatible alternatives (Mallet *et al.*, 2005; Planert *et al.*, 2010). Although both types of MSNs are influenced by 'feed-forward' inhibition from PV+ interneurons, some authors found some preferential connectivity with direct pathway MSNs (Gittis *et al.*, 2010), while others argue that PV+ interneurons provide a strong and homogeneously depressing inhibition of both direct and indirect pathway MSNs (Planert *et al.*, 2010).

1.3.3 Nitric oxide synthase-expressing interneurons

Nitric oxide synthase-expressing GABAergic interneurons are another type of GABAergic interneuron of the striatum that comprises ~0.6% of the total cell population in rodents (Rymar *et al.*, 2004). Many NOS+ interneurons (~75%) also express immunoreactivity for neuropeptide Y (NPY) and somatostatin (SS) (Vincent *et al.*, 1983; Aoki & Pickel, 1990). The functional relevance of these subpopulations of NOS+ interneurons is still unclear. NOS-expressing interneurons innervate mainly the matrix compartment, although their somata are found in patches too and their dendrites often cross compartmental boundaries (Kawaguchi, 1993). They also connect with MSNs (Morello *et al.*, 1997) and with ChAT+ interneurons (Vuillet *et al.*, 1992) although a more recent electrophysiological study did not find evidence of NOS+ interneuron innervating other interneurons (Gittis *et al.*, 2010). NOS-expressing interneurons also receive cortical input, but in contrast with PV+ neurons, they are unlikely to provide a strong feed-forward inhibition of MSNs (Sharott *et al.*, 2012). Electrophysiological investigations of the intrinsic properties of NOS interneurons describe them as characterized by low-threshold calcium spike

(LTS) and with a prolonged calcium-dependent plateau potential. For this reason they have been termed persistent and low-threshold spike (PLTS) neurons (Kawaguchi, 1993; Kawaguchi *et al.*, 1995). By using a genetically modified mouse strain in which green fluorescent protein (GFP) expression is driven under control of the neuropeptide Y (NPY) promoter, Partridge and colleagues (2009) identified NPY interneurons and investigated their function *in vitro*. In accordance with previous studies, they show these neurons display LTS patterns, high input resistances and spontaneous firing between 4-12 spike/s (Koos & Tepper, 1999; Partridge *et al.*, 2009). However, in contrast to these findings, recent *in vivo* studies show how, although exhibiting a prominent burst, NOS+/NPY+ interneurons did not fire typical LTS (Sharott *et al.*, 2012). Understanding the biological function of NOS+ interneurons is challenged by their ability to release multiple neurotransmitters and thus, is still under investigation.

1.3.4 Calretinin-expressing interneurons

The last major class of striatal GABAergic interneuron expresses calretinin (CR), a calcium binding protein that shares 58% homology with calbindin (Jacobowitz & Winsky, 1991). Calretinin-expressing interneurons account for ~0.5% of all striatal neurons (Rymar *et al.*, 2004). Based on immunocytochemical studies, there are at least three, morphologically distinct types of CR+ interneurons which have an organized distribution within the striatum (Tepper *et al.*, 2010).The electrophysiological properties of CR+ interneurons remain to be elucidated (Bennett & Bolam, 1993).

1.4 Target nuclei of striatum

Information processed by the striatum is conveyed “downstream” through the networks of BG via two main routes, one mediated by direct pathway MSNs that monosynaptically innervate with the output nuclei, and the other by indirect pathway MSNs that reach the output nuclei through the GPe and STN. The aim of the following paragraphs is to give an overview of these downstream structures.

1.4.1 External segment of the globus pallidus

The GPe is the main nucleus that integrates information coming from indirect pathway MSNs (Figure 1.1) (Noda *et al.*, 1968; Levine *et al.*, 1974; Ohye *et al.*, 1976; Chang *et al.*, 1981; Park *et al.*, 1982; Wilson & Phelan, 1982; Totterdell *et al.*, 1984; Gerfen, 1985; Nakanishi *et al.*, 1985; Kawaguchi *et al.*, 1990; Kita & Kitai, 1991; Yoshida *et al.*, 1993; Parent & Hazrati, 1995a; Shink & Smith, 1995). The rat GPe is composed of ~46,000 GABAergic neurons (Oorschot, 1996) of which, recently, have been distinguished two main neurochemically and electrophysiologically different populations (Mallet *et al.*, 2012). Mallet and colleagues, in two sets of experiments where different *in vivo* electrophysiological techniques and histochemical staining were combined, were able to elucidate the heterogeneity of this structure. Specifically, the study suggested the presence of two sub-populations of neurons in the GPe with distinct molecular and electrophysiological profiles as well as different connectivity (Mallet *et al.*, 2008a; Mallet *et al.*, 2012). One population of GABAergic GPe neurons, referred to as prototypical neurons, often express parvalbumin and target downstream output nuclei, a sub-group of which innervate the striatum, whereas a second population, referred to as arkypallidal

neurons, express preproenkephalin and project exclusively to the striatum innervating MSNs and interneurons (Bevan *et al.*, 1998; Mallet *et al.*, 2012). Histochemical staining of striatal arborisation in rodents and monkeys has shown that indirect pathway MSNs input in GPe is greatly specific and has a high degree of synaptic convergence with a suggested ratio of 27:1 (Oorschot, 1996). GPe also receive a fraction of inhibitory input from axon collaterals of the direct pathway MSNs (Bolam *et al.*, 2000). The GPe is reciprocally connected to the STN by a series of open and closed loops (Kita & Kitai, 1987; Smith & Bolam, 1990; Shink *et al.*, 1996; Joel & Weiner, 1997; Smith *et al.*, 1998a). The glutamatergic STN is the main source of excitatory input to GPe (Deniau *et al.*, 1978; Perkins & Stone, 1980; Kita *et al.*, 1983b; Kita & Kitai, 1987; 1991; Soltis *et al.*, 1994). Additionally, GPe is also known to receive a sparse dopaminergic projection from the SNc, which can either excite or inhibit GPe neurons (Fallon & Moore, 1978; Lindvall & Bjorklund, 1979; Lavoie *et al.*, 1989; Charara & Parent, 1994; Gauthier *et al.*, 1999; Hedreen, 1999; Jan *et al.*, 2000; Smith & Kieval, 2000). Inputs from the mesopontine tegmentum that are likely to have mixed excitatory and inhibitory effect on GPe neurons (Saper & Loewy, 1982; Gonya-Magee & Anderson, 1983; Jackson & Crossman, 1983; Woolf & Butcher, 1986; Charara & Parent, 1994). The GPe is also innervated by the centromedian-parafascicular complex of the thalamus (Noda *et al.*, 1968; Levine *et al.*, 1974; Kincaid *et al.*, 1991; Mouroux *et al.*, 1997), and receives minor projection from the cortex (Naito & Kita, 1994a; Levesque *et al.*, 1996; Levesque & Parent, 1998). The discharge of GPe neurons can be modulated in response to passive movement or during the planning, initiation, execution and/or termination of active movements (Mink & Thach, 1991; Gardiner & Kitai, 1992; Turner & Anderson, 1997). Nevertheless, further examination of the relationship of different types of GPe

neurons to sensory and motor events is necessary to clarify the importance of such cellular heterogeneity for BG function.

1.4.2 Subthalamic nucleus

The subthalamic nucleus is a small structure localized between the zona incerta and the cerebral peduncle and is densely populated by glutamatergic projection neurons. Despite it relatively small size, the STN is considered to be one of the main regulators of the motor function in the basal ganglia-thalamocortical circuit (Albin *et al.*, 1989; Alexander & Crutcher, 1990). The morphological features of STN neurons have been extensively studied across different species, and although these studies have proposed different classification schemes for STN neurons, there is almost a complete consensus as to the somatic and dendritic morphology (Rafols & Fox, 1976; Iwahori, 1978; Yelnik & Percheron, 1979; Hassler *et al.*, 1982; Chang *et al.*, 1983; Hammond & Yelnik, 1983; Kita *et al.*, 1983a; Afsharpour, 1985a; b; Parent & Hazrati, 1995b). In rats the STN consists of ~13,600 glutamatergic stellate neurons (Oorschot, 1996) with radiating, sparsely spined dendrites with abundant organelles in their somata. The results of tracing studies at the electron microscope level combined with postembedding immunolabelling for glutamate and GABA, have shown that individual neurons of the GP innervate the STN and output structures of the basal ganglia (Bolam *et al.*, 1993; Smith *et al.*, 1998b). The GPe gives rise to massive projections to the STN and in many cases the receiving STN neurons project back to the GPe, hence indicating a strong reciprocal relationship between these structures (Shink *et al.*, 1996). Due to these prominent reciprocal connections, the STN and GPe are classically viewed as a synergistic duo within the indirect

pathway that act in concert with striatal neurons to convey information directly to the output nuclei. During quiet wakefulness STN and GPe neurons fire differently (DeLong *et al.*, 1985; Wichmann *et al.*, 1994a; Nini *et al.*, 1995; Wichmann & DeLong, 1996; Bergman *et al.*, 1998; Raz *et al.*, 2000a), during voluntary or passive movement they display spatiotemporal changes in activity that appears to be related to motor activity (DeLong *et al.*, 1985; Wichmann *et al.*, 1994a; Jaeger *et al.*, 1995; Bergman *et al.*, 1998). Nevertheless, STN also projects to GPi, to the substantia nigra, the striatum, the cerebral cortex, the substantia innominata, the pedunculopontine tegmental nucleus and the mesencephalic and pontine reticular formation (Jackson & Crossman, 1981a; b; Kita & Kitai, 1987; Smith & Parent, 1988). Conversely, the STN receives afferent projections from the cerebral cortex, the centromedian-parafascicular complex of the thalamus and from various brainstem nuclei, principally the substantia nigra, the dorsal raphe and the peduncolopontine tegmental nucleus (Parent & Hazrati, 1995b). In good agreement with the anatomical data, physiological properties of STN neurons have also been demonstrated to be homogeneous (Nakanishi *et al.*, 1987a; Overton & Greenfield, 1995; Beurrier *et al.*, 1999; Bevan & Wilson, 1999; Wigmore & Lacey, 2000). STN neurons exhibit autonomous single-spike firing at a moderate rate and a highly regular pattern in the absence of synaptic input. Studies in awake and anaesthetised animals indicate that STN neurons are tonically active and display moderate (10-40 spikes/s) and regular or irregular firing patterns (Tsubokawa & Sutin, 1972; Rouzaire-dubois *et al.*, 1980; Georgopoulos *et al.*, 1983; Robledo & Feger, 1990; Kreiss *et al.*, 1996; Maurice *et al.*, 1998; Urbain *et al.*, 2000). The discharges of some STN neurons appears to be selectively modulated in response to limb

movement and more specifically to the initiation, execution and often to the termination of motor task.

The involvement of the STN in motor control is evident from studies of Parkinsonism and its resulting treatments. Indeed, subsequent to chronic and progressive dopaminergic loss, the STN shows a prominent hyperactivity in the form of a continuous abnormal bursting mode and increase in the firing rate, whereas in normal physiological conditions it exhibit a more regular pattern of discharge with intervals of burst activity (Magill *et al.*, 2000; Dostrovsky & Lozano, 2002; Urbain *et al.*, 2002; Temel *et al.*, 2005). This STN hyperactivity promotes an excessive inhibition of the target nuclei and it has become, consequently, the principal target for deep brain stimulation (DBS) therapy in Parkinson's disease (Bevan *et al.*, 2002). Also it has been shown in primate that STN is composed of parts that project to associative and limbic areas of the pallidal complex and substantia nigra pars reticulata, but the functionality of these projections remains elusive and requires further investigation (Alexander & Crutcher, 1990; Alexander *et al.*, 1990; Parent & Hazrati, 1995a; b).

1.4.3 Internal segment of the globus pallidus

The GPi and SNr constitute the output nuclei of the basal ganglia (Figure 1.1). These structures share some similarities and are often considered as a functional unit in conveying processed information to the cortex through different thalamic nuclei or conveying information to sub-cortical structures. The homolog of the GPi in rodents, the EPN (entopeducolar nucleus), is a small structure of ~3,200 GABAergic neurons located rostral to the internal capsule and ventral to the medial forebrain bundle

(Oorschot, 1996). The GPi is composed primarily of neurons that innervate structures outside the basal ganglia including the thalamus and brainstem (Bolam *et al.*, 2000). The GPi receives massive inhibitory input from the striatum and the GPe, and excitatory input from STN and mesopontine tegmentum as well as dopaminergic and serotoninergic input from SNc and dorsal raphe nucleus (Bolam *et al.*, 2000).

Tracing studies in primates, cats and rats have shown, based on their projection sites, that GPi neurons form two distinct populations (Nauta, 1974; Filion & Harnois, 1978; van der Kooy & Carter, 1981; Tokuno *et al.*, 1988; Parent *et al.*, 2001). This anatomical evidence was corroborated by *in vitro* studies showing differences in the firing properties of EPN neurons. Nakanishi and colleagues (1990) showed how one population was able to spontaneously fire action potentials at high frequency (~60 spikes/s) in a regular or irregular manner with absence of synaptic input, whereas the second population does not fire spontaneously, do not possess a prominent LTS but rather a ramp depolarization attributable to a A-type potassium current, absent in the other type (Nakanishi *et al.*, 1990). Recently GPi was also electrophysiologically characterized in anesthetized and freely moving rats confirming the previous evidence (Benhamou & Cohen, 2014). The discharge of many (but not all) GPi neurones is tonic with high rate discharges and rapid firing fluctuations and they are modulated during planning, initiation, execution and/or termination of voluntary or passive movement (DeLong, 1971). However due to the physiological complexity of this structure the relationship between motor activity and firing pattern requires further investigation. Finally, GPi is considered to participate in motor control and particularly in movement initiation, sequential organization of movement and predominantly in action selection (Horak & Anderson, 1984b; a;

Mink, 1996; Redgrave *et al.*, 1999). Indeed lesion of this structure can cause motor deficits including reduction of speed as well as acceleration. (Turner & Anderson, 2005; Turner & Desmurget, 2010). Additionally, early studies on GPi neurons showed that they process sensory information related to reward consumption (Lidsky, 1975). Lesion of the GPi leads to improvement of motor symptoms of Parkinson's patients which suggests, again, the powerful influence on motor behaviour (Obeso *et al.*, 2009).

1.4.4 Substantia nigra pars compacta and pars reticulata

The substantia nigra consists anatomically of the pars compacta (SNc), which contains a densely packed population of neurons, and the pars reticulata (SNr), in which the neurons are arranged more diffusely. The SNr in the rat is a nucleus of ~26,000 neurons located in the midbrain, ventral to the SNc (Oorschot, 1996). The SNr together with GPi constitute the output nuclei of the BG (Bolam *et al.*, 2000). Based on their electrical and morphological properties, SNr neurons can be divided in two categories: type I neurons that made up the majority of neurons and are GABAergic projection neurons (Oertel & Mugnaini, 1984). These neurons are characterized by spontaneous repetitive firing, short duration of action potentials, weak spike accommodation and strong delayed rectification during membrane depolarization (Nakanishi *et al.*, 1987b). Type II neurons are dopaminergic projection neurons almost indistinguishable from those located in SNc (Nakanishi *et al.*, 1987a). They present a long duration of action potential, a large post-active hyperpolarization and a less prominent delayed rectification (Nakanishi *et al.*, 1987a). In awake or anaesthetised rats, GABAergic neurons of SNr usually display

a tonic firing with a regular or irregular discharge in the range of 15-70 spikes/s (Dray *et al.*, 1976; Wilson *et al.*, 1977; DeLong, 1983; MacLeod *et al.*, 1990; Robledo & Feger, 1990; Feger & Robledo, 1991; Fujimoto & Kita, 1992; Burbaud *et al.*, 1995; Murer *et al.*, 1997). SNr receives highly-convergent inhibitory input from MSNs (Precht & Yoshida, 1971; Bunney & Aghajanian, 1976; Chevalier *et al.*, 1985; Gerfen, 1985; Bolam *et al.*, 1993; Bevan *et al.*, 1994) and from the GPe (Totterdell *et al.*, 1984; Smith & Bolam, 1989; Bolam *et al.*, 1993; Bevan *et al.*, 1996) and excitatory inputs mainly from the STN (Deniau *et al.*, 1978; Hammond *et al.*, 1978; Kita *et al.*, 1983a; Kita & Kitai, 1987; Nakanishi *et al.*, 1987b; Robledo & Feger, 1990; 1991; Rinvik & Ottersen, 1993; Bevan *et al.*, 1994) and prefrontal cortex (Bunney & Aghajanian, 1976; Kornhuber *et al.*, 1984; Naito & Kita, 1994a). Evidence shows that SNr also receives cholinergic and non-cholinergic afferents from the mesopontine tegmentum (Woolf & Butcher, 1986; Beninato & Spencer, 1988; Lee *et al.*, 1988; Bolam *et al.*, 1991) and input from serotoninergic neurons of the dorsal raphe (Lavoie & Parent, 1990; Corvaja *et al.*, 1993). Although the main target output is towards many regions of thalamus, the superior colliculus, pedunculopontine nucleus and mesenephalic reticular formation (Deniau *et al.*, 1978; Faull & Mehler, 1978; Bentivoglio *et al.*, 1979; Beckstead *et al.*, 1981; Chevalier *et al.*, 1981; Grofova *et al.*, 1982; Deniau & Chevalier, 1992; von Krosigk *et al.*, 1992), a small portion of GABAergic SNr neurons also project to the striatum (Rodriguez & Gonzalez-Hernandez, 1999). Finally, the axon of most of SNr neurons emit local collaterals that broadly ramify within the SNr and SNc (Deniau *et al.*, 1982; Grofova *et al.*, 1982).

The SNc contains dopaminergic neurons that are overall referred to as cell group A9 (Williams & Goldman-Rakic, 1998). These group of neurons provide

massive dopaminergic innervation to the striatum (Beckstead, 1978; Freund *et al.*, 1984; Gerfen *et al.*, 1987b), forming the nigrostriatal projection, but also innervate the GPi, GPe and STN (Smith & Kieval, 2000). This structure receives afferents from the STN (Ricardo, 1980; Kita & Kitai, 1987), cortex (Naito & Kita, 1994b) serotoninergic input from the raphe (Lavoie & Parent, 1990; Corvaja *et al.*, 1993) inhibitory inputs from GPe (Smith & Bolam, 1990) and the SNr (Mailly *et al.*, 2003). The SNc also receives input from neurons of the direct pathway located within the patch compartment (Smith & Bolam, 1990; Fujiyama *et al.*, 2011). Neurons in the ventral tegmental areas (VTA; A10) also project to the striatum, forming the mesostriatal pathway. The SNc provides input to the dorsal, sensorimotor part of striatum, whereas the VTA provides input to the limbic-related areas of striatum (Smith & Kieval, 2000)

Dopaminergic neurons of the SNc have a firing rate of ~5 spikes/s in anaesthetized animals and can exhibit a variety of firing patterns including random, pacemaker and bursting activity (Brown *et al.*, 2009). The SNc is not a homogeneous structures, but can be divided into dorsal and ventral tiers. Many neurons in the dorsal tier express the calcium-binding protein calbindin and display a slower firing rate compared to calbindin-negative ventral tier neurons (Brown *et al.*, 2009).

Dopaminergic innervation of SNc in the BG network plays a pivotal role in a wide variety of motor, cognitive and emotional function. The loss of these neurons is the cause of the cardinal symptoms of Parkinsonism (see section 1.5.1) (Agid, 1991; Gibb & Lees, 1991; Braak *et al.*, 2000). Dopamine has also receive attention in relation to its roles in reward and addiction as midbrain dopaminergic neurons exhibit distinctive firing patterns in relation to rewards, cues that predict reward and

during behavioural tasks in the primate. Indeed, midbrain dopaminergic neurons tend to: (1) increase their firing in response to an unexpected reward; (2) decrease their firing when an expected reward is omitted; and (3) not change their firing in response to an expected reward (Schultz, 1998). Such response patterns, together with other data, support the influential hypothesis that midbrain dopaminergic neurons encode a 'reward prediction error' signal (Schultz, 1998).

Finally the effects of dopamine within the striatum is dependent on the receptors expressed and the level of dopamine available. Dopamine in striatum acts via G-coupled dopamine receptors that mediate its effect through a second messenger cascade that either inhibits or activates specific currents and intracellular messengers.

1.5 Basal ganglia dysfunction

Many insights into the functional roles played by BG come from studies of behavioural and other deficits that are caused by lesions of these structures, either 'natural' (arising in the course of a disease) or experimentally induced. From the extensive body of work, two lines of evidence have arisen to describe the abnormal activity of neurons of BG nuclei in Parkinson's disease (PD). The first line of evidence suggests that changes in the firing rate of BG neurons is the primary cause of motor abnormalities in PD whereas the second argues that the symptoms are a consequence of the emergence of enhanced oscillations and increased synchrony in BG networks. These views have often been perceived as opposed to each other (Bar-Gad & Bergman, 2001). The following paragraphs aim to introduce the reader to the pathology of PD, providing evidence in favour and against both views, with an

emphasis on the role of striatum in this pathology and the operation of the BG network.

1.5.1 Neuropathological features of Parkinson's disease and its treatments

Parkinson's disease is a progressive neurodegenerative disorder that primarily affects the central nervous system. The cause of Parkinson's disease is unknown, but several factors appear to play a role, including: specific genetic mutations, environmental factors (e.g. toxins) and oxidative stress (Braak *et al.*, 2003a). The pathological hallmark of PD is the degeneration of dopaminergic neurons within the substantia nigra (Figure 1.3), the subsequent dopamine depletion of the striatum and the presence of Lewy bodies in surviving dopamine neurons (Bergman & Deuschl, 2002). The motor symptoms resulting from the degeneration of dopaminergic neurons include: bradykinesia, hypokinesia, reduction in movement amplitude and akinesia, the absence of normal/unconscious movement (Dauer & Przedborski, 2003). Tremor is another major symptom of PD, it occurs at rest and typically decreases with voluntary movement. PD patients also exhibit a curved posture and may also lack normal postural reflexes, leading to falls. The inability to begin a voluntary movement (freezing) is another common indicator of the pathology. In the late stages of PD, cognitive and psychological processes are impaired and patients often become passive, depressed and withdrawn (Dauer & Przedborski, 2003). In the initial stages of disease evolution, the clinical manifestation of PD are largely motor due to the neurodegenerative process that is mainly confined to the SN (Braak *et al.*, 2003a). The medial substantia nigra seems

to be more affected in tremor dominant form of PD, whereas the loss of dopaminergic neurons of the lateral substantia nigra is more linked to the akinesia/rigidity-variant of PD (Paulus & Jellinger, 1991). As the disease develops, dopamine loss extends to involve the entire striatum (Hornykiewicz, 1988; Lang & Lozano, 1998), all pallidal areas (Hornykiewicz, 1988; Jan *et al.*, 2000) and the STN (Hornykiewicz, 1988). Additionally, neurons in other brain regions, especially during the late phase, including the cerebral cortex, brainstem and spinal cord, may also be progressively lost (Lang & Lozano, 1998; Braak *et al.*, 2003a). The Braak hypothesis suggests that degeneration begins in the brain stem (or may be the enteric nervous system) and then progresses rostrally in the brain. When it reaches the midbrain, then the motor symptoms follow and when it reaches the forebrain, cognitive symptoms occur. The premotor symptoms may be a consequence of neurons other than dopamine neurons dying.

Currently, only symptomatic treatments are available for PD. The dopamine precursor, Levodopa, is the principal medical treatment for this disease. However the long-term use of Levodopa has been linked to the so-called 'dopamine dysregulation syndrome' that entail several motor complications in up to 80% of the patients (Kondo, 2008). These side effects are often difficult to manage and have led to a renaissance of invasive approaches for late-stage Parkinson's disease, particularly deep brain stimulation (DBS). In a typical implementation of DBS, a multi-contact macro-electrode is implanted in the GPi and/or the STN and current pulses are then delivered at high frequencies (~130 Hz) (Bar-Gad *et al.*, 2004; Carlson *et al.*, 2010; Deniau *et al.*, 2010). The mechanism by which delivery of electrical stimulation to the target area can restore function is not clear. It is possible, however, that this type of surgery works by interfering with and shutting down

abnormal brain activity in those areas where the current is delivered. When abnormal activities are neutralized, motor areas of the brain can resume their function and normal movements are reinstated (Lozano *et al.*, 2002).

1.6 Neural substrates of motor deficits in Parkinson's disease

Because information processing in any neuronal system is bound to an underlying anatomical substrate, and because the BG are the primary locus of the pathology in PD, it is reasonable to assume that PD symptoms are due to abnormalities within these BG-thalamocortical circuits. One of the first attempts to synthesize a unifying concept of BG function and dysfunction came from Albin et al. (1989) and DeLong (1990) who put forward a model that accounts for PD symptoms in light of the dichotomous organization of striatal output (Figure 1.3). As already stated, striatal MSNs can be divided into two main populations according to their projection sites and neurochemical properties (Graybiel, 2000). Direct pathway MSNs preferentially innervate basal ganglia output nuclei (SNr and GPi) and express D1R, whereas indirect pathway neurons exclusively innervate the GPe and express D2R (Gerfen and Surmeier, 2011). Under normal conditions of an intact dopamine innervation, activation of D1Rs on direct pathway MSNs increases their output, thus inhibiting GABAergic basal ganglia output neurons and, thence, disinhibiting basal ganglia targets in thalamus, midbrain and brainstem. This sequence is proposed to facilitate movement. In contrast, activation of D2R on indirect pathway MSNs decreases their output, ultimately reframing the inhibition of basal ganglia targets that reduces movement. Importantly, this model explains PD motor symptoms through changes in the overall firing rates of direct and indirect MSNs as a consequence of adaptation

to the degeneration of SNc dopaminergic neurons (Albin *et al.*, 1989; DeLong, 1990). When dopamine depletion occurs in the SNc, the absence of dopamine in its striatal target area leads to opposite physiological effect of the two pathways. Thus, chronic loss of dopamine leads to both a reduction of activity of the direct pathway, and an increase of the activity in the indirect excitatory pathway, synergistically leading to an increased firing rates of BG nuclei output neurons. Because the GPi/SNr–thalamic projection is inhibitory, increased GPi/SNr discharge leads to inhibition of thalamocortical neurons. The resulting reduction of cortical activation, according to this model, would then account for the hypokinetic symptoms of PD (Albin *et al.*, 1989; DeLong, 1990). The achievement of this model is twofold: first, it predicts a pathophysiological mechanism of PD explained as an under- or over-activity of the direct/indirect pathways. In support of this, recent direct electrophysiological evidence of the imbalance of both pathways became available from studies of rodents in which dopamine neurons have been lesioned by toxin injection. For instance, by combining juxtacellular labelling and immunohistochemistry of recorded cells *in vivo* in a rat model of PD, it has been shown that direct pathway MSNs were hypoactive whereas indirect pathway MSNs were hyperactive after lesions of dopaminergic neurons (Mallet *et al.*, 2006; Ballion *et al.*, 2008). Studies in other nuclei of the BG also corroborate this model illustrating how lesions of the STN and/or GPi ameliorate PD symptoms by reversing the abnormal firing rate increases in these structures (Bergman *et al.*, 1990; Aziz *et al.*, 1991). Second, by taking advantage of the dichotomous nature of MSNs, the direct/indirect pathways model predict how a voluntary movement is performed under the guidance of striatal neurons. Indeed, when a voluntary movement or action is generated by cortex, the indirect pathway MSNs act to inhibit competing

'motor programs'. Concurrently, the direct pathway focally removes the inhibition from the desired 'motor program' (Albin *et al.*, 1989; DeLong, 1990). The basic features of this dichotomous striatal control over voluntary movement have been recently supported by studies using optogenetic approaches (Bateup *et al.*, 2010; Kravitz *et al.*, 2010).

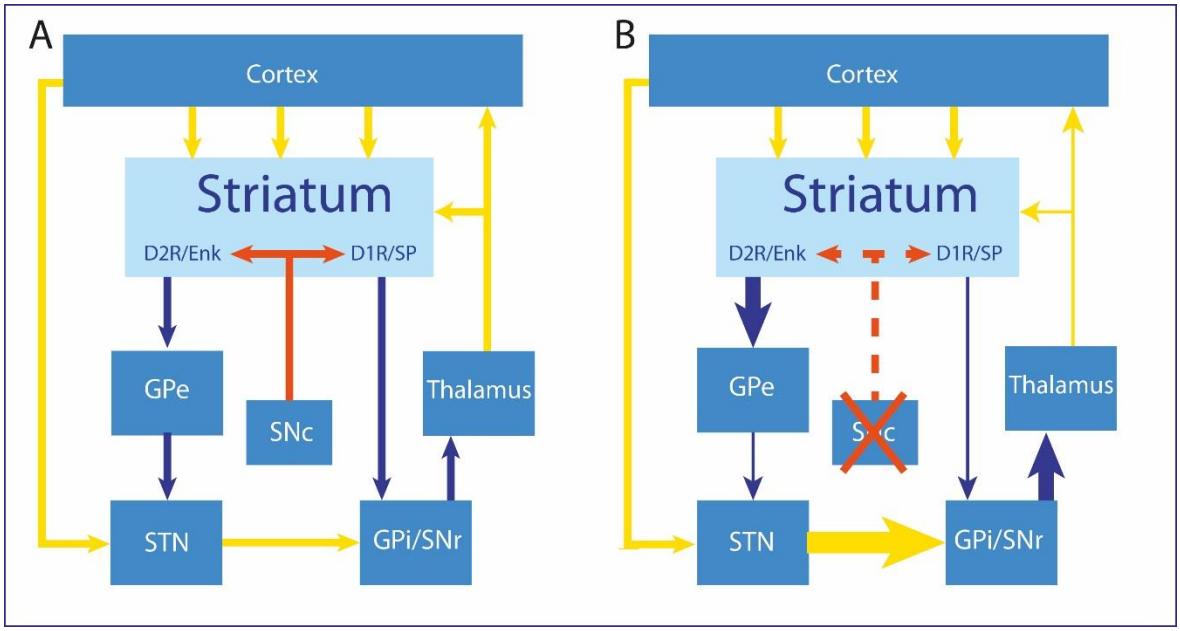

Figure 1.3 **Simplified diagram of direct/indirect pathway model of cortico-basal ganglia-thalamocortical circuitry under normal conditions and in Parkinson's disease. *A*,** According to the classical direct/indirect pathways model, cortical information that reaches the striatum is conveyed to the output nuclei of the basal ganglia, the internal globus pallidus (GPi), and substantia nigra *pars reticulata* (SNr), via two pathways, a direct inhibitory projection from the striatum to GPi/SNr and an indirect pathway, which involves an inhibitory projection from the striatum to the external globus pallidus (GPe) which in turn sends an inhibitory projection to the subthalamic nucleus (STN) and from here excitatory projections reach GPi/SNr. The information is transmitted back to the thalamus or conveyed to various brainstem structure (e.g. peduncolopontine nucleus of mesopontine tegmentum, lateral habenular nucleus, superior colliculus and reticular formation, not shown in the diagram). The activation of direct pathway leads to a disinhibition of neurons in the target of the basal ganglia, whereas activation of the indirect pathway leads to greater inhibition

of neurons in the target regions. The direct pathway MSNs express type 1 dopamine receptors (D1Rs) and substance P (SP); indirect pathway MSNs are enriched of type 2 dopamine receptors (D2Rs) and enkephalin (Enk). The dopaminergic projection from the substantia nigra *pars compacta* (SNc) exerts a net excitatory effect over MSNs giving rise to the direct pathway by the activation of D1Rs, and a net inhibitory effect over MSNs giving rise to the indirect pathway by activation of D2Rs. The overall influence of dopamine within the striatum may be to reinforce cortically-initiated motor circuits by both facilitation of conduction through direct pathways MSNs or suppressing the conduction through indirect pathway. Cortical information can also reach the basal ganglia via the corticosubthalamic projection. Note the connection between thalamus and striatum. ***B*****,** In Parkinson's disease, the loss of dopaminergic neurons in SNc results in an imbalance in the activity of the direct and indirect pathway in favour of the indirect pathway. Relative increases in activity are indicates by *thickening* of arrows and relative decreases in activity by *thinning* of arrows as compared to *A.* The net result of this imbalance is the over-activity of GABAergic neurons in the output nuclei, which leads to excessive inhibition and in turn drastically suppress the activity of cortical and other target areas. Indeed, the excessive thalamic inhibition leads to suppression of cortical motor system, resulting in akinesia and bradykinesia, whereas the overactive inhibition to brainstem structure (not shown) may contribute to abnormalities of gait and posture. It should be noted that these diagrams are a simplification as many connections have not been indicated. Adapted from De Long, 1990.

1.6.1 Limitations of direct/indirect pathways model

Although the direct/indirect pathways model of BG function and dysfunction has advanced the understanding of the pathophysiology of PD, accumulating evidence has challenged this classical view. For example, this model proposes that it is alterations in neuronal firing rates alone that underlie the full spectrum of movement disorders in PD. For instance, akinesia and bradykinesia (main motor symptoms in PD) are explained as a result of the elevated firing rate of BG output nuclei neurons that project to premotor structures. However, studies on PD animal models and PD patients show only a small increase in GPi firing rate in the order of 10-22%, which is not sufficiently strong, according to the authors, to affect thalamic and cortical areas (Wichmann *et al.*, 1994b; Wichmann *et al.*, 1999; Raz *et al.*, 2000b; Levy *et al.*, 2001; Hutchison *et al.*, 2004; Rivlin-Etzion *et al.*, 2008). Also, electrophysiological evidence accumulated for hyperkinetic disorders, such as dystonia and Huntington's disease, show that GPi output is similar to that in PD (Hutchison *et al.*, 2003). Furthermore increased GPi neuron firing induced by STN stimulation in the monkey animal model of PD is actually associated with motor improvement (Hashimoto *et al.*, 2003) and that in turn is incompatible with the direct/indirect model. More invasive approaches such as pallidotomy, which should drastically reduce GPi activity leading to further disinhibition of the thalamo-cortical system, greatly improve akinesia in monkey and humans (Marsden & Obeso, 1994). Similarly, lesions in the thalamus, which should further reduce and impair thalamocortical activity, is not associated with aggravation of motor deficits in PD (Obeso *et al.*, 2000). In recent years, cytoarchitectural studies have also advanced our understanding of BG, suggesting that the neurochemical connection of striatal

neurons are much more complex than those captured in the model. This includes the discovery of the third (Furuta & Kaneko, 2006) and fourth types of MSN (in addition to the classical first direct pathway and second indirect pathway MSNs) (Perreault *et al.*, 2011), as well as the so called 'hyperdirect pathway' that consist in a direct connection between cortex and STN and that bypasses striatum (Nambu *et al.*, 2002). The classical model also fails to capture the influence of striatal interneurons and thalamostriatal projections. Other anatomical studies also show back projections from GPe to the striatum (Kita *et al.*, 1999; Bolam *et al.*, 2000; Mallet *et al.*, 2012), feed-forward projections from the cortex to the GABAergic interneurons of the striatum (Bolam *et al.*, 2000) and collaterals from the direct pathway neurons to GPe (Bolam *et al.*, 2000; Wu *et al.*, 2000). The output from basal ganglia other than to motor thalamus (e.g. to PPN), might play a major role in PD symptoms (Pahapill & Lozano, 2000). Recent studies also indicate that a substantial fraction of D1 and D2 receptors co-localize on striatal neurons (Aizman *et al.*, 2000). Because of the above evidence, several authors have raised the question as to whether rate coding alone is sufficient to account for all the information processing demands performed by the neuronal networks of the BG (Bullock, 1997; Salinas & Sejnowski, 2001; Buzsaki & Draguhn, 2004) and so, in the past decade, attention has shifted from changes in the discharge *rate* to elevations in population synchrony in Parkinsonian BG circuit (Uhlhaas & Singer, 2006). For instance, a model based on neuronal oscillatory synchrony in space and time, that considers PD not just as a mere dysfunctional discharge rate of striatal neurons, could predict that either a lesion or deep brain stimulation would disrupt pathological oscillations leading to an improvement of symptoms.

1.7 Overview of neuronal oscillations

Neurons are connected to form functionally-specialized assemblies. Successful motor, cognitive or associative operations rest on local communication within and long-range communication between these assemblies. An individual task depends on the precise coordination of many brain areas. One mechanism for functional local and long-range neuronal communication is synchronized oscillations. Oscillations are regular fluctuations in neuronal activity present at many levels in the brain and that manifest in a number of physiological process including diurnal rhythm, memory and movement (Hutchison *et al.*, 2004). Oscillations can evolve from the generation of action potentials of a single neuron or in neuronal assemblies within the same nucleus and/or across nuclei. Several studies of BG physiological properties provide evidence showing how different BG neurons are endowed with a battery of intrinsic membrane properties that promote the expression of oscillatory discharge 'at rest' or in response to highly organized synaptic input (Bevan *et al.*, 2002). However, the oscillatory activity of an individual neuron may or may not be synchronized with the activity of another cell or network of cells. Indeed oscillations and synchronization are distinct properties of a neuronal network. In the dopamine-intact BG for instance, the firing patterns of GPe neurons are strongly periodic but their discharge are typically uncorrelated (Mallet *et al.*, 2008a). Conversely, the activity of BG neurons may be synchronized but without being strongly periodic. As such, neurons or populations of neurons oscillate synchronously only if their electrical elements (spike trains, synaptic potentials and membrane potentials) are time locked in a periodic fashion. Starting from this assumption, it could be further assumed that *synchronized oscillations* in space and time may provide the brain with a mechanism

to execute a behavioural task (e.g. reaching a glass of water) that entails the functional contributions of distant and disparate neural assemblies. As an example, how the distributed responses of feature-selective cells are bound together is the core of the so called 'binding problem' (Treisman, 1996). Initially it was hypothesized that axons could act as carrier of responses of specific cells in a hierarchy structure so that they converge on to a common target cell (Singer, 1999a). This strategy, however, is expensive in terms of the number of cells required to code for the infinite number of perceptual combinations in the external environment. Alternatively, it has been suggested that neurons that are synchronised in different processing streams could encode for one object, while remaining desynchronised from neurons responding to different objects (Singer, 1999a; b).

1.7.1 Type of oscillations and methods for their detection

All oscillations have a frequency associated with them and have been reported to occur in the healthy and diseased BG network (Boraud *et al.*, 2002). Oscillations are usually categorized into one of five frequency bands: delta (0.5–3.5 Hz), theta (4–7 Hz), alpha (8–13 Hz), beta (14–35 Hz), and gamma (30-90 Hz).

With the development of large-scale recording systems, oscillatory network can be identified and characterized by electroencephalogram (EEG) and local field potentials (LFPs). Briefly, EEG and LFPs give an indication of the neuronal activity of interest by means of electrode placed on the scalp or directly inside the region of interest, respectively. LFPs are the result of sophisticated interactions of synaptic and cellular mechanisms and the originate mainly from slow subthreshod currents,

primarily those arising with post-synaptic potentials (Eccles, 1951). Likewise, the synchronicity of those oscillations can be detected by several correlation techniques such as the cross correlation histogram (CHH) (see section 2.8.3).

1.7.2 Synchronized oscillations in the healthy basal ganglia

In contrast to evidence showing prominent synchronization of activity in thalamus, neocortex and hippocampus as part of healthy brain functions, early investigations of BG network activity revealed only very low levels of synchronized oscillatory activity in the normal state (Bar-Gad & Bergman, 2001). However, more recent studies in primates and in rodents show that oscillatory activities are not only present in the whole BG circuit but are also a robust phenomenon (Courtemanche *et al.*, 2003; Berke *et al.*, 2004; DeCoteau *et al.*, 2004; Gervasoni *et al.*, 2004; Sharott *et al.*, 2005a). One of the first circuits to be identified to express synchonized activity was the GPe–STN network. It was demonstrated in an in vitro model that the interaction between these two stuctures produces spontaneously occurring slow synchronized oscillatory activity (Plenz & Kital, 1999). A recent recording study, however, performed in a mouse slice preparation in which connections between STN and the GPe were maintained, failed to show coherent activity in the two nuclei, suggesting that mechanisms extrinsic to the immediate GPe–STN interaction may be important to the production of synchronized bursting (Loucif *et al.*, 2005). In other correlational studies, aimed to determine whether two structures are oscillating in a synchronous manner, large amplitude cortical slow oscillations (1 Hz) and faster spindle oscillations (10 Hz) have been shown to be highly coherent with STN activity in deeply anaesthetized rats (Magill *et al.*, 2000). In awake animals, however,

cortico-STN activity synchronization is very low (Sharott *et al.*, 2005a; Sharott *et al.*, 2005b) and even during physiological/ natural sleep (similar to slow wave activity), low frequency cortical oscillations do not correlate with STN activity (Urbain *et al.*, 2000). Other studies performed under general anaesthesia or in awake rodents, show that LFPs recorded in motor cortex, STN and striatum revealed the presence of oscllatory activity at theta (Magill *et al.*, 2006a) and gamma frequencies (Berke, 2009). Oscillatory activity has also been observed in LFPs recorded from rat striatum. The types of oscillation observed change in accordance to the the behavioral state of the animal, and striatal regions. For instance, spindles (8 Hz) are strongly expressed in the dorsal/lateral striatum and occur in awake but immobile animals (Buonamici *et al.*, 1986; Buzsaki *et al.*, 1990). In ventral striatum a strong ~50 Hz gamma oscillation is seen frequently, and beta oscillations infrequently observed in alert rats (whether moving or not) (Berke *et al.*, 2004). During a maze running test, ventral striatum and connected limbic areas also show a theta rhythm (Buzsaki, 2002).

1.7.3 Synchronized oscillations in the Parkinsonian basal ganglia

Our knowledge of the pathophysiology of PD has been greatly enhanced by electrophysiological recordings in animal models and in PD patients. The results of recording of single-unit activity and/or LFPs, have revealed the tendency for BG neurons to aberrantly synchronize (Bergman *et al.*, 1998). In the past two decades of investigation of electrophysiological activity in PD, four main achievements have been obtained: (1) the most prominent oscillatory activity observed in these studies is in the beta band and is enhanced compared to controls; (2) dopaminergic

medication and DBS supress enhanced beta activity; (3) beta synchronization is also suppressed prior to or during movement and (4) excessive beta synchronization has an “antikinetic” role.

1.7.4 Exaggerated beta activity is suppressed by dopaminergic medication and deep brain stimulation

One of the early investigations showing enhanced oscillatory activity in the BG thalamo-cortical loop and its dependence on dopamine, arose when Brown and co-workers investigated shifts in the frequency range of significant coherence (an indicator of neuronal synchronicity) when PD patients were ON or OFF levodopa treatment. By means of simultaneous LFP recordings from the GPi and STN in awake PD patients, they showed that without dopamine medication, the power (predominant frequency) and the coherence between these nuclei was dominated by an oscillatory activity in the beta band of ~15-30 Hz. Treatment with the dopamine precursor, levodopa, reduced the synchronization at beta band and resulted in a new peak at ~70 Hz in the gamma band (Brown *et al.*, 2001). Similar observation of enhanced beta synchronicity in GPi and STN in PD patients has been observed in other studies (Marceglia *et al.*, 2006; Weinberger *et al.*, 2006; Ray *et al.*, 2008; Degos *et al.*, 2009). The presence of prominent LFPs oscillations at beta frequency in STN and GPe nuclei, has been consistently confirmed in several other studies (Bevan *et al.*, 2002; Mallet *et al.*, 2008a; Mallet *et al.*, 2008b; Holgado *et al.*, 2010) and has been described in most BG circuits nodes, including frontal cortex (Mallet et al., 2008a,b), dorsal striatum (Moran et al. 2011), SNr (Avila et al., 2010), STN and GPe (Mallet et al., 2008a,b). In summary, animal models with severe toxin-

induced parkinsonism, as well as PD patients, show enhanced beta band oscillations and coherent beta activity between the basal ganglia and cortex, which can be reversed by dopaminergic therapy (Brown, 2006). Of key importance are also observations of the effect of DBS in PD patients. Although DBS mechanism of action remains unclear, it is possible that DBS suppresses the synchronization of BG neurons at beta frequencies. To explore this, Eusebio and colleagues (2011) recorded from DBS electrodes implanted in the STN in PD patients during simultaneous stimulation (frequency 130 Hz) of the same target using a specially designed amplifier. The authors found that DBS progressively suppressed peaks in local field potential activity at frequencies between 11 and 30 Hz concluding that beta suppression by means of DBS is clinically effective (Eusebio *et al.*, 2011).

1.7.5 Beta-frequency synchronization of neuronal activity and relation to movement

One of the primary hypotheses regarding the functional importance of enhanced synchronization in the beta band, and, as supported by studies of dopamine replacement and DBS therapy, is that excessive beta oscillations have an antikinetic role and inhibit movement (Berns & Sejnowski, 1998). One of the earliest investigations in support of this idea comes from the report of Cassidy and colleagues (2002) who recorded simultaneously the LFPs in STN and GPi during voluntary movement in awake PD patients following neurosurgery for PD. Off dopaminergic medication, the power within STN and the coherence between STN and GPi were dominated by activity with a frequency of ~ 30 Hz. Interestingly, during movement this coupling was attenuated. Likewise after the administration of

dopaminergic medication, beta frequency was dramatically reduced and gamma frequency oscillations appeared and increased with movement (Cassidy *et al.*, 2002). Since then, numerous treatment-induced suppression of the aberrant activity in the beta band in the STN and both GP nuclei, has been repeatedly shown to correlate with motor behaviour (Kuhn *et al.*, 2006; Ray *et al.*, 2008; Kuhn *et al.*, 2009; Eusebio *et al.*, 2011). Enhanced beta band activity also prevalent in cortical motor areas and manifest during steady contractions and it is attenuated prior to or during voluntary movement and greatest during holding periods following movement (Engel & Fries, 2010). Conversely, during the preparation and execution of movement or when on anti-parkinsonian medication, beta activity is replaced by faster rhythms in the gamma-band (Engel & Fries, 2010). Because aberrant beta band activity is prominent at rest and disappears during voluntary movement, it has been suggested that it may correspond to an 'idling rhythm' in the motor system, perhaps indicating a pathological resting state that motor circuits cannot overcome (Pfurtscheller *et al.*, 1996). Indeed one recent hypothesis suggests that (Brittain & Brown, 2014) oscillations in the beta band are enhanced to such extent in PD that voluntary movements are not generated because the motor command for initiation cannot override the enhanced oscillatory state of BG, leading to the poverty of movement characteristic of the disease. According to this theory, therapeutic DBS and dopaminergic therapy act by decreasing the excessive synchronization in beta band and inhibiting and preventing competing motor programs (Jenkinson & Brown, 2011; Brittain & Brown, 2014). To better understand the relationship between motor processing and beta suppression, Kuhn and colleagues (2004) compared the suppression of beta following warning cues in a reaction time task in PD patients. The key finding of this investigation was that the reduction of beta activity is linked

specifically to the facilitation of subsequent movement, and from this it can be reasoned that an increase of power might be predicted when a pre-prepared movement requires cancellation (Kuhn *et al.*, 2004). In summary, BG LFPs activity in the beta band is suppressed prior to and during voluntary movement as well as following behaviourally relevant stimuli such as cues warning that movement is needed. This raises the possibility that in order to perform a task, a motor area has to actively antagonise synchronization in the beta band. If so, rather than reflecting a mere idling state or lack of movement, beta band could work as an active process that works to promote existing motor tasks while counteracting neuronal processing related to new movements (Gilbertson *et al.*, 2005; Androulidakis *et al.*, 2006; Androulidakis *et al.*, 2007; Pogosyan *et al.*, 2009). According to this idea, when voluntary movement is generated by a cortical motor area, the BG network acts to inhibit competing motor programs that would otherwise interfere with the desired movement. In conclusion, BG have a tendency to engage in oscillatory activities, but these oscillations are enhanced in pathological condition such as Parkinson's disease.

1.7.6 Origin of excessive beta oscillations in Parkinson's disease

It is important to understand how and where excessive beta oscillations are generated in basal ganglia-thalamocortical circuits. Evidence in humans and animal models suggests that beta activity is present in every node of the BG circuit (Brown, 2006). Many mechanisms for the generation of beta are favoured, including oscillatory feedback circuits between the STN and GPe or GPi, or between the basal ganglia and the thalamocortical network. In the past, significant attention was given

to GPe and STN neurons, in part because it had been shown to produce spontaneous slow (< 1Hz) synchronized oscillatory bursts in an *in vitro* model (Plenz & Kital, 1999). Because of that, it has been argued that, in an intact brain, these nuclei could underlie the generation of faster and potentially aberrant beta oscillations. However a recent study in a mouse slice preparation in which connections between STN and the globus pallidus were partly maintained, failed to show coherent activity in the two nuclei, suggesting that mechanisms extrinsic to the GPe–STN network may be important for the production of synchronized bursting (Loucif *et al.*, 2005). By means of LFP recording in human PD patients, evidence indicates that the prominent synchrony in STN could be transmitted to the GPi and driving the output nuclei in a synchronous manner (Brown *et al.*, 2004). Direct and single unit recording has not yet been performed and further investigations are required. Even the contribution of thalamic inputs has not been explored in detail. Indeed inputs arising from the intralaminar nuclei or from the thalamic ventral anterior and ventro lateral nuclei may be important (Gatev *et al.*, 2006). Due to its strong connection to the BG, the cortex has also been considered as driving force for excessive oscillations because its oscillations involves the entire basal ganglia-thalamocortical system, particularly the STN (Alexander *et al.*, 1986; Kelly & Strick, 2004). In an attempt to test the putative role of initiator of beta oscillations, Nambu and Tachibana (2014) selectively and pharmacologically inactivated BG nuclei in a MPTP-treated monkey model of PD. They found that (1) inactivation of the STN by muscimol (GABA receptor agonist) injection ameliorated Parkinsonian symptoms and suppressed GPi oscillations; (2) the blockade of glutamatergic inputs to the STN by local injection of a mixture of NMDA and AMPA receptor antagonists suppressed neuronal oscillations in the STN; and (3) STN oscillations were also attenuated by

the blockade of GABAergic neurotransmission from the GPe to the STN by muscimol inactivation of the GPe. These results suggest that cortical inputs to the STN and reciprocal GPe-STN interconnections are both important for the generation and amplification of the oscillatory activity of GPe and STN neurons in the parkinsonian state. Such oscillatory activity is subsequently transmitted to GPi neurons, and finally reaches the thalamus, cortex and brain stem, contributing to motor symptoms (Nambu & Tachibana, 2014). With respect to the activity of MSNs in Parkinsonism, the only evidence of enhanced beta activity comes from computational and LFPs studies (McCarthy *et al.*, 2011; Moran *et al.*, 2011; Nevado-Holgado *et al.*, 2014) and therefore the specific cell-type contribution in the generation and propagation of beta activity is still not clear. Certainly, however, striatal neurons have many of the canonical features required to generate and disseminate, to the downstream network, this kind of excessively synchronized activity. First, MSNs are highly and recurrently connected and this in turn is necessary to establish neuronal network groups, whose synchronized activity is seen during deep state of anaesthesia (Grillner, 2006). In support of this view comes from a recent work showing that the blockade of MSNs abolishes the reverberation of network beta-state in striatum (Carrillo-Reid *et al.*, 2008). Second, a fraction of striatal population is composed of interneurons that possess strong feed-forward and feed-back network activities (Sporns *et al.*, 2002; Grillner, 2006). Because interneurons are modulated by dopamine, they are in the perfect position to aberrantly synchronize their activity with recipient MSNs (Carrillo-Reid *et al.*, 2008). Third, striatal interneurons are capable of active, tonic self-modulated pacemaker activity, such as excitatory ChAT+ (Grillner *et al.*, 2005) or inhibitory interneurons such as PV+ interneurons (Koos & Tepper, 1999; Berke *et al.*, 2004; Tepper *et al.*,

2010). If so, the reciprocal connection between overall striatal network might create sustained network activity, even at higher frequency.

1.8 Aims

Striatum is one of the major nuclei of the BG. It receives wide glutamatergic inputs from cortex and thalamus, as well as dopaminergic inputs from the midbrain. Its position in the BG circuit is critical in regulating the flow of cortical information to other basal ganglia nuclei. Indeed, direct and indirect pathway MSNs, by acting synergistically or in opposition, provide a balanced output back to cortical areas. In Parkinsonism, chronic loss of dopamine affects striatal physiology. Despite intensive studies of the anatomical and functional organization of BG and the large amount of data gathered on the pathophysiology of PD, many of the mechanisms governing information processing within the striatum remain obscure. Similarly, the role of direct and indirect MSNs is crucial for information processing, but their functions in pathological condition, such as PD, remain largely undefined. Previous evidence from mathematical models and LFP studies suggest pathological changes in striatal neuron firing rate and in pattern in PD (McCarthy *et al.*, 2011; Moran *et al.*, 2011) but these studies have not accounted for the complex intrinsic organization and cellular heterogeneity of striatum. As such, the specific *in vivo* contributions of neurochemically-distinct striatal cell types to aberrant oscillations in the Parkinsonian brain are unknown**.** These important issues need to be addressed in order to gain a better understanding of the functions of striatum in health and disease.

The overall objective of this thesis research was to elucidate how chronic loss of dopamine alters the activity of direct and indirect pathway neurons of striatum. Two complementary studies were performed (see Chapters 3 and 4), with the following specific aims in mind:

- To define the brain state-dependent activity of direct pathway MSNs and indirect pathway MSNs in the dopamine-intact brain.
- To investigative how chronic dopamine loss affects the activity of striatal MSNs *in vivo.*
- To elucidate the cell-type specific contribution of striatal neurons to excessive beta oscillations in PD.

CHAPTER 2

Materials and Methods

All experimental procedures were performed on adult male Sprague Dawley rats (Charles River, Margate, UK) and were conducted in accordance with Animals (Scientific Procedures) Act, 1986 (United Kingdom). Rats were group housed and maintained on a 12/12 h light/dark cycle, with access to food and water *ad libitum*.

2.1 Surgical protocol and procedures for in vivo electrophysiology

All *in vivo* electrophysiological recordings were performed in animals under general anaesthesia. Anaesthesia was induced with 4% v/v isoflurane (Isoflo; Schering-Plough, Welwyn garden City, UK) in O_2, and maintained with urethane (1.3 g/kg, i.p.; ethyl carbamate; Sigma, Poole, UK) and supplemental doses of ketamine (30 mg/kg, i.p.; Ketaset; Willows Francis, Crawley, UK) and xylazine (3 mg/kg, i.p.; Rompun; Bayer, Leverkusen, Germany) as described previously (Magill *et al.*, 2006b). All wound margins were infiltrated with the local anaesthetic, bupivacaine (0.75% w/v; Astra, Kings Langley, UK). Animals were then placed in a stereotaxic frame (Kopf, Tujunga, CA). Body temperature was maintained at 37 ± 0.5° using

homoeothermic heating device (Harvard Apparatus, Edenbridge, UK). Anaesthesia levels were assessed by examination of the electrocorticograms (ECoGs, see section 2.2), and by testing reflexes to a cutaneous pinch or to gentle corneal stimulation. ECoG activity and respiration rate were monitored constantly to ensure animals' well-being (Magill *et al.*, 2006b). A small craniotomy (4mm²) was made directly above the dorsolateral striatum (0.6 mm anterior and 3.0 mm lateral of bregma; Paxinos & Watson, 2007) with a hand-held dental drill (Bracon Ltd., Hurst Green, UK) and the dura mater was carefully removed. Saline solution (0.9% w/v NaCl) was applied to all areas of exposed cortex to prevent dehydration.

2.2 Electrocorticogram and cortical activity

Ongoing states of activity in the motor cortex was assessed using an electrocorticogram. The ECoG is an invasive analogue of the electroencephalogram (EEG) in which the signal is measured on or below the dura and where the noise and filtering effects created by the skull are radically reduced. The ECoG measures the activity of a population of neurons as fluxes in electrical field potential as a function of time (Magill *et al.*, 2004; Sharott *et al.*, 2005b). In all *in vivo* experiments, the ECoG was recorded via 1-mm-diameter steel screw juxtaposed to the dura mater above the right frontal (somatic sensory-motor) cortex (4.5 mm anterior and 2.0 mm lateral of bregma; Paxinos and Watson, 2007), and was referenced against another screw implanted in the skull above the ipsilateral cerebellar cortex. ECoG was recorded from frontal (motor) cortical areas because these regions are the most relevant to the study of excitatory inputs to dorsolateral 'motor' striatum. Defining

how the firing of striatal neurons is related to ongoing cortical activity is important in understanding their function and dysfunction. Thus, the firing of striatal neurons was recorded under urethane/ketamine and xylazine anaesthesia during two distinct, spontaneous brain states as defined in ECoGs: (1) slow-wave activity (SWA); Figure 2.1), which is similar to activity observed during natural non-rapid eye movement sleep and drowsiness; and (2) “cortical activation” (ACT, Figure 2.1), which contains patterns of activity that are more analogous to those observed during the alert, behaving state (Steriade, 2000). In frontal ECoGs, SWA is characterized by a slow (~1 Hz) oscillation of large amplitude (~0.5 mV). Higher-frequency, lower-amplitude activity, including spindle oscillations, was often superimposed on slow oscillations (Steriade, 2000). In contrast to SWA, the activated brain state contains predominantly lower-amplitude, higher-frequency (>10 Hz) oscillations. Although neuronal activity patterns present under this anaesthetic regimen are only qualitatively similar to those present in the unanaesthetised brain, it is still useful for assessing the impact of extremes of brain state on functional connectivity within and between the cortex and basal ganglia (Magill *et al.*, 2006b; Mallet *et al.*, 2008a; Mallet *et al.*, 2008b). Raw ECoG was bandpass filtered (0.3-1500 Hz, - 3 dB limits) and amplified (2000X; DPA-2FS filter/amplifier; npi electronic) before acquisition.

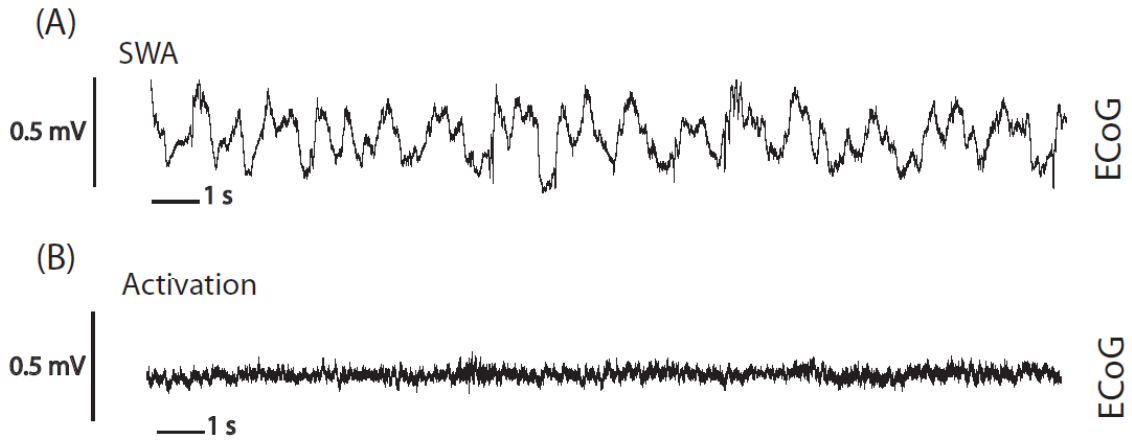

Figure 2.1 **Two spontaneous brain states recorded under urethane anaesthesia**. ***A,*** Frontal electrocorticogram (ECoG) showing typical slow-wave activity (SWA). Note large amplitude, slow (~1 Hz) oscillations. ***B,*** Frontal ECoG showing typical activated brain state

2.3 Extracellular recordings of single units

The suprathreshold activity of individual striatal neurons ('units') was monitored by extracellular recordings of action potential ("spike") trains. Electrodes for extracellular recordings were made from borosilicate glass capillary tubes (Harvard Apparatus Ltd, Firocroft way, Edenbridge, Kent. GC120F- 10, 1.2 mm O.D x 0.69 mm I.D.) using a vertical puller unit (Tokyo; PE-2 N8702). Electrodes were broken back under a microscope to an external tip diameter of ~1.5 µm and filled with 0.5 M NaCl solution containing 1.5% w/v of the tracer substance neurobiotin™ (Vector Laboratories). Electrodes with a resistance of 15-25 MΩ *in situ* were selected and then lowered into the dorsal striatum under stereotaxic guidance using a computer-controlled stepper motor (IVM-1000; Scientifica) that allowed the electrode depth to be determined with a resolution of 0.1 µm. Electrode signals were amplified (10X)

through the bridge circuitry of an Axoprobe-1A amplifier (Molecular Devices), AC-coupled, amplified another 100X, and bandpass filtered at 300–5000 Hz (DPA-2FS filter/ amplifier) before acquisition. The ECoG and single-unit activity were each sampled at 16 kHz using a Power1401 Analog-Digital converter and a PC running Spike2 acquisition and analysis software (Version 7.2; Cambridge Electronic Design). Spikes of single units were often several millivolts in amplitude and the recording of spontaneous activity generally lasted for 5- 15 min. Lastly, to overcome electrical interference originating from the power supply, that has a frequency of 50 Hz in Europe, we used HumBug™ units which constructs a real-time replica signal of the mains noise and continuously subtracts it from the input signal. This has the advantage of only removing noise elements of the signal, leaving physiological activity around these frequencies intact, without causing signal distortion.

2.3.1 Juxtacellular labelling of single neurons

Following electrophysiological characterization of single striatal neurons, they were juxtacellularly labelled with neurobiotin, to identify their location, morphological characteristics and molecular profile (Pinault, 1996). The electrode tip was advanced into a “juxtamembranous” position as identified by an increase in background noise and large (> 3mV) spikes (Pinault, 1996). Once in position, microiontophoretic current pulses (1-10 nA anodal current, 200ms duration, 50% duty cycle) were applied, which then deliver the tracer contained in the electrode to the neuron. The optimal position of the electrode for the labelling was identified when the firing pattern of the neuron was robustly modulated by the microiontophoretic current pulses. On average, neurons were labelled for ~ 10-15

min. Once the tracer substance neurobiotin is inside the neuron, it is anterogradely transported into dendritic and axonal process at ~1 mm per hour (Kita & Armstrong, 1991). In these experiments the neurobiotin was then left to transport along neuronal processes for up to 5 h. After the recording and labelling sessions, the animals were given a lethal dose of ketamine (150 mg/kg) and perfused via the ascending aorta with ~100 ml of 0.01 M phosphate buffered saline (PBS) at pH 7.4, followed by 300 ml of 0.1% w/v glutaraldehyde and 4% w/v paraformaldehyde in 0.1 M phosphate buffer, pH 7.4, and then by 200 ml 4% w/v paraformaldehyde in 0.1 M phosphate buffer. Brains were then left in fixative solution at 4°C for <12 h and then in PBS until they were sectioned 24–72 h later.

2.4 Electrical stimulation of the motor cortex

Parallel, bipolar tungsten stimulating electrodes (constructed from nylon-coated stainless steel wires; California Fine Wire), with tip diameters of ~ 100 µm, a tip separation of ~150 µm, and an impedance of ~ 10 kΩ, were implanted in two regions of the motor cortex (3 mm and 1 mm anterior to bregma, and 2.6 mm and 2.8 mm lateral to the medial line respectively; ~2.0 mm below the cortical surface). Paired electrical stimuli (800 µA, pairs [100 ms interval] delivered to the cortex every 2 seconds) were applied while searching for and recording striatal neuron activity (Mallet *et al.*, 2005; Mallet *et al.*, 2006). Responsive neurons were juxtacellularly labelled and processed for anatomical identification (see section 2.7.1). In the case of 6-OHDA lesioned animals (see section 2.6), stimulating electrodes were place in the cortex, ipsilateral to the lesion. First spikes in each stimulus trial was used to measure the response latency. Neurons were considered to respond significantly if

20% of first spikes after the stimulus were fired in a response window of 1.5 – 20 ms. The mean latencies of the first spikes in a given time window were compared using a Mann–Whitney U test or Wilcoxon signed-rank test as appropriate. The same short-latency analysis windows were also used for both paired-pulse and high-frequency train stimulation. For paired-pulse stimulation, latencies and firing probabilities across the first and second pulse were compared using Wilcoxon signed-rank tests as long as there were ~5 spikes in this window in response to both pulses.

2.5 Extracellular recording of populations of neurons

Simultaneous extracellular recordings of the spiking activity of striatal neurons were made using "silicon probes" (NeuroNexus Technologies, Ann Arbor, MI). The probes had 16 recording contacts arranged in a single vertical plane, with a contact separation of 100 μm. Each contact had an impendance of 0.9 -1.3 MΩ (measured at 1000 Hz) and an area of ~ 400 μm^2 (Magill *et al.*, 2006a). The probe was manually advanced into the dorsal striatum under stereotaxic control (0.6 mm anterior and 3.0 mm lateral of bregma) (Paxinos and Watson, 2007). On average, 4 penetrations of striatum were made with the same probe during each experiment. Typically, recordings were made (for ~ 20 min) at just one depth (relative to the cortical surface) during each penetration. On average, action potentials could be readily observed on 10 out of 16 probe contacts; small movements of the probe (<10 µm) were occasionally made during the course of a recording to optimise the signals on some contacts. The same probe was used throughout the series of experiments, but it was cleaned after each experiment in proteolytic enzyme solution (Magill *et*

al., 2006a). This was sufficient to ensure that contact impedances and recording performance were not altered by probe use and reuse. Monopolar probe signals were recorded using high-impedance operational amplifiers (Advanced LinCMOS; Texas Instruments, Dallas, TX) and were referenced against a screw implanted above the contralateral cerebellum. After initial preamplification (x1), extracellular signals were further amplified (x1000) and low-pass filtered at 6000 Hz using programmable differential amplifiers (Lynx-8; Neuralynx, Tucson, AZ). The ECoG and probe signals were each sampled at 16 kHz using a Power1401 Analog-Digital converter and a PC running Spike2 acquisition and analysis software (Cambridge Electronic Design). Finally, all recording locations were verified after the experiments using standard histological procedures. After the recording sessions, animals were sacrificed with lethal dose of anaesthetic and transcardially perfused with fixative as described above.

2.6 6-Hydroxydopamine lesions of dopamine neurons

The primary hallmark of Parkinson's disease is the progressive loss of dopaminergic neurones within the SNc which is responsible for the cardinal motor symptoms of this disease (Braak *et al.*, 2005; Braak & Del Tredici, 2008). Thus, to investigate how striatal function is altered in Parkinson's disease, midbrain dopaminergic neurons were lesioned by unilateral intracerebral injection of the neurotoxin, 6-hydroxydopamine (6-OHDA). Being molecularly and structurally similar to dopamine, 6-OHDA shows high affinity for the dopamine transporter, which carries the toxin inside the dopaminergic neurons. Once in the neuron, 6-OHDA accumulates in the cytosol and undergoes auto-oxidation, promoting free radical

formation. This in turn stresses neurons such that they no longer exert their normal physiological functions and, eventually, die (Blum *et al.*, 2001). This loss of dopaminergic neurons is maximal within 12-14 days after 6-OHDA injection, and is apparently maintained *ad infinitum* (Schwarting & Huston, 1996a; b). Lesions of midbrain dopaminergic neurons will lead to reductions in dopamine in some or all of the brain regions that are usually innervated by these cells, including the striatum (dorsal and ventral), GPe, EPN, STN, neocortex and hippocampus. The neurotoxin injections were made near the medial forebrain bundle (MFB), the area where the axons of dopaminergic neurons of the SNc and VTA collect together and run towards the striatum (Deumens *et al.*, 2002). Twenty-five min before the injection of 6-OHDA, all animals received a bolus of desipramine (25 mg/kg, i.p.; Sigma) to minimize the uptake of 6-OHDA by noradrenergic neurons (Breese & Traylor, 1971; Schwarting & Huston, 1996a) ; note, however, that it is not possible to rule out that some noradrenergic neurons were still affected by the 6-OHDA injections. Anaesthesia was induced and maintained with isoflurane (Isoflo, Schering-Plough) (4% v/v for induction, 2% v/v or 3% v/v for maintenance) in O_2. Experimental procedures were performed on young adult male Sprague Dawley rats (180-200 g) (Charles River, Margate, UK). Animals were placed in a stereotaxic frame (Kopf Instruments) and body temperature was maintained at 37 ± 0.5 °C with the use of a homeothermic heating device (Harvard Apparatus). Anaesthesia level were assessed by testing reflexes to a cutaneous pinch or to gentle corneal stimulations. The rate and depth of respiration was also constantly monitored to ensure animals' well-being. The 6-OHDA (hydrochloride salt; Sigma) was dissolved immediately before use in ice cold 1.2% w/v NaCl solution containing 0.02% w/v ascorbate to a final concentration of 12 mg/ml. Then, under stereotaxic guidance, 1 µl of 6-OHDA

solution was injected into the region adjacent to the medial forebrain bundle (4.1 mm posterior and 1.4 mm lateral of bregma, and 7.9 mm ventral to the dura) (Paxinos and Watson, 2007) using a graduated glass micropipette (Blaubrand® intraMARK, 708707). Following injections of 6-OHDA, the pipette was left in place for 1 min and then slowly withdrawn. The scalp incision wounds were then sutured (5/0 coated Vicryl, Ethicon™, Johnson and Johnson Intl., Brussel, Belgium) and bonded with tissue adhesive (Vetbond, 3M), and the animal was then removed from the stereotaxic frame. Animals received a dose of long-lasting analgesic, buprenorphine (30 μgkg-¹, s.c.; Vetergesic™, Reckitt and Coleman Products Ltd., Hull, UK) before being returned to cages, and for the three consecutive days of recovery after the surgery. Subcutaneous injections of saline solution were also given as necessary to prevent dehydration.

2.6.1 Assessment of the efficacy of 6-OHDA lesions

Because unilateral lesion of the MFB causes a dopaminergic imbalance between the two hemispheres, the extent of the dopamine loss was assessed 14 days after 6-OHDA injection by challenge with apomorphine (0.05 mg/kg, s.c.; Sigma) (Schwarting & Huston, 1996b) a dopamine receptor agonist. When challenged with apomorphine, 6-OHDA animals display active rotational behaviour (Ungerstedt, 1968), away from the lesioned side (Ungerstedt, 1971). The lesioning procedure was considered successful in those animals that made at least 80 contraversive rotations in 20 min. This number of rotations is indicative of a loss of greater that 90% of dopamine content from the ipsilateral striatum, with a concomitant depletion of greater that 50% of dopamine content in the corresponding SNc (Hudson *et al.*,

1993). Nearly 60% of rats receiving 6-OHDA injections achieved the criterion in the rotation test. The reason(s) for some rats failing to reach this criterion are unclear. However, suboptimal delivery of the toxin (arising, for example, from animal-to-animal variation in the accuracy of stereotaxic coordinates) and thence, only a minor loss of dopamine, are a likely explanation. Electrophysiological recordings were performed ipsilateral to 6-OHDA lesions at 4 weeks after surgery (on average), when pathophysiological changes in the basal ganglia are likely to have levelled out near their maxima (at ~2 weeks)) (Vila *et al.*, 2000) and when the apomorphine was fully metabolized (after ~1 week).

2.7 Histochemistry and immunocytochemistry

2.7.1 Histochemical identification of juxtacellularly-labelled neurons

Parasagittal sections (50 µm) were cut from each brain using a vibrating microtome (VT1000S; Leica), collected in series and washed in PBS. Free-floating sections were then incubated overnight at room temperature in 'Triton PBS' (PBS containing 0.3% v/v Triton X-100 [Sigma]) containing Cy3-conjugated streptavidin (1:3000 dilution; Life Technologies). Sections were examined with Carl Zeiss AxioVision M.2 microscope and those containing neurobiotin-labelled neuronal somata (identified by the Cy3) were then isolated for molecular characterization by immunofluorescence. Those labelled neurons with medium-sized cell body (~15 µm) and densely-spiny secondary and higher-order dendrites were classified as MSNs and were thus tested for the expression of preproenkephalin (PPE;

encephalin precursor expressed by indirect pathway MSNs). Briefly, sections containing neurobiotin-labelled MSN somata were incubated overnight at room temperature in Triton PBS containing 1% v/v normal donkey serum (NDS; Jackson ImmunoResearch) and rabbit anti-preproenkephalin (PPE; 1:5000 dilution; Lifespan, Ls-C23084,). To optimize immunolabelling for PPE in projection neurons, a heat pre-treatment (Citrate Buffer pH 6, 1h at 80 °C) was used as a means of antigen retrieval (Jiao *et al.*, 1999). After exposure to primary antibodies, sections were washed in PBS and incubated overnight at room temperature in Triton PBS containing AlexaFluor 488 (1:500; Life Technologies A13201). In some cases, MSNs were localized to patch/matrix by revealing with high affinity to MOR immunolabeling (goat anti-MOR, 1:300 dilution; Santa Cruz, SC-7488. Aspiny neurons were tested for expression of parvalbumin (guinea pig anti-PV 1:1000; Synaptic Systems, 195004), choline acetyltransferase (ChAT; goat anti-ChAT 1:500; Millipore, AB144P), nitric oxidase synthase (mouse anti-NOS 1:500; Sigma, N2280) and/or calretinin (rabbit anti-CR 1:1000; Synaptic Systems, 214-102) to define interneuron identity. After washing in PBS, sections were mounted on glass slides in Vectashield (Vector), coverslipped, and viewed in a laser-scanning confocal microscope (Zeiss LSM 710). For neurochemical characterization, single-plane confocal images were acquired using a 1 µm optical section and a 40x objective lens. A neuron was classified as not expressing the tested molecular marker only when positive immunoreactivity could be observed in other cells on the same focal plane as the tested neuron. Occasionally, multiple-plane images were taken, and *z*-stack montages created, to better highlight the somatodendritic structure of labelled neurons.

2.7.2 Identification of the location of labelled neurons

The distributions of identified striatal neurons in the dorsal striatum of dopamine-intact and 6-OHDA-lesioned animals were mapped on to representative parasagittal sections of striatum that were defined according to a standard rat brain atlas (Paxinos and Watson, 2007): Sections containing neurobiotin-labelled neuronal somata (identified by the CY3) were first isolated and examined on an epifluorescence microscope (AxioVision M.2 microscope; Carl Zeiss), and then the location of each neuron was visually registered to one of six parasagittal sections that ranged from 1.55 mm to 3.70 mm lateral to Bregma (Paxinos and Watson, 2007).

2.7.3 Verification of the locations of the silicon probes

Recording locations were histologically verified in two animals. Before recording in these animals, the silicon probe was evenly coated with the red fluorescent dye, 1,1-dioctadecyl-3,3,3,3-tetramethylindocarbocyanine perchlorate (DiI) (Invitrogen, Carlsbad, CA), by immersion of the probe in a 100 mg/ml DiI solution (in 50:50 acetone:methanol) under microscopic control. No differences in recording quality (signal-to-noise ratio) or neuronal activity were observed when the probe was coated with DiI, in agreement with the findings of others (Blanche *et al.*, 2005; Magill *et al.*, 2006b). Because DiI is nontoxic to neurons and highly lipophylic, it is taken up into cell membranes and white matter tracts when the probe is *in situ*. Parasagittal sections (50 µm) were cut from each brain using a vibrating microtome (VT1000S; Leica), collected in series, washed in PBS and viewed on a light microscope using a 10X objective. Probe locations were indicated by discrete

red/pink staining of the tissue (Figure 3.2). Images of sections were captured using a laser-scanning confocal microscope (Zeiss LSM 710).

2.8 Data analysis

2.8.1 Analysis of single unit and multiunit activity

Putative single unit activity was extracted with standard “spike-sorting” procedures (Mallet *et al.*, 2008a), including template matching, principal component analysis, and supervised clustering (Spike2). Isolation of a single unit was verified by the presence of a distinct refractory period in the interspike interval (ISI) histogram. For further analysis, single-unit activity was converted so that each spike was represented by a single digital event (Spike2). Each single unit was considered as an independent sample, even though (by virtue of using silicon probes) several units were necessarily recorded at the same time from the same animal. All data analyses were performed using MATLAB (MathWorks) and associated toolboxes. Mean firing rate (spikes/s) was calculated from the total number of spikes per data epoch. To evaluate the regularity of units firing, I analysed the distribution of the intervals between two subsequent spikes and then the coefficient of variation of the ISI was calculated (CV2; the lower the CV value, the more regular the unit activity (Holt *et al.*, 1996; Schulz *et al.*, 2011). Statistical comparisons of spontaneous firing properties were performed using a nonparametric Kruskal–Wallis ANOVA on ranks, followed by Dunn’s test for post hoc definition of significant pairwise differences, or by using Mann–Whitney U Tests, as appropriate. The significance level for these statistical tests was taken to be $p < 0.05$. All box plots in figures show the medians,

the interquartile ranges (box), and extremes of the range (whiskers, within 99% of the distribution).

In addition to the analysis of single units, I constructed a multi-unit activity (MUA) from the background activity or “hash” of every silicon probe contact. MUA and LFP as well are extracellularly recorded signals from local network of neurons. The LFP, the low frequency (<500 Hz) content of the raw recording, is believed to be generated by membrane currents of the neurons in the local neighbourhood of the recording electrode. MUA, the high frequency (> 1000 Hz) portion of the recording represents the spiking of an indiscriminate number of local neurons around the recording contact (Bullock, 1997) and has been successfully used to estimate the population activity of STN neurons (Moran & Bar-Gad, 2010). This signal has the potential to be particularly advantageous to detect population level activities (such as oscillations) in structures like the striatum, where single neurons fire at low rates. As in Moran *&* Bar-Gad (2010), I removed large single unit activities in the raw high-passed unit signal and replaced them with background noise. Specifically, large action potentials were detected as events that were over 4 times the standard deviation of the high pass filtered unit signal. The signal 1ms before and 2ms after the peak of the action potential was then replaced by a randomly selected section of 3ms of data from elsewhere in the recording (that did not contain an action potential). Following this process, signal was down-sampled to 2048 Hz and the rectified signal was used for further analysis.

2.8.2 Phase locking analysis and circular statistics

To investigate how the activity of individual striatal neurons varied in time with respect to ongoing cortical network activity, I analysed the instantaneous phase relationships between striatal spike times and cortical oscillations in specific frequency bands. After recordings experiments ECoG and single-unit activity were each sampled at 16 kHz using a Power1401 Analog-Digital converter and a PC running Spike2 acquisition and analysis software (Version 7.2; Cambridge Electronic Design). Artifact-free data were visually inspected and epochs of robust spontaneous SWA or spontaneous cortical activation were first identified in ECoGs according to the previously described characteristics of these brain states (Magill *et al.*, 2001; Sharott *et al.*, 2012). Recording epochs for a given neuron were only included in group analyses when they had a minimum duration of 70 s for SWA and 60 s for cortical activation; the majority of epochs analysed were between 100 and 500 s. ECoG signals containing robust SWA were first filtered, using a band- pass filter (Butterworth filter, first order for SWA/second order for beta), to isolate slow (0.4–1.6 Hz) or beta (15–30 Hz) oscillations. Subsequently, the instantaneous phase and power of the ECoG in these frequency bands were separately calculated from the analytic signal obtained via the Hilbert transform (Lachaux *et al.*, 1999). In this formalism, peaks in the ECoG oscillations correspond to a phase of 0° and troughs to a phase of 180°. Linear phase histograms, circular phase plots, and circular statistical measures were calculated using the instantaneous phase values for each spike. Descriptive and inferential circular statistics were then calculated using the Circ Stat toolbox (Berens, 2009) for MATLAB. For the calculation of vector lengths and statistical comparisons, I included only those neurons that fired ≥40

spikes during the entire analysed epoch. These neurons were then tested for significantly phase-locked firing (defined as having $p<0.05$ in Rayleigh's uniformity test). For each of the neurons that were significantly phase locked, the mean phase angle was calculated. Differences in the mean phase angles of groups of neurons were tested for using the Watson–Williams F test ($p < 0.05$ for significance). The mean resultant vector length (referred to hereafter as simply vector length) of the phase distribution, bound between zero and one (the closer to one, the more concentrated the angles), was used to quantify the level of phase locking around the mean angle for individual neurons (computed using the angles of each spike) and for populations of neurons (computed using the mean angle for each neuron). The population vector lengths and mean angles for each cell type are shown as bold, black lines emanating from the centre of circular plots. Where data are displayed in circular plots, lines radiating from the centre are the vectors of the preferred phases of firing. The small open circles on the perimeter of each circular plot represent the preferred firing phase of each neuron.

2.8.3 Spectral analysis

ECoG is traditionally modelled as a series of sine waves of different frequencies overlapping in time and with different phase angles with respect to a stimulus. A sine wave is defined in terms of its frequency, its power and its phase. The frequency of a sine wave refers to the number of complete cycles or oscillations within 1 second time period and has a unit of Hertz (Hz = cycle per second). The power refers to the maximum height of the sine wave's peaks with respect to the x axis.

The phase refers to where specific time points fall within a cycle of the sine wave, ranging, from 0° to 360°. The most common way of evaluating oscillations is in the frequency domain by taking the Fourier transform (FFT) of the time series and using it to compute a frequency power spectrum. The result is a single power spectrum that captures the average power (or magnitude) of oscillations for individual frequency bins integrated over the entire time period analysed in a linear or logarithmic scale. Power spectra thus, indicate the power of each frequency component present in the source time domain waveform. Spectral parameters for both time series (ECoG and MUA) were evaluated using FFT as described in Halliday et al. (1995). ECoG and MUA were down sampled to 500 Hz and spectra were calculated with a FFT size of 2000 giving a frequency resolution of 0.25Hz. The same resolution was used for MUAs recorded during SWA, whereas spectra for recordings made during global activation were calculated using a frequency resolution of 1Hz (2048 sampling rate and FFT size). FFT windows overlapped by 50%. For some analysis of MUA, where the impedance of the probe contact could affect the absolute power, each individual power spectrum was normalised to "% total power". This was achieved by converting taking the power of each frequency bin as a percentage of the total power between 1 and 80 Hz, excluding the 49 – 51Hz range that contained mains noise in some recordings.

The most common method of looking at synchronisation between the spike trains of two neurons is the CCH which provides an estimation of the probability that neuron B will fire as a function of the time, before or since, a spike was fired by neuron A. The possible results of a CCH computed between two tonically firing neurons are shown in Figure 2.2. If the firing of the neuron A is not predictive of a spike in neuron B the CCH will be flat, reflecting the independent nature of the two

point processes. A sharp peak, displaced in relation to zero, indicates a possible monosynaptic connection between the two cells. If this is the case, the time interval from zero indicates the sum of the axon conduction and synaptic delay. A peak around zero in the CCH indicates that both cells are being driven from a common, third neuron at equal axonal and synaptic delays causing them to fire synchronously (Nowak & Bullier, 1998). Oscillatory activity in and between single neurons can also be detected using the correlation techniques described above. A CCH between two oscillatory cells which are synchronised at the same frequency will give a similar result, with the offset from zero reflecting a positive or negative phase difference between the two point processes. Although time domain measures can be used to detect and measure synchronisation, it is more common to analyse such signals in the frequency domain.

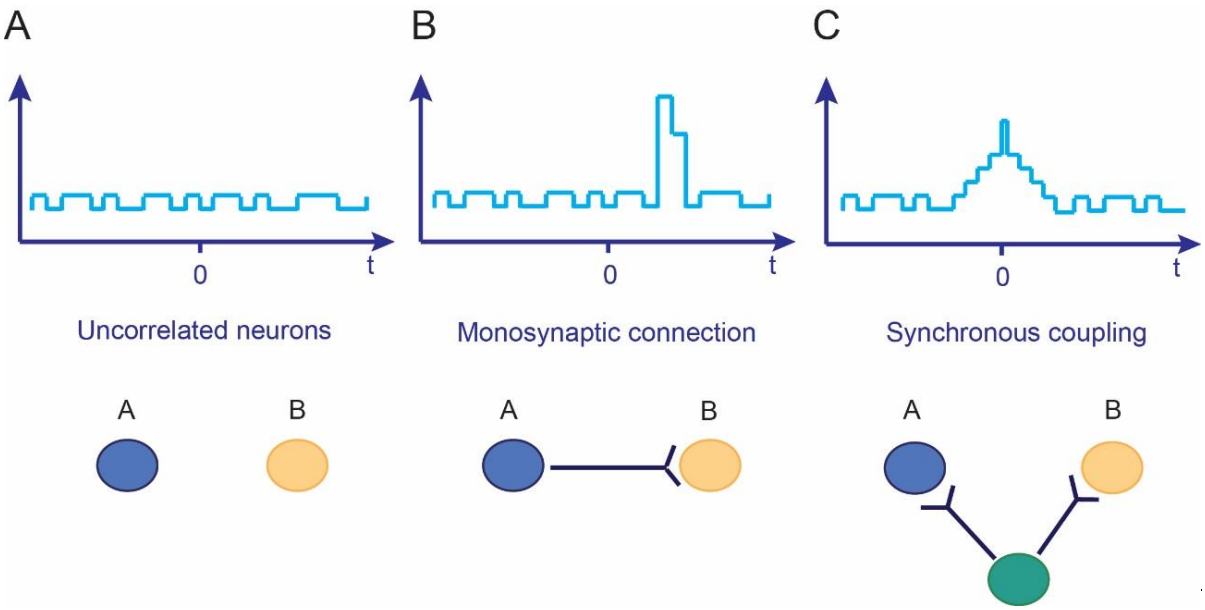

Figure 2.2 **Detecting neuronal synchronization.** Synchronisation between the firing patterns of single neurons is most commonly detected using the cross correlation histogram (CCH) ***A,*** A flat CCH indicates the firing of two neurons is completely independent ***B,*** A sharp peak indicates a monosynaptic connection between two neurons. The displacement of the peak from zero is equal to the sum of the axonal and synaptic delay. **C,** A broad peak around zero indicates that the two neurons are being driven by a common third neuron.

Raw cross correlations were calculated for every pair of sorted striatal single units recorded on a silicon probe using 5ms windows with 1s lag. The aim of the analysis was to detect pairs of spike trains where the number of coincidences and/or oscillatory properties where significantly different to those that would be predicted by the first order characteristics of the spike train (i.e. rate and interspike interval distribution). To this end, cross correlations were calculated using surrogate spike trains constructed by globally shuffling the interspike intervals of both neurons and calculating their cross correlation 100 times (Sharott *et al.,* 2009). This produced a null hypothesis distribution for each lag point. The real correlation was then

converted to a z-score (the number of standard deviations of the true correlation from the mean of the null hypothesis) that was used as a measure of the correlation strength, as it is dependent mainly on the temporal locking of the two spike trains. A cross correlation was considered significant at a given lag if it was outside two standard deviations of the null hypothesis and this criteria was used to construct significance histograms, which were used to investigate the likelihood of significant correlation between a specific pair type at a given lag. The oscillatory content of the cross correlation (CCH power) was evaluated by computing the FFT of the central 250ms (± 0.125s) of the z-scored cross correlation histogram. As the power was computed on the z-score, it therefore reflected oscillatory interaction that was not predicted by the primary spike train statistics. In order to give multiple windows for the FFT, for a given data set (e.g. putative PPE+ MSNs), 50% of the CCHs were selected at random and the FFT was calculated using non-overlapping windows. This procedure was repeated 1000 times to allow a mean and 99% confidence limits to be constructed for each group. Frequency bins at which these confidence limits did not overlap were considered significant. As the cross correlation histograms were often noisy, a multi-taper power spectral density estimate (Matlab function “pmtm”) was used to further smooth the spectral estimate. Confidence limits for zero-lag correlation versus distance plots were calculated in a similar manner by using half of the sample (1000 times) to create a distribution of percent significant zero-lag correlations at a given distance.

CHAPTER 3

In vivo electrophysiological activity of populations of striatal neurons in dopamine-intact and 6-OHDA-lesioned animals

3.1 Study background

The striatum is a key integrative structure in the circuitry of the basal ganglia. It receives excitatory inputs from the cortex and thalamus, and conveys information to the other nuclei of the basal ganglia via two main routes. The direct pathway MSNs monosynaptically convey information to the GPi and SNr, whereas the indirect pathway MSNs relay information to the GPe. Striatal projection neurons are differentially modulated by dopaminergic inputs from the SNc and VTA. Dopamine release in the striatum leads to the excitation of the direct pathway MSNs via activation of D1-receptors, and the inhibition of the indirect pathway MSNs via activation of D2-receptors. In PD, the dysfunction and loss of midbrain dopaminergic neurons is predicted to imbalance direct and indirect pathways, in favour of the latter (DeLong, 1990).The physiological alteration of identified direct and indirect pathway MSNs arising from chronic dopamine loss has been investigated at the level of single cells during SWA activity (Mallet *et al.*, 2006); this study shows a clear imbalance within the striatum, with some indirect pathway neurons displaying an

enhanced firing, whereas some direct pathway neurons are almost quiescent. However, little is known about how dopamine loss impacts on the spatiotemporal organization of population activity in striatum.

Excessive synchronization of neuronal population activity at beta frequencies (15-30 Hz) has been linked to the absence of dopaminergic receptor stimulation in PD and have been shown to emerge in the cortex and in many nuclei of the basal ganglia (Brown, 2006). With respect to the striatum, excessive beta oscillations have been detected in LFPs (Moran *et al.*, 2011). However, whether and how striatal neurons engage in suprathreshold (spiking) activity during these beta oscillations are unknown. This is a critical issue; if MSNs fire in time with beta oscillations (in cortex or striatum), then they could play a key role in the dissemination of these abnormal rhythms to other BG nuclei. Hence, the aims of this study (see Table 3A and Figure 3.1) were to: (1) evaluate differences in the firing rate and patterns of striatal neurons occurring after chronic loss of dopamine during different brain state conditions; and (2) to define whether the firing of striatal neurons is abnormally synchronized at beta frequencies in Parkinsonism. To address these, I simultaneously recorded single-unit and multiunit activity from multiple (up to 16) sites in the dorsal striatum of anaesthetized dopamine-intact or 6-OHDA-lesioned rats.

Animal group	DOPAMINE-INTACT		6-OHDA LESIONED	
Brain state	ACT	SWA	ACT	SWA

Table 3A **Study plan for the recording of populations of striatal neurons *in vivo***. Striatal population activity is recorded in two experimental groups: dopamine-intact and 6-OHDA-lesioned animals. Within each group, the aim is to record the activity of striatal neurons during two well-defined brain states defined by the ECoG (ACT, spontaneous activation; SWA, slow-wave activity).

3.2 Unilateral 6-hydroxydopamine-lesioned rat model of Parkinson's disease

Animal models of PD have been widely used to investigate the pathogenesis and pathophysiology of this neurodegenerative disorder. Indeed, most of our current knowledge of the cellular and network mechanisms underlying PD derives from studies of rodent models that are able to replicate many of the key phenotypic features of idiopatic PD including bradykinesia and akinesia (Schwarting & Huston, 1996a).

The neurotoxin 6-OHDA is a synthetic organic compound that is analogous in structure to dopamine and has a strong affinity for the dopamine transporter (DAT). Because 6-OHDA is unable to cross the blood brain barrier, local (intracerebral) injection of 6-OHDA is required to induce Parkinsonism. Although many brain sites are available for 6-OHDA injections, including striatum, the medial forebrain bundle is the preferred target when it is desirable to induce a degeneration of most (> 90%) midbrain dopaminergic neurons. This bundle conveys the efferent

fibres from nigral cell bodies to the striatum and other forebrain structures. When 6-OHDA is delivered in this location, and is taken up into dopaminergic neurons via DAT, profound retrograde dysfunction and degeneration start to occur within 12 h of injection (Schwarting & Huston, 1996a; b). Toxin injection is usually carried out unilaterally because of the high level of morbidity associated with bilateral injections. Because dopamine is the precursor of noradrenaline, a reasonable selectivity of 6-OHDA action for dopaminergic neurons is achieved by pre-treating rodents with desipramine, a noradrenaline transporter blocker that minimises 6-OHDA uptake into the noradrenergic neurons. The mechanism of toxic action of 6-OHDA is related to its oxidative properties: once inside the neuron, 6-OHDA accumulates in the cytosol and promotes the formation of free radicals that in turn disrupt cell metabolism. Unilateral lesions induced by 6-OHDA leads to typical sensorimotor asymmetries, which manifest as florid turning behaviour upon administration of apomorphine, a D1/D2 dopamine receptor agonist. If at least 80% of dopaminergic neurons are killed after 6-OHDA lesion (Hudson *et al.*, 1993), rats will rotate contralateral to (away from) the lesioned hemisphere: the rate of rotation correlates with the severity of the lesion.

3.3 Experimental procedures

Before the electrophysiology recording session, some animals underwent unilateral injection of 6-OHDA and an apomorphine rotation test to verify the extent of dopamine loss (see section 2.6). To ensure that the apomorphine used in the rotation test was fully metabolised/excreted before recordings, successfully lesioned animals were allowed to recover for one week before recording. Electrophysiological

recordings in dopamine-intact and 6-OHDA animals were carried out on male Sprague-Dawley rats (390-500g). Anaesthesia was induced with 4% isoflurane and maintained with urethane (1.3g/kg, i.p.) and supplemental doses of ketamine (30 mg/kg, i.p.) and xylazine (3 mg/kg, i.p.; see section 2.1). A multi-electrode array (or 'silicon probe') was evenly coated with a red fluorescent dye before the recording, and its location was verified after perfusion and fixation (Figure 3.2). The silicon probe was advanced into the striatum, in accordance with stereotaxic coordinates, to record activity of striatal neurons in control and 6-OHDA-lesioned animals during SWA and spontaneous cortical activation (see section 2.2). Simultaneous recordings of striatal neurons and ECoG were performed ipsilateral to the 6-OHDA lesion.

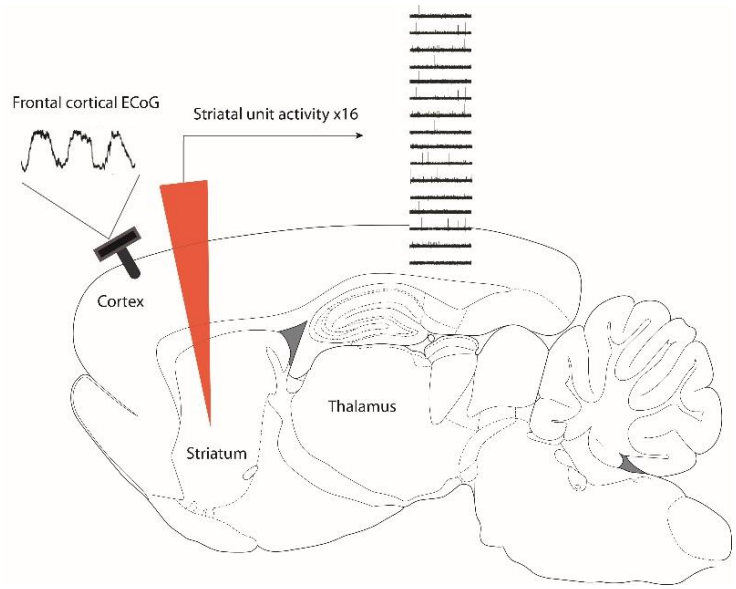

Figure 3.1 **Experimental design and set-up.** A parasagittal section of the rat brain (Paxinos and Watson, 2007). Activity of striatal neurons is recorded with a 16-channel silicon probe in anaesthetised rats (control and lesioned). Frontal cortical activity was simultaneously determined from the ipsilateral ECoG, which was registered through a screw juxtaposed to the dura mater.

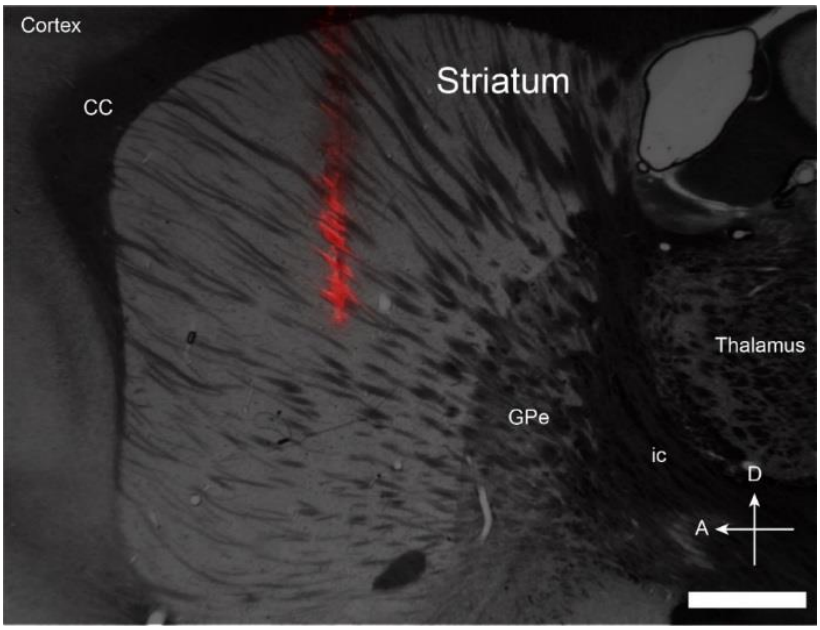

Figure 3.2 Verification of the location of the recording site of the silicon probe in dorsal striatum. Parasagittal section of rat brain showing the vertical distribution of DiI red marker in the striatum. Silicon probe tip was immersed in DiI solution prior to recording. Scale bar 1mm. (CC, corpus callosum; GPe, external segment of the globus pallidus; ic, internal capsule; D, dorsal; A, anterior).

3.3.1 Cortical input and brain state conditions for investigating striatal physiology

Because the cerebral cortex provides massive glutamatergic inputs to striatum, defining how the firing of striatal neurons is related to ongoing cortical activity is important to understand striatal function/dysfunction. Thus, the firing of striatal neurons in both dopamine-intact and 6-OHDA-lesioned rats was recorded under urethane anaesthesia during two distinct, spontaneous brain states, as defined in ECoGs: slow-wave activity (SWA) and cortical activation. During SWA, frontal ECoG is dominated by a slow (~1 Hz) oscillation of large amplitude (>400 μV). Higher-frequency, lower-amplitude activity, including spindle oscillations, is often

superimposed on slow oscillations (Steriade, 2000). In contrast to SWA, the activated state consists of predominantly low-amplitude (<100 μV), higher-frequency (>10 Hz) oscillations. Although neuronal activity patterns present under this anaesthetic regimen are only qualitatively similar to those present in the unanaesthetised brain, it is still useful for assessing the impact of extremes of brain state on functional connectivity within and between the cortex and basal ganglia (Magill *et al.*, 2006b; Mallet *et al.*, 2008a; Mallet *et al.*, 2008b). Importantly, the utility of urethane-anaesthetised (lesioned) rats for studying the emergence of pathological beta oscillations after dopamine loss has already been established (Mallet *et al.*, 2008a; Mallet *et al.*, 2008b).

3.4 Results

3.4.1 Firing rate and pattern of striatal neurons in dopamine-intact and 6-OHDA-lesioned rats during slow-wave activity

I recorded the spontaneous activity of 396 striatal neurons (single units) in control dopamine-intact rats (n = 8; n of cells 20-40, min-max) and 350 striatal neurons (single units) in 6-OHDA-lesioned rats (n = 8; n of cells 20-40, min-max) during SWA (Figure 3.3 A, B). In control animals, the majority of striatal neurons fired at low rates (~0.7 spike/s) and with irregular firing patterns: these units occasionally fired single spikes or bursts of 2 or 3 spikes around the peaks of the cortical slow oscillations (Figure 3.3 A). In lesioned animals, while some neurons were still nearly quiescent, many other neurons fired high-frequency bursts of spikes around the

peaks of the slow oscillation (Figure 3.3 B). The average firing rate of striatal neurons in lesioned animals (1.2 ± 0.08 spikes/s; mean ± SEM) was significantly higher than that of neurons in controls (0.78 ± 0.07 spikes/s, mean ± SEM; Mann Whitney, $p = 0.7 \times 10^{-8}$. Figure 3.3 C). However, this average increase appeared to reflect an increase in the firing rate of a specific population of neurons; although the proportion of units firing >1 spike/s increased, many neurons still fired at rates <1 spike/s (Figure 3.3 D). The mean interspike interval (ISI) histograms showed that while the firing of striatal neurons at the around the interval of the slow oscillation was similar between the two groups (i.e. the incidence of interspike intervals around 1s was unchanged), there was a clear increase in the incidence of smaller intervals (10-100 ms) for neurons in lesioned rats, i.e. more high-frequency firing for neurons in lesioned rats (Figure 3.3 E). An analysis of the firing regularities showed that the firing of striatal neurons in the lesioned group (CV2 of 1.17 ± 0.01) was significantly less regular compared to the neurons in control (CV2 of 1.12 ± 0.01; Mann Whitney, $p = 5.35 \times 10^{-7}$; Figure 3.3 F).

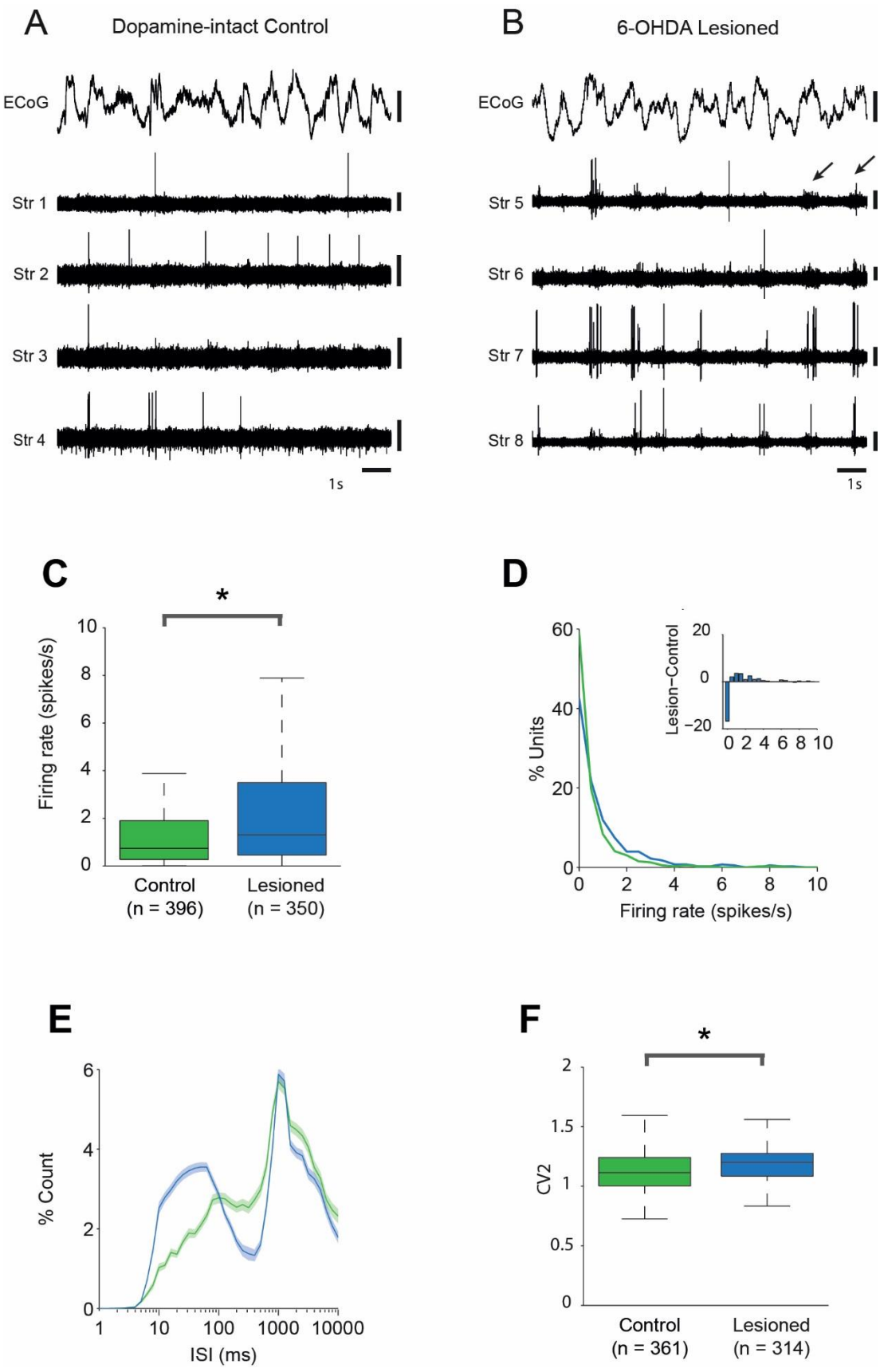
A
Dopamine-intact Control
ECoG
Str 1
Str 2
Str 3
Str 4
1s
B
6-OHDA Lesioned
ECoG
Str 5
Str 6
Str 7
Str 8
1s
C
*
Firing rate (spikes/s)
Control
(n = 396)
Lesioned
(n = 350)
D
% Units
Firing rate (spikes/s)
Lesion−Control
E
% Count
ISI (ms)
F
*
CV2
Control
(n = 361)
Lesioned
(n = 314)

Figure 3.3 **Single-cell and network activity in the striatum of dopamine-intact and 6-OHDA-lesioned rats during cortical slow-wave activity.** ***A, B,*** Typical simultaneous recordings of striatal neurons during cortical SWA in a control rat (A, Str neurons 1-4) and a lesioned rat (B, Str neurons 5-8). Cortical activity (ECoG) is dominated by slow oscillations at ~1 Hz. Calibration: 500 µV (ECoG), 100 µV (units). Note the prominent rhythmicity in the background multiunit activity in lesioned animals (B, arrows). ***C,*** Mean firing rate of all striatal single units in control (green) and lesioned animals (blue). All box plots in figures show the medians, the interquartile ranges (box), and extremes of the range (whiskers, within 99% of the distribution). Black bar and asterisk above box plot indicate significant differences across experimental groups ($p < 0.05$, Mann-Whitney). The number of neurons included in each group is shown in parenthesis. ***D*****,** Histogram of the firing rates of all striatal single units in control and lesioned animals. *Inset*, the difference in the proportion of neurons firing in each rate bin in lesioned and control. ***E,*** Normalized ISI histograms (means ± SEMs) for neurons in control and lesioned animals. ***F,*** Firing regularities of striatal neurons in control and lesioned animals. Regularity was quantified by CV2 measures, with a lower CV2 reflecting more regular firing.

3.4.2 Firing of striatal neurons in relation to cortical slow oscillations

I next examined the firing of single striatal neurons in relation to the cortical slow oscillations. Striatal neurons in both control and lesioned animals preferentially discharged just before the peak of the cortical slow oscillation (Figure 3.4 A, B). The mean angles of the significantly phase-locked striatal neurons (Rayleigh, $p<0.05$) in control (346.1±2.7º) and lesioned rats (344.1±1.65º) were not significantly different, and the population vector lengths for each group were similar (control/lesion: 0.78/0.89, Figure 3.4 A, B). There were, however, more neurons significantly locked to the slow oscillations in lesioned rats (96.4% of neurons) than in control rats (63.3%, bootstrap resampling, $p<0.05$). The proportion of neurons that preferentially fired around the slow oscillation troughs appeared larger in lesioned rats as compared to control rats (Figure3.4 A, B). Because it was not possible to verify the identities of recorded neurons, the nature and contributions of these cells firing around the troughs is obscure and was not further investigated. However, given that MSNs are the majority of striatal neurons, it is possible that a new/different population of MSNs, with unusual electrophysiological properties, might tend to fire around the troughs after chronic dopamine loss. The power of the ECoG slow oscillation was not significantly different between control and lesioned animals, suggesting that differences in striatal neurons firing were not caused by any systematic difference in cortical activity (Figure 3.4 C). In summary, individual striatal neurons locked with similar timing and precision to the cortical slow oscillation in lesioned and dopamine-intact animals, but more neurons tended to do so after chronic dopamine loss. To further explore striatal output, I utilised the high-pass filtered multiunit signal that represents the firing of many neurons around the

electrode. In contrast to the discrete firing of single units, this multiunit signal is continuous, enabling spectral analysis that is not corrupted by firing rate. The proportion of total multiunit spectral power (0-80 Hz) that was contained in the slow oscillations frequency band (0.4-1.6 Hz), was considerably higher in 6-OHDA-lesioned animals (lesioned 2.74 ± 0.08; control 1.24 ± 0.03, Mann Whitney, $p = 0.6 \times 10^{-38}$), suggesting that, after dopamine loss, the net output of striatal neurons populations was altered to better represent these slow oscillations (Figure 3.4 D).

To understand how chronic dopamine loss affected the synchronization of ensemble activity in striatum during SWA, I used cross-correlation analysis of pairs of neurons. The analysis of pairs of neurons in dopamine-intact and lesioned animals revealed that the oscillatory discharges of striatal neurons were significantly more synchronized after chronic dopamine loss (Figure 3.5 A, B, C). Indeed ~60% of striatal neurons pairs in lesioned animals versus ~37% of neuron pairs in dopamine-intact animals were significantly synchronized during SWA. Finally, I analysed the level of firing synchrony in relation to the distance between neurons in a paired recording. As shown in Figure 3.5 D, the synchronicity between pairs of neurons in both control and lesioned animals is moderately stable across hundreds of micrometres.

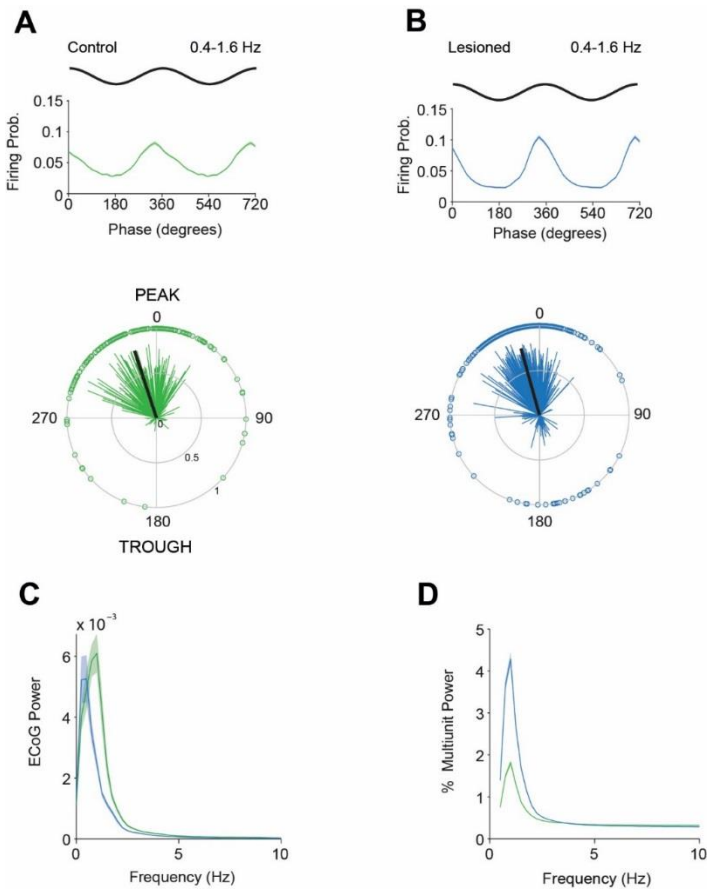

Figure 3.4 **Striatal neuron activity in relation to the cortical slow oscillations in control and 6-OHDA-lesioned animals.** ***A, B*****,** Mean linear phase histograms for all single units (upper) and circular plot of significantly-locked units (lower) recorded in control animals (green) and in lesioned animals (dark blue) during SWA. For clarity, two cortical slow oscillations cycles are shown in phase histograms. Shaded areas show the SEM. Vectors of preferred firing of individual neurons are shown as lines radiating from the centre of circular plots. Greater vector lengths indicate lower variance in the distribution around the mean phase angle of an individual neuron. Black line radiating from the centre indicates the mean phase angle of all the neurons. Each circle on the plot perimeter represents the preferred phase angle of an individual neuron. Striatal neurons in control and lesioned animals tended to fire along the ascending portion of the slow oscillation. ***C,*** Mean power spectra of all ECoGs recorded during SWA in control (green) and lesioned rats (dark blue). ***D,*** Mean power spectra of all striatal multiunit recordings in control (green) and lesioned animlas (dark blue).

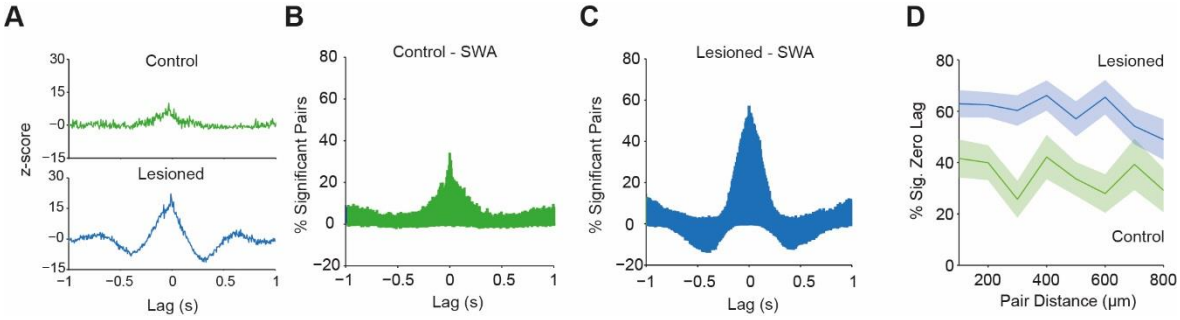

Figure 3.5 **Temporal and spatial correlations between striatal neurons during SWA in control and lesioned animals.** ***A,*** Representative examples of cross-correlation histograms (CCHs) calculated between pairs of striatal units recorded during SWA in dopamine-intact (green) and lesioned animals (dark blue). ***B,*** Histogram of the percentage of striatal unit pairs in controls that were significantly correlated (z-score >2) at a given lag during SWA. Negative values indicate a significant trough in the CCH. ***C,*** As in B, for striatal unit pairs recorded in lesioned animals. ***D,*** Mean percentage of significant correlations at zero lag as a function of the distance between the contacts at which they were recorded in dopamine intact (green) and lesioned animals (dark blue). Shaded areas show the SEM.

3.4.3 Characterisation of ECoG activity during spontaneous activation

Spontaneous global ECoG activation was defined as a clear reduction in the amplitude of the cortical slow oscillations and related spindle oscillations (compare Figures 3.3 A, B and 3.6 A, B). Concomitant with the loss of these low-frequency oscillations, the activated brain state was heralded by an increase in gamma oscillations (30-90 Hz) in control animals, and beta oscillations (15-30 Hz) in lesioned rats.

3.4.4 Firing rate and pattern of striatal neurons in dopamine-intact and 6-OHDA-lesioned rats during spontaneous cortical activation

I recorded the spontaneous activity of 181 striatal neurons in control rats (n = 9; n of cells 20-40, min-max) and 822 striatal neurons in lesioned rats (n = 9; n of cells 20-40, min-max) during spontaneous cortical activation (Figure 3.6 A, B). In dopamine-intact animals, the majority of striatal neurons fired single spikes once every few seconds (Figure 3.6 A). In lesioned animals, some neurons fired at similarly low rates (See Str 15 and 16 in Figure 3.6 B). However, after dopamine loss, more neurons fired at faster rates that were rarely seen in dopamine-intact animals (Figure 3.6 B, C). On average, the firing rate of striatal neurons in lesioned animals (3.39 ± 0.19; spikes/s; mean ± SEM) was significantly higher than that of neurons in controls (1.45 ± 0.15, spikes/s; Mann Whitney, $p = 0.4 \times 10^{-8}$; Figure 3.6 C). Moreover, in lesioned animals, the proportion of neurons firing at very low rates (<1 spike/s) decreased by about 15% across the whole sample of single units, whereas the proportion of neurons firing at > 3 spike/s increased (Figure 3.6 D). Striatal neurons in lesioned animals also had a greater tendency to fire spikes at

short intervals (5-100 ms; Figure 3.6 E). Analysis of the firing regularities showed that the firing of striatal neurons in lesioned animals (CV2 1.01 ± 0.0041) was significantly more regular compared to the control group (CV2 0.99 ± 0.013. Mann Whitney, p = 0.0472; Figure 3.6 F).

To understand whether brain state has an impact on striatal neuron firing properties, I analysed the firing rate and pattern of neurons recorded in control or lesioned groups during different brain states. I found that the firing rate and pattern of striatal neurons in dopamine-intact rats was significantly higher and more regular during the activated state than during slow-wave activity (Firing rate: control SWA 0.78± 0.07, spikes/s; control ACT 1.45 ± 0.16; spikes/s; Mann Whitney p = 0.1×10^{-7}. Firing pattern: control SWA CV2 1.12 ± 0.09, control ACT CV2 0.99 ± 0.01; Mann Whitney = 0.16×10^{-13}). Analysis of neurons in lesioned animals revealed a similar scenario. The firing rate of striatal neurons recorded in the lesioned group was higher during spontaneous activation (lesion SWA 1.23 ± 0.09, spikes/s; lesion ACT 3.38 ± 0.19, spikes/s; Mann Whitney = 3.2804e-19) and the firing pattern become more regular (lesion SWA CV2 1.17 ± 0.01, lesion ACT CV2 1.01 ± 0.04; Mann Whitney = 0.2×10^{-59}).

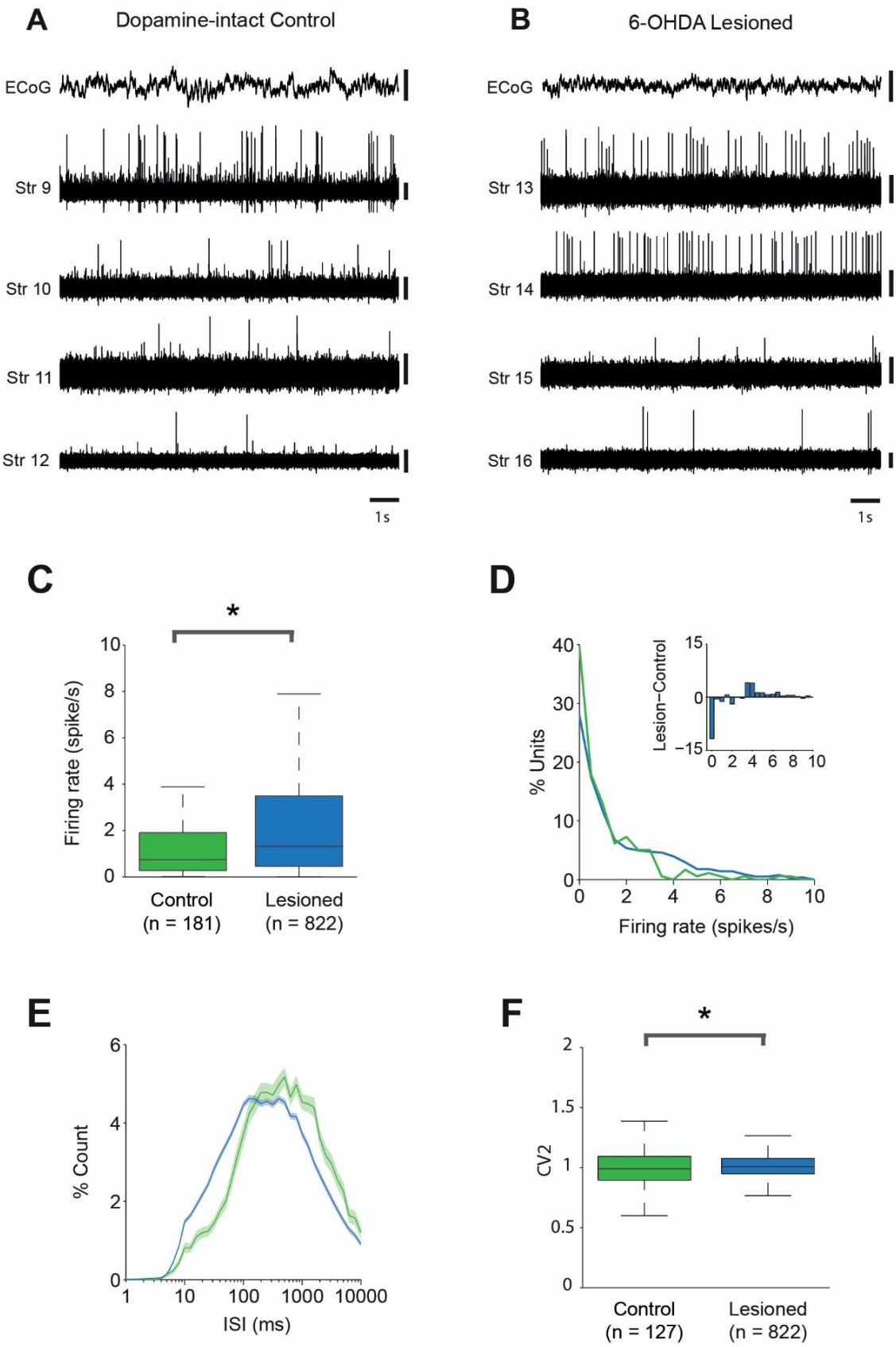
A
Dopamine-intact Control
ECoG
Str 9
Str 10
Str 11
Str 12
1s
B
6-OHDA Lesioned
ECoG
Str 13
Str 14
Str 15
Str 16
1s
C
*
Firing rate (spike/s)
Control
(n = 181)
Lesioned
(n = 822)
D
% Units
Firing rate (spikes/s)
Lesion−Control
E
% Count
ISI (ms)
F
*
CV2
Control
(n = 127)
Lesioned
(n = 822)

Figure 3.6 **Single-cell and network activity in the striatum of dopamine-intact and 6-OHDA-lesioned rats during spontaneous cortical activation.** ***A, B,*** Typical simultaneous recordings of striatal neurons during cortical activation in a control rat (A, Str neurons 9-12) and a lesioned rat (B, Str neurons 13-16). Cortical activity (ECoG) is dominated by high-frequency oscillations. Calibration: 500 µV (ECoG), 100 µV (units). ***C,*** Mean firing rate of all striatal single units in control (green) and lesioned animals (blue). All box plots in figures show the medians, the interquartile ranges (box), and extremes of the range (whiskers, within 99% of the distribution). Black bar and asterisk above box plot indicate significant differences across experimental group ($p < 0.05$, Mann-Whitney). The number of neurons included in each group is shown in parentheses. ***D,*** Histogram of the firing rates of all striatal single units in control and lesioned animals. *Inset*, the difference in the proportion of neurons firing in each rate bin in lesioned and control. ***E,*** Normalized ISI histograms (means ± SEMs) for neurons in control and lesioned animals. ***F,*** Firing regularities of striatal neurons in control and lesioned animals during activation. Regularity was quantified by CV2 measures, with a lower CV2 reflecting more regular firing.

3.4.5 Firing of striatal neurons in relation to cortical beta oscillations during spontaneous activation

Because chronic disruption of dopamine transmission also affects the frequency-domain interactions of neurons in cortico-basal circuits, I compared the synchronization of the firing of striatal neurons to ongoing cortical oscillations at beta frequencies (15-25 Hz) in both control and lesioned animals. The power of beta-frequency oscillations in the cortical ECoG was significantly higher in 6-OHDA-lesioned animals (Mann Whitney, $p = 0.04$, Figure 3.7 A). In lesioned animals, the firing of around 40% of striatal neurons was significantly locked to the cortical beta (Figure 3.7 B) and neurons tended to fire around the troughs of these oscillations (Figure 3.7 C, D). Conversely, only 6% of striatal neurons in the control group fired in phase with these oscillations (Rayleigh, $p<0.05$; Figure 3.7 B) and they did not exhibit any clear phase preference (Figure 3.7 C). The above evidence obtained for the lesioned group was consistent with a clear peak of power in the beta-frequency range in the multiunit activity recorded in striatum, which compared to controls, was significantly higher (lesion: 1.35 ± 0.01; control: 1.32 ± 0.001; Mann Whitney $p = 6.6073 \times 10^{-33}$, Figure 3.7 E). Moreover, around 30% of the multiunit spectral power was coherent with cortical beta oscillations in lesioned animals, whereas coherence in dopamine-intact animals was at chance level (Figure 3.7 F). Thus, a large proportion of striatal neurons became engaged in pathological beta oscillations in 6-OHDA-lesioned animals.

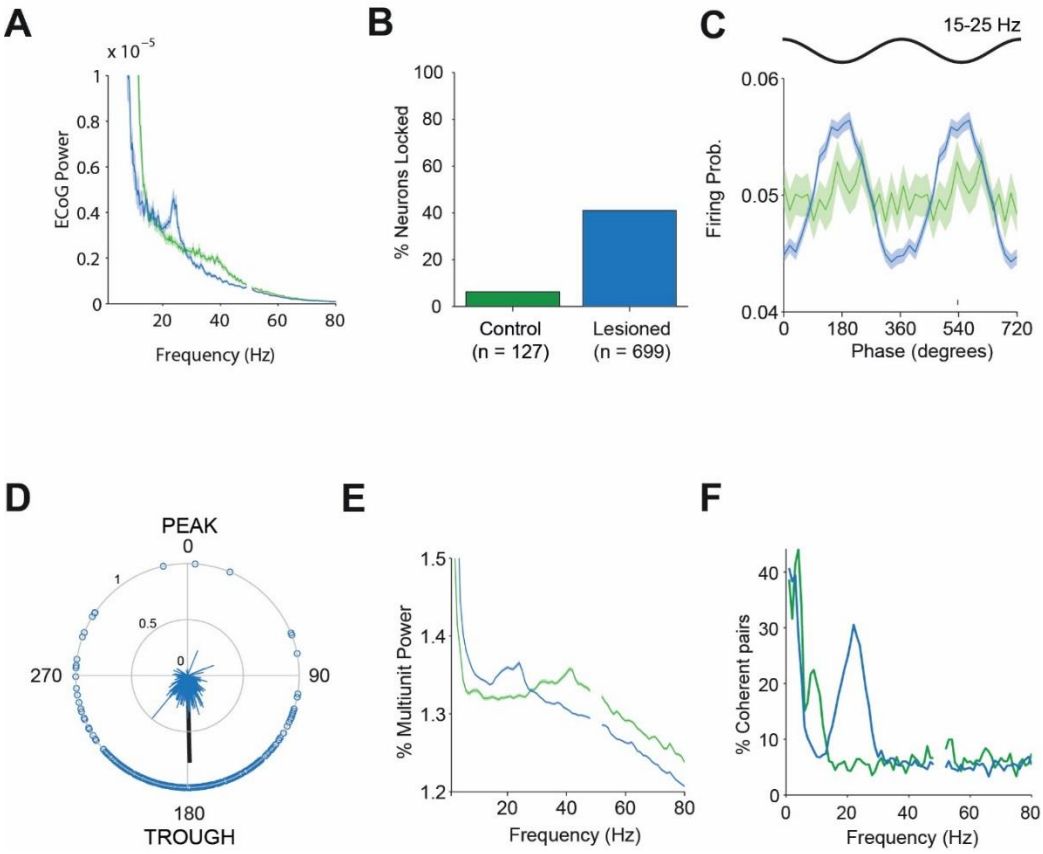

Figure 3.7 **Striatal neuron activity in relation to cortical beta oscillations in control and 6-OHDA-lesioned animals.** ***A****,* Mean power spectra of all ECoG recordings during cortical activation in control (green) and lesioned (blue) animals. ***B***, Percentages of neurons in control and lesioned animals whose firing was significantly locked to cortical beta oscillations (Rayleigh, $p < 0.05$). Number of neurons tested are in parentheses. ***C****,* Mean linear phase histograms for all single units recorded in control (green) and lesioned (blue) animals for cortical beta oscillations. Shaded areas show the SEM. ***D****,* Circular plot of significantly-locked single units recorded in lesioned animals. Vectors of preferred firing of individual neurons are shown as lines radiating from the center. Greater vector lengths indicate lower variance in the distribution around the mean phase angle for each neuron. Black line radiating from the centre indicates the mean phase angle of all neurons. Each circle on the plot perimeter represents the preferred phase angle of an individual neuron. ***E,*** Mean power spectra of all striatal multiunit recordings in control (green) and lesion (blue) animals during cortical activation. ***F,*** Percentage of striatal multiunit recordings that were significantly coherent with the ECoG in control (green) and lesioned (blue) animals.

3.4.6 Synchronization of striatal neurons during the activated brain state is enhanced by dopamine depletion

The cross correlation histograms (CCHs) of striatal unit pairs recorded during cortical activation in both dopamine-intact and lesioned animals showed wide peaks of around 200ms (Figure 3.8 A, B). CCHs from lesioned animals often had sharper peaks at zero-lag and this manifested as larger peaks in histograms of significant cross correlations across all recorded pairs (Figure 3.8 C, D). Accordingly, the percentage of pairs correlated at zero-lag was significantly higher in lesioned animals (Permutation T-test, $p = 1.14 \times 10^{-29}$) and the z-scores at zero-lag were significantly higher for unit pairs in 6-OHDA-lesioned than dopamine-intact animals (Mann Whitney, $p = 0.04$). In 6-OHDA-lesioned animals, individual CCHs and the histogram of significant pairs displayed side lobes in the beta range (i.e. 40-50 ms cycle length; Figure 3.8 B, D). The power of the CCH z-scores displayed a significant peak in the beta range (15-25 Hz), which was not present in data from dopamine-intact animals (Figure 3.8 E). The percentage of significant correlations at zero lag as a function of the distance between contacts of the silicon probe showed that the closer striatal units were, the more correlated was their firing (Figure 3.8 F). However, there was no interaction between control group and lesioned group as a function of the distance ($p = 0.89$). In summary, these data show that after chronic dopamine loss, neurons in striatum tend to be more synchronized, compared to the control, in a specific frequency range (15-25 Hz) during cortical activation.

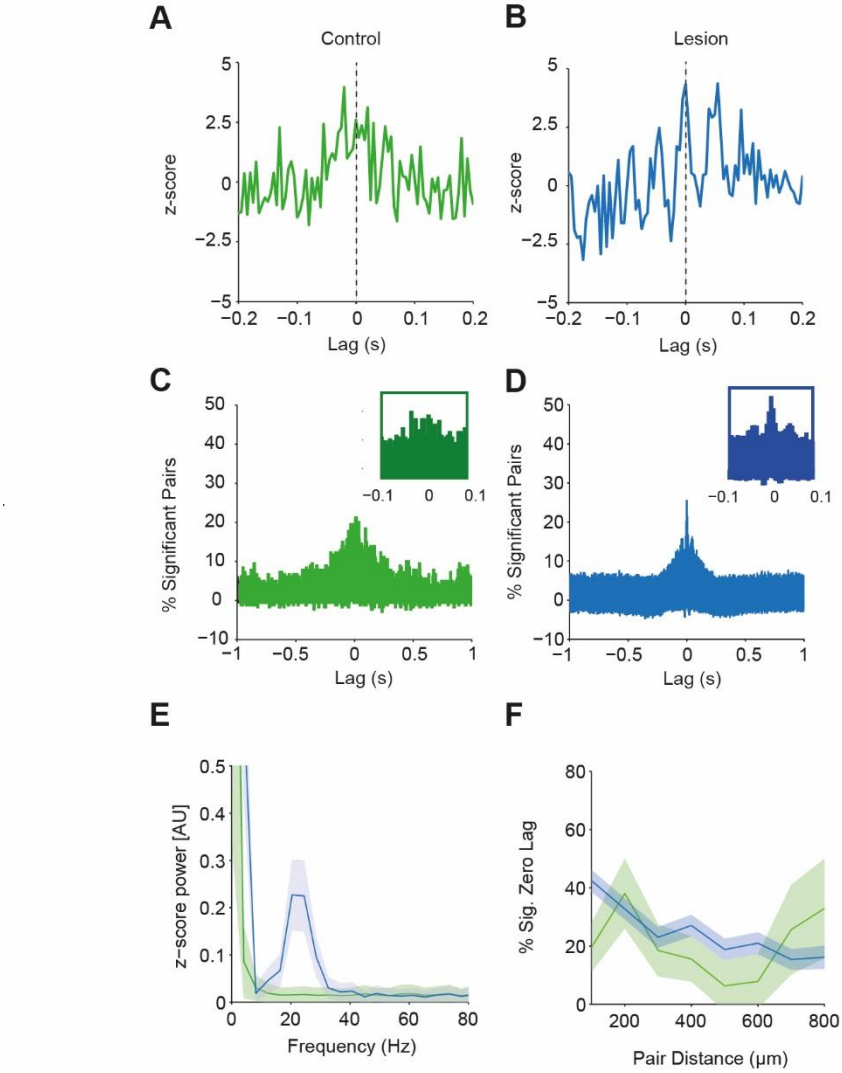

Figure 3.8 **Temporal and spatial correlations between striatal neurons during the activated brain state in dopamine-intact and 6-OHDA-lesioned animals.** ***A, B,*** Representative examples of CCHs calculated between pairs of striatal units recording during spontaneous activation in dopamine-intact (A, green) and 6-OHDA-lesioned animals (B, dark blue). ***C, D,*** Histograms of the percentage of striatal unit pairs that were significantly correlated (z-score >2) at a given lag, in dopamine-intact (green) and lesioned (dark blue) animals. Negative values indicate a significant trough in the CCH. ***E,*** Power spectra of the z-scored CCHs from dopamine-intact (green) and lesioned animals (dark blue). Note the prominent peak in the beta range for lesioned animals. Shaded areas show the SEM. ***F,*** Mean percentage of significant correlations at zero lag as a function of the distance between the contacts at which they were recorded in dopamine-intact (green) and lesioned (dark blue) animals. Shaded areas show the SEM.

3.5 Discussion

The results of this study demonstrate that chronic loss of midbrain dopaminergic neurons alters the firing rates, patterns and synchronization of striatal neurons in a brain-state dependent manner. Simultaneous recordings of populations of striatal neurons in both SWA and spontaneous cortical activation showed: (1) a significant increase in the average firing rate of striatal neurons in 6-OHDA-lesioned animals; and (2) that, during spontaneous activation, a prominent synchronization of striatal neurons at beta frequencies arose in 6-OHDA-lesioned animals, suggesting the striatum is involved in the propagation of these aberrant oscillations through the BG in Parkinsonism.

Firing rate of striatal neurons is altered after chronic dopamine loss

Understanding the brain-state dependent activity of striatal neurons after chronic dopamine loss is important to elucidate the neuronal basis of the pathophysiology of Parkinsonism. The prevailing model describing the critical function/dysfunction of BG circuitry after chronic dopamine loss, suggests that two routes of information flow, the direct and indirect pathways, originate from two distinct populations of spiny projection neurons (Albin *et al.*, 1989; DeLong, 1990). Striatal neurons of the direct pathway express D1-dopamine receptors, that when stimulated, promote firing, whereas striatal neurons of the indirect pathway express D2-dopamine receptors that inhibit the firing of these neurons. According to this model, dopamine loss, as occurs in PD, imbalances these two pathway to a level at which one population, (striatal neurons of the direct pathway) become hypoactive, and the other (indirect

pathway) become hyperactive. The imbalanced output of the direct and indirect pathways would then be propagated to the downstream network of the BG and be one of the causes of the antikinetic symptoms of PD. In this thesis, and in agreement with previous observations obtained from *in vivo* recordings of putative MSNs in rodents (Schultz & Ungerstedt, 1978; Alloway & Rebec, 1984; Kish *et al.*, 1999; Chen *et al.*, 2001; Tseng *et al.*, 2001; Zold *et al.*, 2012), I found that the firing rate of striatal neurons recorded in the 6-OHDA-lesioned animals was significantly higher, compared to neurons in control animals. The pathological enhancement of the firing rate was further validated through the analysis and comparison of the duration of interspike intervals in both control and lesioned group showing that, in 6-OHDA-lesioned animals, the duration of interspike was markedly reduced, irrespective of the brain state. Additionally, some neurons in the lesioned group still fired at low rates (in both brain states), that were similar to those observed in the control group. The use of multi-electrode arrays did not allow for the verification of the identity (cell-type) of recorded neurons. With this in mind, it is only possible to assume that differences in the firing rate of recorded striatal neurons in the lesioned group, in agreement with what has been described in the classical model (Albin *et al.*, 1989; DeLong, 1990), correspond to direct and indirect pathway neurons, with the first group of neurons showing a very low firing rate and the second displaying a higher firing, after chronic dopamine loss. If these assumptions are correct, then they would be consistent with previous literature showing similar differences in the firing rate within the striatal population. For instance, in rodents (Schultz & Ungerstedt, 1978; Alloway & Rebec, 1984; Kish *et al.*, 1999; Chen *et al.*, 2001; Tseng *et al.*, 2001; Zold *et al.*, 2012) and in monkeys (Crutcher & DeLong, 1984; Alexander & DeLong, 1985b; Kimura, 1992; Aosaki *et al.*, 1994) it has been

repeatedly shown that, after toxin-induced dopamine loss, the firing of striatal neurons is segregated into two distinct populations, with one (on average) firing below 3 spike/s and the other firing above 3 spike/s. There is some evidence, however, that indicates that the firing of unidentified striatal neurons can reach very high frequencies after dopamine loss (Liang *et al.*, 2008) and in some documented cases (Liang *et al.*, 2008; Calabresi *et al.*, 2014) it has been suggested that the enhanced firing involves all MSNs: i.e. both striatal output pathways. The reasoning behind such a generalized mechanism, which does not distinguish between direct and indirect pathways, could be related to exaggerated glutamatergic input from the cortex after loss of presynaptic dopamine regulation (Liang *et al.*, 2008) or to critical intrastriatal connections between MSNs that make them structurally and functionally intertwined (Calabresi *et al.*, 2014). Although these findings raise doubts concerning the classical model of the direct/indirect pathway, the literature needs to be integrated with more compelling findings, considering for example, that the cell-type specific contributions have not been elucidated in these studies. At present, the firing rate of identified MSNs during both SWA *and* spontaneous activation has not been reported. However, Mallet and colleagues (2006) showed that some identified indirect pathway MSNs increased their firing during SWA to a greater degree than in control animals, demonstrating for the first time that histochemically-identified striatal neurons display different electrophysiological properties *in vivo* after chronic dopamine loss.

Finally, because of the technical limitation of the multi-electrode array technique, it was not possible to identify striatal interneurons. In a recent study, Sharott and colleagues (2012) showed that, in control animals, PV+, NOS+ and

ChAT+ striatal interneurons have distinct temporal signatures *in vivo*, with some of those firing at similar rate and patterns to the striatal unit activities I recorded under the same brain state and dopamine-intact conditions. Hence, although it is not possible to rule out that some interneurons were included in my analyses, their proportion in striatum is very low (<5% of all striatal neurons) and therefore it is likely that the majority of the unit activities I recorded correspond to MSNs. The electrophysiological properties of neurochemically-identified interneurons in a 6-OHDA-lesioned model of PD are still under investigation.

Striatal firing rate and pattern is modulated by different cortical brain state and dopamine

All experimental procedures in this thesis were conducted under general anaesthetic. In agreement with previous studies performed under the same anaesthesia regime, the frontal electroencephalogram reflected two main brain states. The first is characterized by slow oscillations (~1 Hz) of large amplitude and the second, called here as 'spontaneous activation', is characterized by sustained high-frequency oscillations and an absence of the slow oscillations (Tseng *et al.*, 2001; Mallet *et al.*, 2005; Sharott *et al.*, 2012). Although general anaesthesia may interfere with a number of neurophysiological variables, previous studies indicate that slow oscillations in the ECoG are correlated with a depolarized state in both corticostriatal and striatal neurons under a variety of anaesthetic conditions (Mahon *et al.*, 2001). The striatum receives extensive glutamatergic input from the cortex (Bolam *et al.*, 2000) whose state transition is thought to control basal ganglia function by shaping striatal output (Mahon *et al.*, 2006). Thus, understanding how

cortical information is processed and integrated into the striatal microcircuit and how in turn striatal neurons shape their firing with respect to the ongoing cortical activity was one of the aims of this research study. In agreement with previous investigations, my data suggests that extremes of brain state have a prominent impact on the firing rate and pattern of striatal neurons in both control and lesioned animals (Mallet *et al.*, 2005; Mahon *et al.*, 2006; Sharott *et al.*, 2012). Specifically, I found that, irrespective of the experimental group (control or lesioned group), striatal neurons tended to fire at higher frequencies during spontaneous activation. In agreement with previous studies, up and down shifts of highly synchronized cortical neurons superimpose a specific time-window during which MSNs can fire (Wilson, 1995; Mahon *et al.,* 2006). During spontaneous activation in contrast, the noise-like membrane potential fluctuations probably originate in the uncorrelated firing of many convergent corticostriatal neurons that are in a position to trigger action potentials from epochs of relatively coherent cortical activity (Murthy & Fetz, 1992; Mahon *et al.*, 2006). Hence during SWA striatal neurons are forced to follow a rhythmic pattern of cortical activity (of ~1 Hz) and can only fire during the up state of this pattern. During spontaneous activation, because epochs of synchronized and highly coherent corticostriatal neurons is lost, striatal neurons are not forced to follow a pattern, therefore they fire more. Also, in line with this assumption, I also found that the firing pattern of striatal neurons become more regular during spontaneous activation. Because cortical and thalamic projections innervate the main population of striatal neurons to a similar degree (Doig *et al.*, 2010), it is possible that thalamic projections may have an impact on striatal firing properties as well. For instance, during spontaneous activation, thalamic neurons fire tonically and are thus in a position to contribute to the excitatory synaptic bombardment of striatal neurons

(Lacey *et al.*, 2007). Another result of this investigation showed that the firing of both striatal neurons in the control and lesioned groups was significantly locked to the ascending portion of cortical slow oscillations during SWA, which is to be expected because cortical neurons are most active at this phase in the cycle (Stern *et al.*, 1998).This finding is in agreement with previous studies in control animals, showing how the activity of striatal neurons is dependent on spatio-temporal and highly convergent cortical inputs that shape their membrane potential to a depolarized state of few milliseconds, during which striatal neurons fire (Stern *et al.*, 1998; Sharott *et al.*, 2012). As mentioned before, I did not take into account thalamic projections to striatum which could provide functionally distinct inputs to striatum. For instance, Lacey and colleagues (2007) found that neurons of the central lateral and parafascicular nuclei of the thalamus, which project to the striatum, provide different temporally patterned inputs to distinct striatal targets that in turn could shape striatal physiology. In contrast to slow oscillations, the preferred phase angle of discharge of striatal neurons during beta activity is at the descending portion of the oscillation, at around 180°. This is line with previous studies showing that most GPe neurons fire less during this phase of cortical beta oscillation (Mallet *et al.*, 2008a). As some inhibitory striatal neurons send projections to the GPe, it is possible that the reduced firing in the latter structure is due to the pathologically-enhanced inhibitory striatal firing. Then, in turn, the peak activity of GPe neurons during a beta oscillation, coincides with minimal activity of STN (Mallet *et al.*, 2008a). However, the specific dynamics of indirect pathway- GPe- STN network and the spatio-temporal reciprocal inhibition needs to be further clarified. For example, future studies should try to account for the fraction of GPe neurons that also project back to striatum because they could play an important role in the modulation of

striatal neuron physiology. Interestingly, a few striatal neurons fired with the peak of beta oscillations and showed a preferred phase angle at around 0°. The functional role and identity of these specific neurons are not known and need to be further investigated. In line with the analysis of the preferred phase angle of striatal cell discharges, here I suggest that the sub-population of striatal neurons that showed a preferred angle at the trough of the oscillations could be in a position to orchestrate the emergence of beta oscillations in the GPe and other downstream BG targets in Parkinson's disease. Although some striatal neurons fired at low rates, and only half were entrained to cortical beta, striatal neurons greatly outnumber GPe neurons (~25:1) and so convergent, synchronised striatal output could play a key role in the propagation of beta oscillations. Indeed, a recent computational modelling study places special emphasis on abnormal activity along the indirect pathway (as a whole) being particularly important for excessive beta oscillations and movement impairments in PD (Moran *et al*., 2011). The mean vector length of striatal neurons showing phase-locked activity in 6-ODHA animals is also indicative of the strength at which neurons are locked to beta oscillations. In behavioural terms this analysis may be informative not only in relation to a specific motor symptoms but also to the severity of the symptoms. For instance, a recent study in PD patients has shown that the percentage of STN units oscillating at beta frequencies was positively correlated with axial and limb rigidity, and in contrast, the percentage of units oscillating at gamma frequency negatively correlated with bradykinesia (Sharott *et al.*, 2014).

Finally, dopamine inputs from the substantia nigra converge with glutamatergic inputs from the cerebral cortex and thalamus at the dendrites of

striatal projection neurons as well (Moss & Bolam, 2008). Extracellular recordings of single-unit activity have established that the pattern of activity of neurons in nuclei receiving strong dopamine innervation (i.e. SNr), shifts from a regular pattern to a rhythmic firing bursting mode after chronic dopamine loss (Murer *et al.*, 1997). With respect to striatum, there is an indication that ionic conductances shaping the fluctuation of membrane potential of striatal neurons, are carefully modulated by the neurotransmitter dopamine (Nicola *et al.*, 2000). Hence, if corticothalamic neurons are in a position to depolarize striatal membrane potential to a level in which striatal neurons can become active, then there are probably dopaminergic afferents that promote or inhibit their firing, depending on the striatal dopaminergic receptor. When I compared the firing of control and lesioned animals, I found that, irrespective of the brain state, striatal neurons recorded in the lesioned group fire higher frequency rate compared to the control group. One explanation for this alteration in the firing rate, comes from *in vivo* intracellular recording of striatal projection neurons during SWA after dopamine loss that have revealed how striatal projection neurons present a more depolarized membrane potential after chronic dopamine loss during both up and down state, and an increased firing probability during the up state (Tseng *et al.*, 2001). This study also shows that lesioned animals have significantly fewer silent neurons than in control rats, an observation that is consistent with my data.

Chronic loss of dopamine alters the engagement of striatal neurons with oscillations

Enhanced oscillations at beta frequencies (15–25 Hz) are a signature of neuronal dysfunction in the basal ganglia and cortex of Parkinson's disease patients. The

mechanisms underlying these pathological beta oscillations remain elusive. Only computational models so far provide suggestions that robust beta oscillations can emerge in the striatal microcircuit at the level of the single cells. (McCarthy *et al.*, 2011; Damodaran *et al.*, 2015). Thus, the key aim of this study was to investigate the neural basis of (abnormally) synchronized beta oscillations *in vivo,* at the level of single neurons in the striatum and to elucidate their functional significance. To achieve this aim, I sampled single-unit activity from numerous sites in the dorsal striatum, using linear arrays with multiple, spatially-defined recording contacts (Magill *et al*., 2006; Mallet *et al*., 2008). Then, I analysed the activity of populations of striatal neurons in control and lesioned animals in relation to the ongoing cortical activity, during spontaneous activation. The results of this investigation provide the first direct evidence that striatal neurons fire action potentials in phase with cortical beta oscillations and that such engagement is greatly increased after dopamine loss. Specifically, ~40% of striatal neurons became entrained to the beta oscillations in lesioned rats compared to only ~6% of neurons in controls. When the power spectra of all striatal multiunit activity was compared between the control and the lesioned group, a clear peak in the range of beta frequency was observed only in the latter group, suggesting, in agreement with previous LFP studies (Moran *et al*., 2011), that a large portion of striatal neurons became synchronously engaged in pathological beta oscillations after chronic dopamine loss occurs. Additionally, around 30% of the spectral power of multiunit activity in lesioned animals was also significantly coherent with cortical beta oscillations, whereas no direct relationship with cortex was observed in the control group. I also found that the oscillatory discharges of striatal neurons were significantly more synchronized after chronic dopamine loss irrespective of the brain state, and that the closer striatal neurons

were, the more correlated was the firing. This in turn suggests that chronic dopamine loss enhances the synchronicity of large ensembles of neighbouring striatal neurons. A few neurons in control animals were also phase-locked with cortical beta oscillations; this observation deserves further investigation, for example to define their neurochemical identity. However, this result is partially consistent with previous studies of the striatal LFP in an awake dopamine-intact monkey (Courtemanche *et al.*, 2003) that showed some neurons engaged in beta activity. This study did not investigate the striatal LFP after chronic dopamine loss, so it is not possible to draw conclusion to what extent neurons are locked to beta in Parkinsonism. However, this study suggests that in order to effectively inhibit/impair the basal ganglia downstream structures, the number of neurons in the control group firing in phase with cortical beta oscillations should be higher. When similar analyses were applied at the level of the multiunit activity during SWA, the power of 1 Hz activity was significantly higher in the lesioned group, suggesting that even in this brain state, dopamine loss strongly affects the strength at which neurons engage with specific oscillations, that in turn could have a stronger impact to the downstream basal ganglia network.

Concluding remarks

My current data suggest that subpopulations of striatal neurons play a key role in the generation and propagation of aberrant beta oscillations in the BG network. However, the striatum has been largely ignored as a source of beta oscillations. For instance, in the past, most of the investigations regarding pathological oscillatory

activity have been conducted on STN and GPi given the possibility of recording from this structure during the implantation of DBS electrodes as a treatment for PD (Brown, 2006). In animal models, as well as in PD patients, these nuclei display bursting activity at 15–30 Hz (Brown, 2006). Clinical improvement obtained with DBS implantation or levodopa administration is related to the decrease of beta-band oscillatory activity in STN and GPi nuclei (Cassidy & Brown, 2001; Williams *et al.*, 2002; Brown, 2003; Priori *et al.*, 2004; Silberstein *et al.*, 2005; Marceglia *et al.*, 2006; Stoffers *et al.*, 2008a; Stoffers *et al.*, 2008b; Kuhn *et al.*, 2009). Also, experimentally augmented beta oscillations have been shown to disrupt motor functions in the same nuclei (Timmermann *et al.*, 2004; Fogelson *et al.*, 2005; Chen *et al.*, 2007; Eusebio *et al.*, 2008). Here, I suggest, in agreement with previous studies on striatum (Moran *et al.,* 2011), that because this structure is also pathologically synchronized at beta frequencies, it could be a potential therapeutic target for the treatment of Parkinsonian symptoms as well.

How aberrant synchronization arises in the basal ganglia in Parkinsonism is still unclear. Although it is unlikely that the complex pathology of PD is limited to only beta oscillations, or conversely that beta oscillations subserve a single motor function/dysfunction, it is well established that PD is intimately linked with recorded activity at this specific frequency band. It is still unclear whether the origin of the pathological oscillations resides in striatum, it being the source of direct and indirect pathway and the major recipient of dopaminergic neurons, or if aberrant oscillations arise from interactions across entire BG-thalamocortical circuit. In an attempt to understand how MSNs shift from up and down states, Zold and colleagues (2012b) showed that not only do MSNs have intrinsic mechanisms that may allow self-

generated plateau depolarization in certain circumstances, but also that the activation of glutamatergic receptors from corticostriatal synapses is not required for spontaneous up states *in vivo* (Zold *et al.*, 2012). Indeed delivering an NMDA receptor antagonist during an *in vivo* intracellular recording of MSNs, only reduces up state amplitude by a few millivolts, not affecting the up state duration. Likewise, if applied to aberrant synchronization, it is possible that beta activity occurring in striatum is a mechanism by which striatal cells modulate themselves and that the cortex only shapes and eventually reinforces these striatal phenomena. Another mechanism suggested as an intrinsic factor for the generation of beta oscillations is the effect of PV-expressing interneurons on MSNs. Indeed, it has been shown that PV interneurons have intrinsic properties that could contribute to MSN entrainment in oscillatory activity in cortex-striatum co-cultures with no thalamus present (Plenz & Aertsen, 1996). However, other observations implicate other nuclei (i.e. cortex) as the most likely origin of enhanced beta rhythm (Hammond *et al.*, 2007; Gradinaru *et al.*, 2009; Litvak *et al.*, 2011). The idea is that the cortico-subthalamic pathway is enhanced through disinhibition of STN by a suppressed GPe, allowing the STN to become entrained by excitatory cortical projections (Hammond *et al.,* 2007).

In conclusion, this study enabled the recording of hundreds of neurons that gave a robust sample size useful for the comprehension of the wide range of activities in striatum. However, this strategy did not allow for the identification of the cell type(s) of recorded neurons, and therefore I could not directly investigate how differences in the firing rate and pattern correlate to a specific class of striatal neuron. Hence, having established that aberrant synchronization occur in striatum (at the level of the single cell, multiunit activity) and cortex, an important next step is to elucidate the cell-type specific contribution of striatal neurons to excessive beta

oscillations in PD. Indeed, defining how identified neurons shape their firing rate and pattern with respect to aberrant synchronization, will help us to understand which striatal circuit components have a role in the generation of beta oscillations. I will address these issues in chapter 4.

CHAPTER 4

In vivo electrophysiological activity of neurochemically-identified striatal neurons in dopamine-intact and 6-OHDA-lesioned animals

4.1 Study background

The striatum is mainly composed of GABAergic medium-sized densely-spiny neurons (MSNs) whose long-range axonal projections provide the sole output to other basal ganglia nuclei. Striatal MSNs can be divided into in two main populations according to their projection sites and neurochemical properties (Albin *et al.*, 1989; DeLong, 1990). One MSN population preferentially innervates basal ganglia output nuclei and expresses type 1 dopamine receptors (D1Rs) and a second MSN population exclusively innervates the GPe and expresses type 2 dopamine receptors (D2Rs) (Gerfen and Surmeier, 2011). This dichotomous organization of striatal MSNs and their outputs is a core component of the highly influential "direct/indirect pathways" model of basal ganglia functional organization. In this model, D1R-expressing MSNs constitute the so-called "direct pathway". Activation of D1Rs on these MSNs increases their output, thus inhibiting GABAergic basal ganglia output neurons and, thence, disinhibiting basal ganglia targets in thalamus,

midbrain and brainstem. This sequence is believed to facilitate movement. In contrast, activation of D2Rs on the enkephalin-expressing MSNs of the “indirect pathway” decreases their output, ultimately providing increased inhibition of basal ganglia targets and thence reducing movement.

In Parkinson’s disease, midbrain dopaminergic neurons selectively degenerate. According to the classic model, loss of dopaminergic innervation of the striatum in PD imbalances the two striatal output systems (in favour of the indirect pathway), ultimately resulting in excessive inhibition of basal ganglia targets and hence, impaired movement (Albin *et al.,* 1989). Although this scheme of basal ganglia function and dysfunction has advanced understanding of the pathophysiology of Parkinsonism, accumulating evidence challenges this classical view. For example, the afferent and efferent connections of basal ganglia neurons are much more complex than those captured in the model. Moreover, the model suggests that the basal ganglia influence behaviour through changes in their firing rates; this does not fit well with the fact that disturbed firing patterns are more evident in Parkinsonism than the predicted firing rate abnormalities. Indeed, dopamine loss greatly enhances the tendency of neurons in basal ganglia-thalamocortical circuits to generate synchronized, oscillatory firing patterns (Hammond et al., 2007). In bradykinetic PD patients, this excessive oscillatory synchronization preferentially occurs at beta (15-25 Hz) frequencies (Brown et al., 2001). Clinical evidence suggests that excessive beta oscillations are essentially “antikinetic” in nature (Brown et al., 2001; Chen et al., 2007) and arise in most circuits nodes, including frontal cortex, dorsal striatum, subthalamic nucleus (STN), GPe, and SNr in lesioned rats (Mallet *et al*., 2008a,b; Moran *et al*., 2011; Avila *et al*., 2010). With respect to striatum, however, previous work only shows excessive beta activity in striatum at

the level of the LFP (Moran *et al*., 2011) and has not accounted for the complex intrinsic organization and cellular heterogeneity of striatum. Other studies show an alteration in the firing rate of striatal neurons as a consequence of chronic dopamine loss; the data indicate that direct pathway MSNs were hypoactive whereas indirect pathway MSNs were hyperactive, during SWA activity only, in 6-OHDA-lesioned animals (Mallet *et al.*, 2006). Data collected in Chapter 3 showed an excessive synchronization of neuronal activity at beta frequencies at every level of the analysis (ECoG, MUA, and pairs of striatal neurons) after dopamine loss. As reiterated before, the use of the multi-electrode arrays does not provide information about the neurochemical and morphological identity of recorded neurons. Hence, the general goal of this study was to identify cell-type specific contributions of neurons to striatal network dynamics, with a view to understanding their impact on downstream BG nuclei and their (dys)functional roles in Parkinson's disease. Specific aims were to (1) evaluate differences in the firing rate, pattern and level of synchronization of identified MSNs before and after dopamine loss, and (2) evaluate the impact of different cortical brain states on the firing of identified (subtypes) of MSNs, before and after dopamine loss. To pursue this goal, I recorded the spontaneous firing of MSNs *in vivo* in both dopamine-intact control rats and 6-OHDA-lesioned rats during two well defined brain states (see Table 4A). After the physiological characterization, I labelled individual recorded neurons with neurobiotin using the juxtacellular method (Pinault, 1996). I then recovered the neurobiotin-labelled neurons to define their somatodendritic structure, neurochemical properties, and precise location in order to distinguish direct pathway MSNs from indirect pathway MSNs (on the basis of the expression or not of preproenkephalin; PPE).

Animal Group	DOPAMINE-INTACT				6-OHDA-LESIONED			
Peptide	PPE+		PPE-		PPE+		PPE-	
Brain state	ACT	SWA	ACT	SWA	ACT	SWA	ACT	SWA

Table 4A **Study plan for *in vivo* recording and juxtacellular labelling of single neurons.** Striatal unit activity is recorded in two experimental groups: dopamine-intact and 6-OHDA-lesioned animals. Within each group, neurochemically-identified indirect pathway MSNs (PPE+) and direct pathway MSNs (PPE-) were recorded during two well-defined brain states (ACT, spontaneous activation; SWA, slow-wave activity).

4.2 Anatomical identification of individual, electrophysiologically-recorded striatal neurons

To characterize and compare the firing of neurochemically-distinct striatal projection neurons, I developed an (immuno)fluorescence protocol for use on recorded and neurobiotin-labelled neurons that allows the positive identification of indirect pathway MSNs. First, the densely-spiny higher-order dendrites of recorded/labelled MSNs distinguished them from aspiny interneurons. Second, direct and indirect pathway MSNs were differentiated on the basis of their selective expression of immunoreactivity for preproenkephalin (PPE), a precursor of the neuropeptide enkephalin, that is expressed only in indirect pathway MSNs (Gerfen & Surmeier, 2011). Thus, PPE-expressing (PPE+) MSNs were defined as indirect pathway neurons. The MSNs that did not express PPE immunoreactivity (PPE-) were considered direct pathway neurons (see Table 4A). In some early experiments, an

immunofluorescence test for preproenkephalin A (PPTA), a substance P precursor, was also used to verify the identity of direct pathway MSNs. However, the intensity and pattern of PPTA immunoreactivity was inconsistent across trials, and could not be optimised in timely manner. As such, the tests for PPTA expression were discontinued. . It is important to note that, despite not using a positive marker (e.g. PPTA) for direct pathway MSNs, previous work (Reiner *et al.*, 1999) shows that, in all but a small minority of cases (~ 2%), the presence or absence of immunoreactivity for PPE in MSNs is sufficient to accurately distinguish them as neurons of the indirect pathway or direct pathway, respectively. Recorded/labelled neurons were also localized to striatal patches or matrix on the basis of immunoreactivity for μ-opioid receptor (MOR) in surrounding tissue (Crittenden & Graybiel, 2011); those neurons with somata located in regions of relatively intense MOR immunofluorescence signal were defined as patch neurons.

4.3 Experimental procedures

Before the electrophysiology recording session, some animals underwent unilateral injection of 6-OHDA and a drug-induced rotation test to verify the extent of dopamine loss (see section 2.6). Successfully lesioned animals, as verified by the rotation test, were allowed to recover for one week between the test and the recording session. Electrophysiological recording and juxtacellular labelling experiments were performed in 57 anaesthetized rats weighing 300-500 g at the time of recording (32 dopamine-intact and 25 6-OHDA-lesioned). Anaesthesia was induced with 4% isoflurane in O_2 and maintained with urethane (1.3g/kg, i.p.) and supplemental doses of ketamine (30 mg/kg, i.p.) and xylazine (3 mg/kg, i.p.; see section 2.1).

Extracellular recordings of single-unit activity in the dorsal striatum were made using glass electrodes (10-20 MΩ *in situ;* tip diameter ~1.2µm) containing 0.5 M NaCl solution and neurobiotin (1.5% w/v); the glass electrode was then lowered into the striatum using a stepper motor and guided by stereotaxic coordinates (see section 2.1). Both sets of recordings in dopamine-intact and 6-OHDA-lesioned animals were performed during slow-wave activity and cortical activation (Magill *et al.*, 2006a), characterized by means of an ECoG recorded in the frontal region. Following electrophysiological recordings, individual neurons were juxtacellularly labelled with neurobiotin (Pinault, 1996; Bevan *et al.*, 1998; Sharott *et al.*, 2012). After the recording and labelling session, the animals were euthanized with a lethal dose of anaesthetic and transcardially perfused as in section 2.3.1. Brain sections with neurobiotin-labelled neurons were then processed for immunofluorescence labelling (see section 2.7).

4.4 Results

4.4.1 Firing rate and pattern of direct and indirect pathway MSNs in dopamine-intact and 6-OHDA-lesioned rats during slow-wave activity

I recorded, juxtacellularly labelled and identified a total of 90 MSNs in the dorsal striatum of 32 anaesthetised dopamine-intact rats (*n* of cells per animal 1-6, min-max). On the basis of their PPE expression, and brain state ongoing at the time of recording, 29 PPE+ and 33 PPE- MSNs were recorded during SWA, and 12 PPE+ MSNs and 16 PPE- MSNs were recorded during cortical activation. Similarly, I recorded, labelled and identified 98 MSNs in 6-OHDA-lesioned animals (n = 25; *n*

of cells per animal 1-6, min-max) of which 36 were identified as PPE+ MSNs and recorded in SWA, 8 PPE- MSNs recorded in SWA, 46 PPE+ MSNs recorded in ACT and 8 PPE- MSNs recorded in ACT. Only a small fraction of these MSNs were found in patches in control and lesioned groups (see section 4.7 and Table 4D for details). Because of this small sample size and because the electrophysiological properties of MSNs located in the matrix and striosomes were similar, they were combined for the analyses detailed below.

To ensure that recorded MSNs were located in a common aspect of the dorsal striatum, that is, the area that receives dense projections from motor cortex, a map displaying the positions of identified direct and indirect neurons was created. As shown in Figure 4.1, all recorded and labelled MSNs were located in the dorsal striatum, and a similar area of striatum was sampled in control and lesioned animals. No significant correlation was observed when the firing rate and vector length of recorded MSNs were analysed as a function of their location in striatum (data not shown). In control animals, the majority of PPE+ MSNs fired at very low rates (< 0.5 spike/s) and with irregular patterns during SWA (Figure 4.2 A, E). These indirect pathway neurons occasionally fired single spikes around the peak of the cortical slow oscillations. In lesioned animals, while some PPE+ MSNs were still virtually quiescent (Figure 4.2 E), many others fired high-frequency bursts of spikes around some of the peaks of the slow oscillations (Figure 4.2 C). Analysis of the firing rates of PPE+ neurons recorded in dopamine-intact and 6-OHDA-lesioned animals during SWA showed that PPE+ neuron activity in lesioned animals was significantly increased (Control 0.34 ± 0.01 spikes/s; mean ±SEM. Lesioned: 1.2 ± 0.04 spikes/s; mean ±SEM. Mann Whitney, $p = 0.003$). The mean interspike interval (ISI) histogram showed that while the firing of PPE+ MSNs at the around the interval of

the slow oscillations (at ~1000 ms) was similar between animal groups, there was an increase in the incidence of smaller intervals (10-100 ms) for neurons in lesioned rats (Figure 4.2 F). After chronic dopamine loss, PPE+ MSNs firing was significantly more regular (CV2 Control 1.30 ± 0.01; Lesioned 1.14 ± 0.01. Mann Whitney 0.0048; Figure 4.2 G).

In control and lesioned animals, PPE- MSNs also tended to fire at low rates (< 0.5 spike/s) with irregular patterns. These MSNs occasionally fired single spikes at around the peak of the slow oscillations (Figure 4.2 B). An analysis of the firing rates of PPE- MSNs in both control and lesioned animals showed a modest but significant increase in their activity after dopamine loss (Control 0.31 ± 0.02 spike/s, mean ± SEM; Lesioned 0.84 ± 0.14 spike/s, mean ± SEM. Mann Whitney, p = 0.03; Figure 4.2 B, D, H). As for PPE+ MSNs in the lesioned group, PPE- MSNs showed a greater tendency to fire short intervals (10-100 ms; Figure 4.2 I) compared to MSNs in controls, although the firing around the interval of the slow oscillation was similar between the two groups. Chronic dopamine loss did not affect the firing regularities of PPE- neurons (CV2 Control 1.3 ± 0.01; Lesioned 1.16 ± 0.03. Figure 4.2 J).

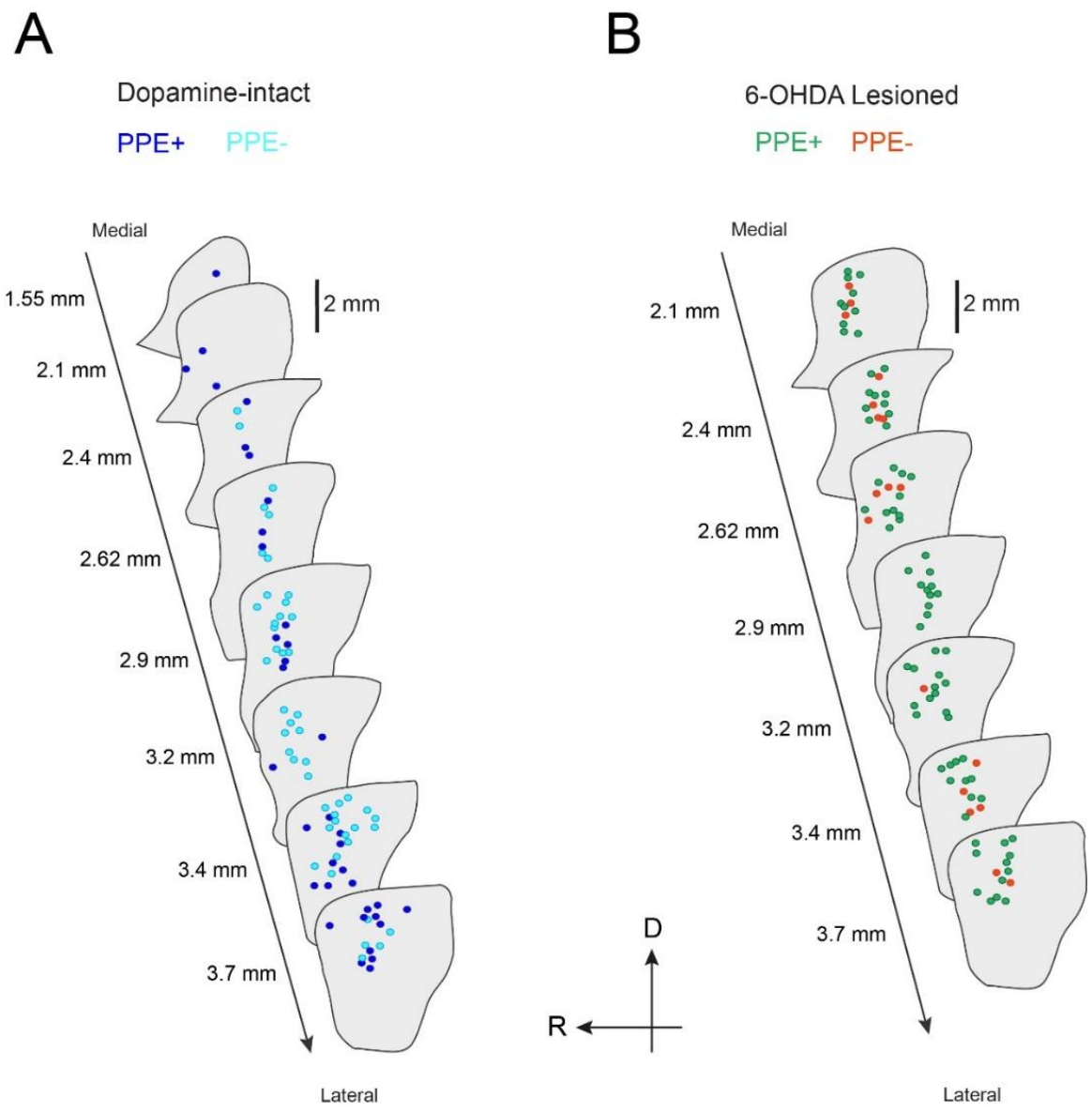

Figure 4.1 **Distribution of recorded and labelled MSNs on parasagittal sections of dorsal striatum in dopamine-intact and 6-OHDA lesioned rats. *A, B,*** Circles represent the location of identified PPE+ and PPE- neurons in dopamine-intact (A) and 6-OHDA-lesioned animals (B) within sections between 1.55 mm and 3.7 mm lateral to Bregma. Identified neurons were all located in the dorsal striatum. Circles represent PPE+ neurons (green, lesioned animals; dark blue, control animals) and PPE- neurons (orange, lesioned animals; light blue control). Adapted from Paxinos & Watson, (2007). D, dorsal; R, rostral.

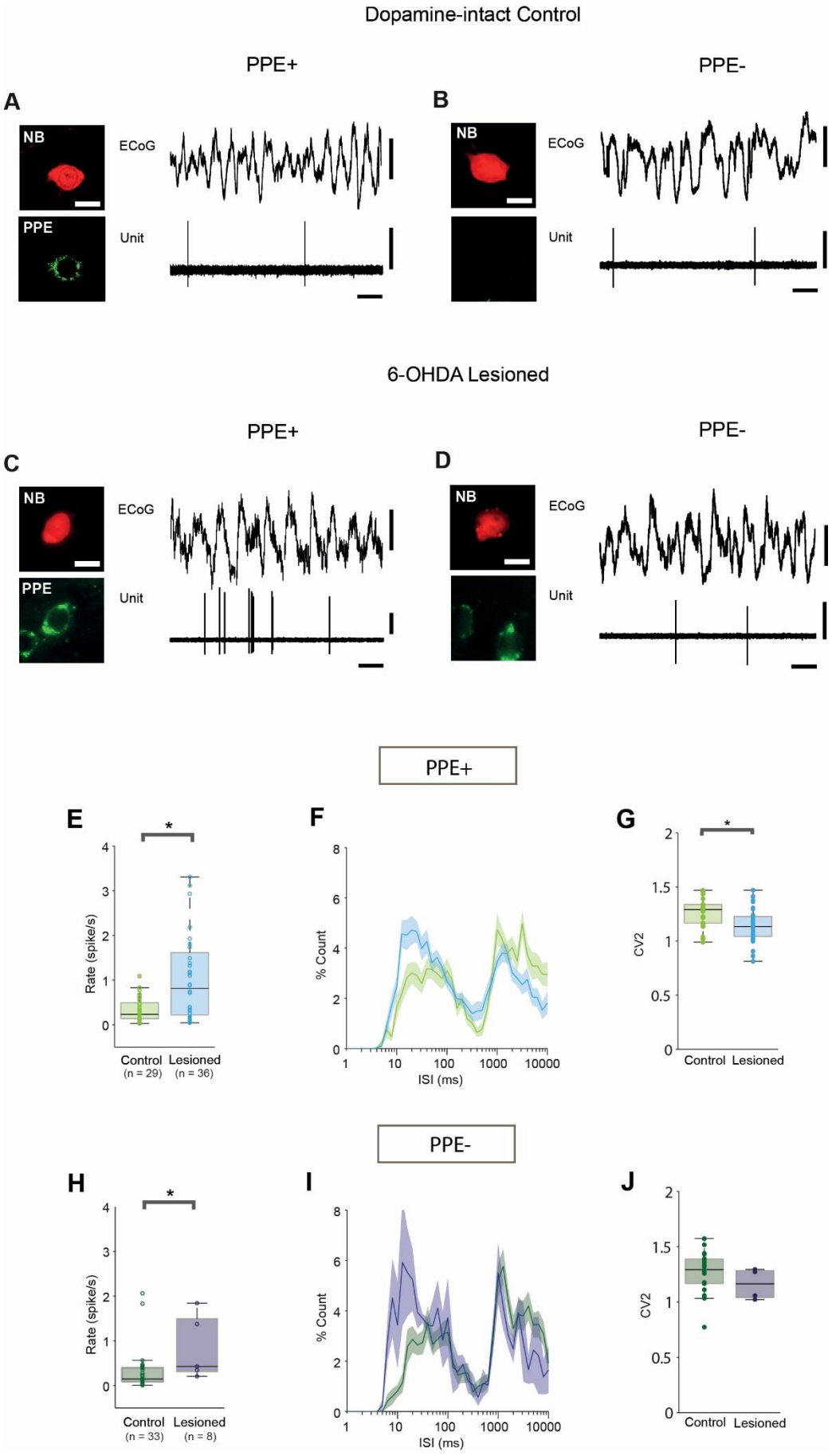
Dopamine-intact Control
PPE+
PPE-
A
B
NB
PPE
ECoG
Unit
6-OHDA Lesioned
C
D
PPE+
PPE-
E
F
G
H
I
J
Rate (spike/s)
Control
Lesioned
(n = 29)
(n = 36)
% Count
ISI (ms)
CV2
(n = 33)
(n = 8)
*

Figure 4.2 **Spontaneous firing of identified indirect and direct pathway MSNs during slow-wave activity in dopamine-intact and 6-OHDA-lesioned rats.** ***A, C,*** Left side, single-plane confocal fluorescence micrographs of neurobiotin (NB)-labelled striatal projection neurons of the indirect pathway that expressed immunoreactivity for preproenkephalin (PPE) in control (A) and in lesioned animals (C). Note PPE immunoreactivity is punctate and largely restricted to somatic cytoplasm. Right side, the action potentials (unit) fired by the same MSNs during spontaneous cortical SWA, as recorded in the electrocorticogram (ECoG). Note that the neurons tended to fire around the peaks of the cortical slow oscillation and that PPE+ MSNs were more active in lesioned animals. ***B, D,*** Single-plane confocal fluorescence micrographs of neurobiotin (NB)-labelled neurons that did not express immunoreactivity for PPE. These cells were identified as striatal projection neurons (of the direct pathway) because their higher-order dendrites were densely laden with spines (not shown). Note neighbouring PPE+ neurons acting as positive controls for the immunoreaction in panel D. Note that PPE- MSNs also tended to fire around the peaks of the cortical slow oscillation. (A-D scale bars of micrographs: 15 µm; Vertical calibration bar, ECoG: 0.5 mV; unit activity 1 mV. Horizontal calibration bar, 1 s) ***E,*** Firing rate of PPE+ MSNs in control (green) and lesioned (blue) animals. All box plots in figures show the medians, the interquartile ranges (box), and extremes of the range (whiskers, within 99% of the distribution). Black bar and asterisk above box plot indicate significant differences across experimental group ($p < 0.05$, Mann-Whitney). The number of neurons included in each group is shown in parenthesis. ***F,*** Mean interspike interval (ISI) histogram for PPE+ neurons recorded in control (green) and lesioned animals (blue). Data are means ± SEM. ***G,*** Firing regularities of PPE+ neurons in control (green) and lesioned animals (blue). Regularity was quantified by CV2 measures, with a lower CV2 reflecting more regular firing. ***H,*** Firing rate of PPE- neurons in control (dark green) and lesioned (violet) animals. *I,* Mean interspike interval (ISI) histogram for PPE- neurons recorded in control (dark green) and lesioned animals (violet). *L,* Firing regularities of PPE- neurons in control (dark green) and lesioned animals (violet). No difference in the firing regularities was observed.

4.4.2 Firing of direct and indirect pathway MSNs in relation to cortical slow oscillations

To investigate the fine temporal relationship between the spike discharges of individual MSNs and the simultaneously-recorded cortical activity, I analyzed how PPE+ and PPE- neurons fired in time with respect to ongoing cortical slow oscillations. Both types of MSNs (PPE+ or PPE-), in both dopamine-intact and lesioned animals fired near the peak of the cortical slow oscillations (Figure 4.2 and 4.3 A-D). The spikes fired by most PPE+ and PPE- were significantly phase-locked to the cortical slow oscillation in both control and lesioned animals as indicated in Figure 4.3 A-D (% of neurons phase-locked to slow oscillations: Control PPE+, 96%; Control PPE-, 87%; Lesioned PPE+, 75%; Lesioned PPE-, 100%). Similarly, population vector lengths, as an indicator of the strengh of phase-locking, were similar across cell types, and relatively large, suggesting the mean angle of firing was highly consistent within each population (Population vector length: Control PPE+, 0.80; Control PPE-, 0.80; Lesioned PPE+ 0.58; Lesioned PPE-, 0.64). Thus, when the dopamine system is intact, direct pathway and indirect pathway MSNs cannot be readily distinguished on the basis of their spontaneous firing rates and patterns *in vivo*. There were no significant differences in mean vector length of individual PPE+ neurons between control and lesioned animals suggesting that the precision of locking to a specific phase of the slow oscillation was unaffected by dopamine loss. However, the population vector length of individual PPE+ neurons was lower in lesioned animals (Control 0.8/Lesion 0.6), suggesting the mean angle of locking across PPE+ neurons was less consistent following dopamine depletion. Only a small number of PPE- neurons were recorded in 6-OHDA-lesioned animals;

of these, only a fraction were useful to compute a phase-locking analysis. Although their distribution as in Figure 4.3 D appears to be random, on average, they were phase-locked to the ascending portion of the cortical slow oscillation as for the other neurons.

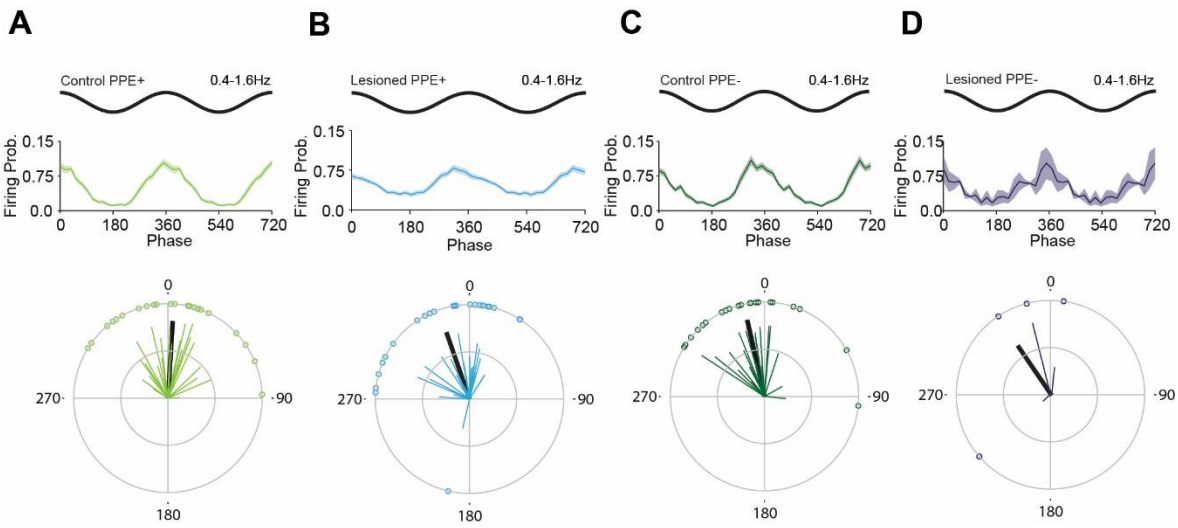

Figure 4.3 **Firing of direct and indirect pathway neurons in relation to ongoing cortical slow oscillations.** ***A-D***, Mean linear phase histograms of all PPE+ MSNs and PPE- MSNs (upper) and circular plots (lower) showing their phase-locked firing during slow oscillations in control and lesioned animals. (Shaded areas in linear phase histograms show SEM). Only those neurons with significantly phase-locked firing are shown in circular plots. Only neurons that fired >40 spikes in a recording session were analysed. Vectors of preferred firing of individual neurons are shown as lines radiating from the centre. Greater vector lengths indicate lower variance in the distribution around the mean phase angle of an individual neurons. Black line radiating from the centre indicates the mean phase angle of all neurons. Each circle on the plot perimeter represents the preferred phase angle of an individual neuron.

4.4.3 Firing rate and pattern of direct and indirect pathway MSNs in dopamine-intact and 6-OHDA-lesioned rats during spontaneous activation

Having established the electrophysiological properties of PPE+ and PPE- MSNs during SWA in dopamine-intact and 6-OHDA-lesioned animals, I next examined the spike firing of these cells types during a brain state of spontaneous cortical activation. In dopamine-intact animals, PPE+ MSNs fired single spikes or small groups of spikes in a sporadic manner (Figure 4.4 A), whereas in 6-OHDA-lesioned animals, most PPE+ neurons fired more sustained trains of spikes at higher frequencies (> 2 spike/s for several seconds; Figure 4.4 C). On average, the firing rate of PPE+ MSNs in lesioned animals was significantly higher compared to neurons control (Control 0.49 ± 0.03 spike/s; mean ± SEM; Lesioned 2.92 ± 0.07 spike/s, mean ± SEM. Mann Whitney, $p = 0.0008$; Figure 4.4 E). It should be noted, however, that a number PPE+ MSNs maintained low firing rates in the same range as those neurons in control animals (Figure 4.4 E). The mean ISI histogram of PPE+ neurons in lesioned animals showed an increase in the proportion of ISIs between 20 ms and 1 s and a decrease in very long (> 2 s) intervals (Figure 4.4 F). The firing regularities of PPE+ neurons significantly changed after dopamine loss. Indeed PPE+ neurons in lesioned animals showed a small, but significant shift to more regular firing compared to those in controls (CV2 Control 1.1 ± 0.08; Lesion 0.98 ± 0.03; Figure 4.4 G). I next tested whether these changes for PPE+ neurons also applied to PPE- neurons. There was no significant difference in the firing rates of PPE- MSNs in control and lesioned animals (Control 1.04 ± 0.1 spike/s; mean ± SEM; Lesioned 1.14 ± 0.2 spike/s, mean ± SEM. Figure 4.4 B, D, H). The ISI

histograms of PPE- neurons in control and lesioned animals was also similar (Figure 4.4 I). Moreover, no differences were observed in the firing regularities of PPE- neurons in control and lesioned animals (CV2 Control 1.09 ± 0.01; Lesioned 1.0 ± 0.03. Figure 4.4 J). In summary, following dopamine depletion, PPE+/indirect pathway MSNs significantly increased their firing rates and regularities during cortical activation, whereas PPE-/direct pathway MSNs were not likewise affected.

Finally, to understand whether brain state had an impact on the activities of identified MSNs, I compared the firing rates of control and lesioned PPE+ and control and lesioned PPE- neurons during different brain states. I found that the brain state has only a minor impact on the firing rate of most of the group analyzed, with the exception of PPE+ MSNs which showed a significant increase in their firing rates during cortical activation as compared to SWA (Mann Whitney = 0.0050).

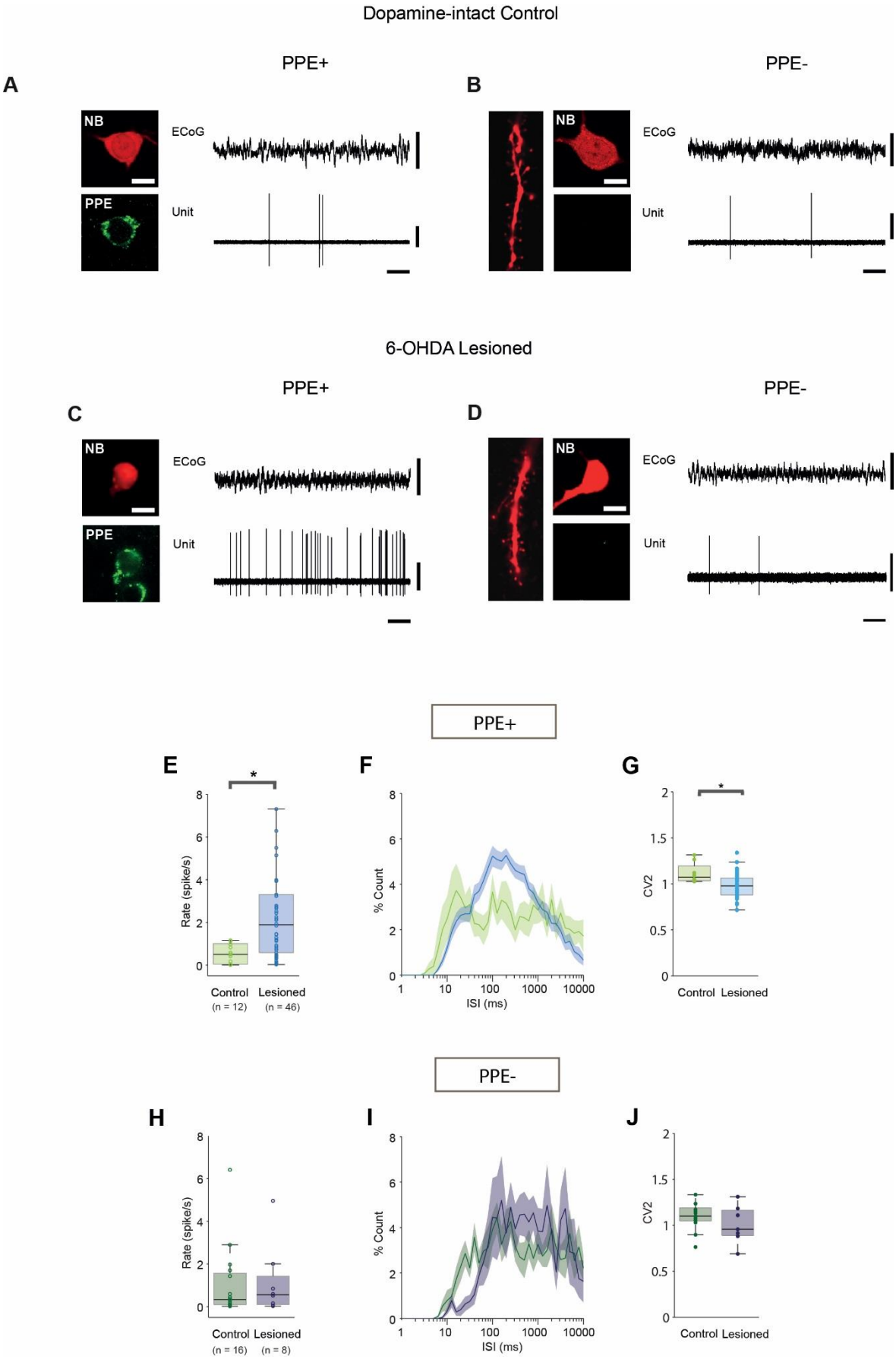
Dopamine-intact Control
PPE+
PPE-
A
B
NB
PPE
ECoG
Unit
6-OHDA Lesioned
C
D
PPE+
PPE-
E
F
G
H
I
J
Rate (spike/s)
% Count
ISI (ms)
CV2
Control
Lesioned
(n = 12)
(n = 46)
(n = 16)
(n = 8)

Figure 4.4 **Spontaneous firing of identified indirect and direct pathway MSNs during spontaneous activation in dopamine-intact and 6-OHDA-lesioned rats.** ***A, C,*** Left side, single-plane confocal fluorescence micrographs of neurobiotin (NB)-labelled striatal projection neurons of the indirect pathway that expressed immunoreactivity for preproenkephalin (PPE) in control (A) and in lesioned animals (C). Note PPE immunoreactivity is punctate and largely restricted to somatic cytoplasm. Right side, the action potentials (unit) fired by the same MSNs during spontaneous activation, as recorded in the electrocorticogram (ECoG) Note that PPE+ MSNs are more active in lesioned animals. ***B, D,*** Single-plane confocal fluorescence micrographs of neurobiotin (NB)-labelled neurons that did not express immunoreactivity for (PPE). These cells were identified as striatal projection neurons (of the direct pathway) because their higher-order dendrites were densely laden with spines. (A-D scale bars of micrographs: 15 µm; ECoG: 0.5 mV; unit activity 1 mV). ***E,*** Firing rate of PPE+ MSNs in control (green) and lesioned (blue) animals. The number of neurons included in each group is shown in parenthesis. All box plots in figures show the medians, the interquartile ranges (box), and extremes of the range (whiskers, within 99% of the distribution). Black bar and asterisk above box plot indicate significant differences across experimental group ($p < 0.05$, Mann-Whitney). ***F,*** Mean interspike interval (ISI) histogram for PPE+ MSNs recorded in control (green) and lesioned animals (blue; shaded areas shows SEM). ***G,*** Firing regularities of PPE+ MSNs in control (green) and lesioned animals (blue) during cortical activation. Regularity was quantified by CV2 measures, with a lower CV2 reflecting more regular firing. ***H,*** Firing rate of PPE- MSNs in control (dark green) and lesioned (violet) animals. No significant differences were observed. ***I,*** Mean interspike interval (ISI) histogram for PPE- neurons recorded in control (dark green) and lesioned animals (violet). ***L,*** Firing regularities of PPE- MSNs in control (dark green) and lesioned animals (violet). No difference in the firing regularities was observed.

4.4.4 Firing of direct and indirect pathway MSNs in relation to cortical beta oscillations during spontaneous activation

To better understand the temporal relationship between the spike firing of individual, identified MSNs and ongoing cortical beta activity, analyses of the preferred phase of firing of PPE+ and PPE- neurons in control and lesioned animals were performed. In the control animals, PPE+ MSNs had, on average, a weak preference to fire around the troughs of the cortical beta oscillation, with only 12.5% of neurons being significantly locked (Figure 4.5 A, E). In lesioned animals, PPE+ neurons also preferentially fired around the troughs of the beta oscillation, but with a much stronger tendency (Figure 4.5 B) such that 50% of the individual neurons were significantly locked (Figure 4.5 E, F). In contrast, PPE- MSNs showed no obvious phase preference in dopamine-intact animals, with only 7.7% of neurons phase-locked to cortical beta oscillations (Figure 4.5 C, E). Finally only 14.3% of PPE- MSNs in lesioned group were significantly phased-locked (Figure 4.5 D, E). This is the first evidence that the firing of neurochemically-identified striatal MSNs is temporally related to ongoing beta activity and, importantly, that a large proportion of indirect pathway PPE+ MSNs are entrained to cortical beta oscillations in Parkinsonism.

Given that identified PPE+ MSNs recorded in the lesioned animals showed the greatest propensity to fire phase-locked to cortical beta oscillations, I hypothesized that these neurons would comprise the majority of units in the synchronized striatal neuron pairs recorded in lesioned animals by means of multi-electrode arrays (see Chapter 3).To test this, I first isolated 264 pairs of units that had properties matching those of most identified PPE+ MSNs, namely a firing rate

of 2-8 spike/s (Figure 4.4 E) and a preferred phase angle, with respect to cortical beta, between 90° and 270° (Figure 4.5 F). I also isolated 250 pairs of units that had properties similar to those of the most identified PPE- MSNs (firing rate <1 spike/s and mean cortical beta angle from 270° and 90°). I then recomputed CCHs for pairs of putative PPE+ MSNs (pPPE+), for pairs of putative PPE- MSNs (pPPE-) and for pairs consisting of one pPPE+ and one pPPE- neuron (70 pairs of neurons). The results of this investigation showed that nearly 50% of the pPPE+/pPPE+ unit pairs were significantly correlated at zero lag, in comparison to under 20% for the other pair types (Figure 4.6 A-C). Moreover, the power spectra of the CCHs of pairs of pPPE+ MSNs had a prominent peak in the beta range, which was significantly larger than the spectral powers of the CCHs of other pair types (Figure 4.6 D). Additionally, when these pair groups were plotted as a function of distance between the two recorded units, there were at least twice as many synchronized pairs of PPE+ MSNs at zero lag than there were for the other pair types across distances of up to 900 μm (Figure 4.6 E). Thus putative PPE+ MSNs become highly synchronized across large areas of striatum after dopamine loss.

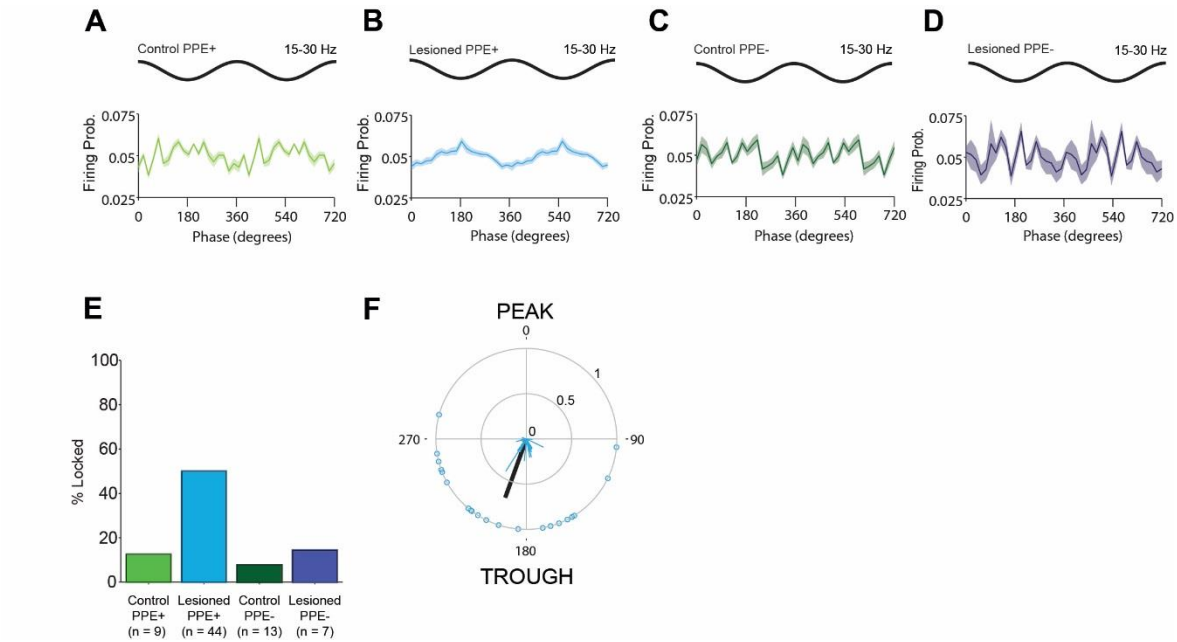

Figure 4.5 **Firing of direct and indirect pathway MSNs with respect to cortical beta oscillations in dopamine-intact and 6-OHDA-lesioned animals.** ***A-D,*** Mean linear phase histograms of all PPE+ and PPE- MSNs recorded in control and lesioned animals during cortical beta oscillations. For clarity, two oscillations cycles are shown. Shaded areas show SEM. ***E,*** Histogram showing the percentage of neurons phase-locked to beta oscillations. ***F,*** Circular plot of preferred firing angles of significantly-locked PPE+ neurons in lesioned animals. Each circle on the plot perimeter represents the preferred phase angle of an individual neuron. PPE+ neurons in lesioned animals tended to fire around the troughs of the cortical beta oscillations. Vectors of preferred firing of individual neurons are shown as lines radiating from the centre. Black line radiating from the centre indicates the mean phase angle of all neurons. Greater vector lengths indicate lower variance in the distribution around the mean phase angle of an individual neurons.

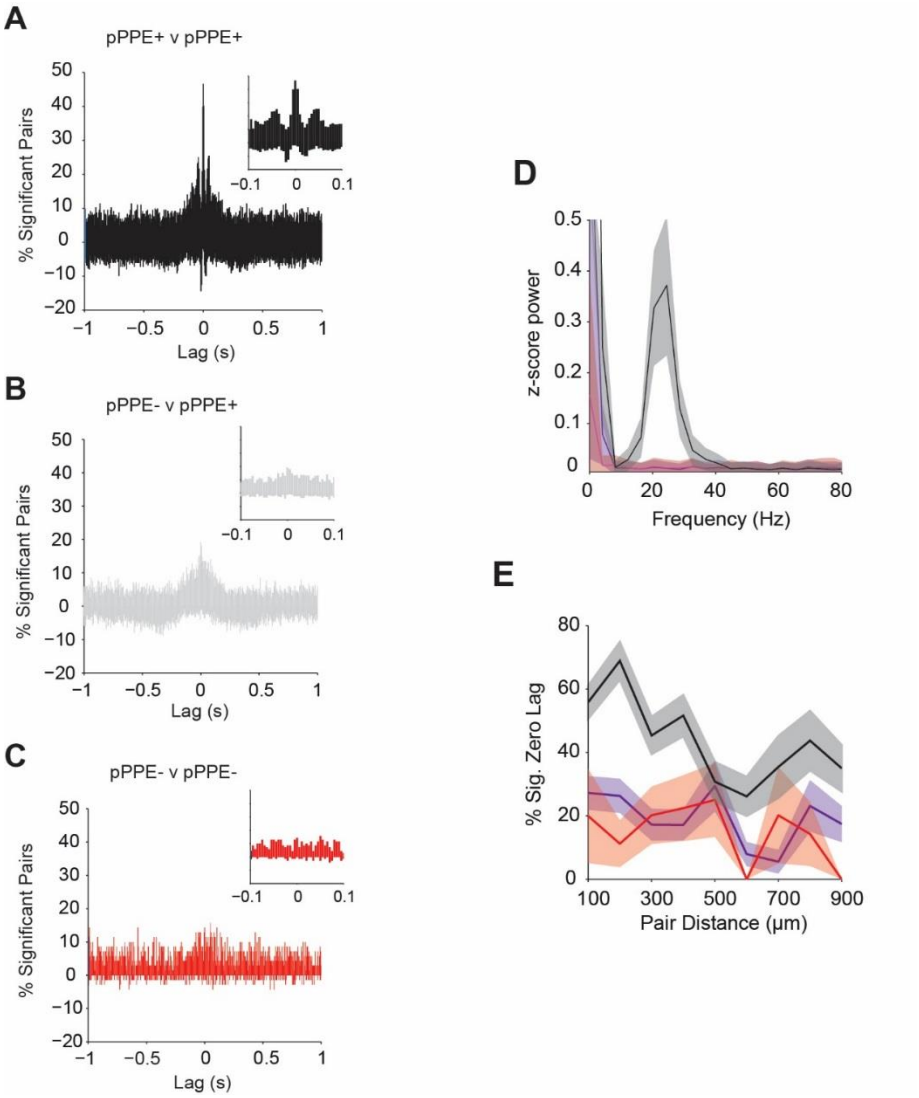

Figure 4.6 **Dopamine loss leads to a selective increase in the synchronization of firing in ensembles of putative PPE+ MSNs.** ***A-C,*** Unit pairs from 6-OHDA-lesioned animals were divided into three categories based on whether neither, one or both units displayed the characteristics of PPE+ MSNs. Histograms of the percentage of striatal unit pairs that were significantly correlated at given lags during beta activity, for units divided into putative PPE+/PPE+ (A), PPE-/PPE+ (B) and PPE-/PPE- unit pairs (C). Note that only the pPPE+/pPPE+ neurons pair present strong synchronization at beta frequency. ***D,*** Power spectra of the CCHs of the different types of striatal unit pairs in A-C (colours are the same). ***E,*** Mean percentage of significant correlations at zero lab between the putative neuron pairs in A-C (colours are the same) as a function of the distances between the probe contacts on which they were recorded.

4.5 Both direct and indirect pathway MSNs can be quiescent after dopamine loss

Previous observations in this thesis (see Chapter 3 and Figure 4.2) suggest (in agreement with previous studies), that in 6-OHDA-lesioned animals, a significant proportion of direct pathway neurons are silent, irrespective of the brain state (Albin *et al.*, 1989; DeLong, 1990; Mallet *et al.*, 2006). Hence, I examined which types of MSN were apparently silent during cortical activation when aberrant beta oscillations are present. Thus, I used paired-pulse cortical stimulation (see section 2.4) to elicit action potentials from 19 MSNs recorded in 5 lesioned rats (see Table 4B for details) that would be otherwise silent, and then identified them as direct or indirect pathway neurons (Figure 4.7). The spontaneous firing rate of each of these neurons was assessed from recordings in the absence of cortical stimulation, which was reinstated at the end of the recording session to ensure the neuron was suitable for labelling (Figure 4.7 A, B).

MSN type	n	Brain state	Latency (ms)		Spontaneous firing
			Stim 1	Stim 2	Rate (spike/s)
PPE+	10	Activated	7.9 ± 0.84	8.8 ± 0.89	0.05 ± 0.02
PPE-	9	Activated	7.7 ± 0.75	8.4 ± 1.1	0.02 ± 0.02

Table 4B **Detection of quiescent MSNs in Parkinsonian rats by ipsilateral cortical stimulation.** Spontaneous firing rate was assessed during spontaneous activation in the absence of cortical stimulation. Latency of first spike fired in response to first or second stimulation pulse (Stim 1, Stim 2). Similar numbers of direct and indirect MSNs are virtually quiescent (< 0.1 spike/s).

Stimulation-“detected” neurons that showed periods of quiescence lasting hundreds of seconds were subsequently found to be MSNs of both pathways (Figure 4.7 A, B). Approximately half of these quiescent MSNs were identified as PPE+, showing that in addition to a population of silent direct pathway MSNs, there is also a similarly-sized population of silent indirect pathway MSNs (Figure 4.7 A, B). With respect to responses to cortical stimulation, PPE+ MSNs, but not PPE- MSNs, fired with higher probability after delivery of the second stimulation pulse (Figure 4.7 C, D, G, H). However, both types of quiescent MSNs responded with a longer latency to the second pulse (Figure 4.7 E, I), but only PPE+ neurons had significantly less variability in the latency of firing to the second pulse (Figure 4.7 F, J). These data show that, first, both types of MSNs can be quiescent (and have approximately equal chance of being so) during cortical activation and, secondly, that direct and indirect pathway MSNs have different responses to cortical input in lesioned animals.

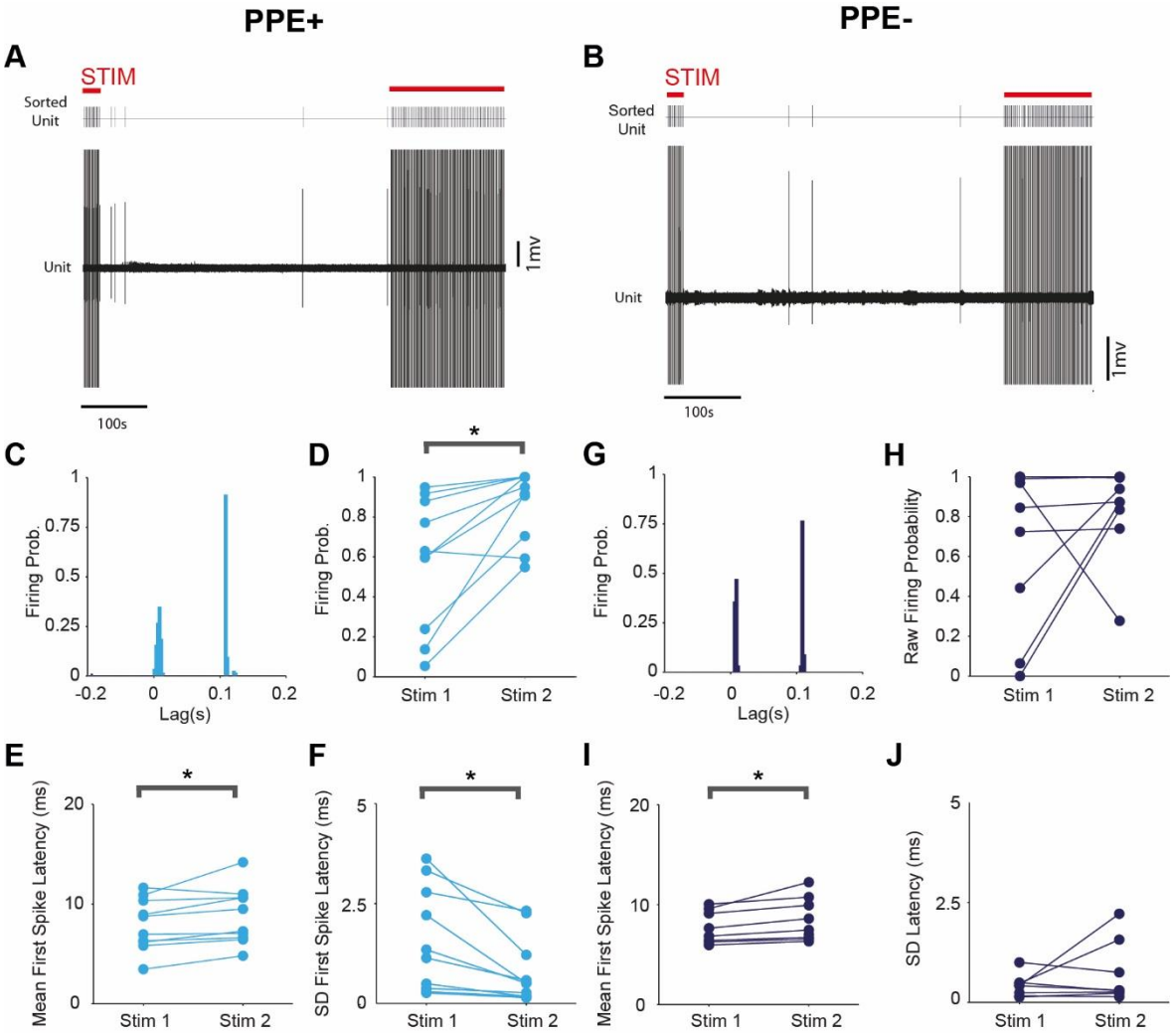
PPE+
PPE-
A
B
STIM
Sorted Unit
Unit
1mv
100s
C
D
G
H
Firing Prob.
Lag(s)
Raw Firing Probability
Stim 1
Stim 2
*
E
F
I
J
Mean First Spike Latency (ms)
SD First Spike Latency (ms)
SD Latency (ms)

Figure 4.7 **Both direct and indirect pathway MSNs are quiescent during the activated brain state in lesioned animals.** ***A,*** Representative trace of a quiescent PPE+ (indirect pathway) MSN “detected” by paired cortical stimulation. When the stimulation is off, the neuron does not fire for extended periods (hundreds of seconds) defining it as quiescent. The neuron then responds to virtually every electrical pulse when cortical stimulation resumes (see sorted unit). ***B,*** Representative trace of a quiescent PPE- (direct pathway) MSN detected by paired cortical stimulation. The neuron displays similar firing to that in A. ***C,*** Representative responses of a quiescent PPE+ MSN to paired cortical stimulation. ***D,*** Quiescent PPE+ neurons MSNs exhibit a significantly greater probability of firing in response to the second stimulation pulse (Stim 2). ***E*****,** Quiescent PPE+ neurons had a significantly longer latency to respond to the second stimulation pulse. ***F*****,** Quiescent PPE+ neurons had significantly less variability in firing latency on the second stimulation pulse. ***G,*** Representative responses of a quiescent PPE- MSN to paired cortical stimulation. ***H*****,** Although some PPE- MSNs responded with a higher probability to the second pulse, the average response of these neurons did not change between the first and second pulses. ***I*****,** Quiescent PPE- neurons had significantly longer latency to respond to the second cortical stimulation. *J*, Quiescent PPE- neurons had did not have a significantly different latency between first and second pulses.

4.6 Spontaneous firing of identified striatal interneurons in 6-OHDA-lesioned animals

Striatal interneurons comprise only 5-10% of all striatal neurons and are believed to powerfully modulate MSN activity (Tepper *et al.,* 2010). Defining the activity of striatal interneurons *in vivo* is challenging, not only because of their scarcity, but also because of the functional heterogeneity of these cell populations (see sections 1.2 and 1.3). Recently, Sharott and colleagues (2012) defined the spontaneous firing of cholinergic interneurons (ChAT+), parvalbumin-expressing interneurons (PV+), and nitric oxide synthase-expressing interneurons (NOS+) in anaesthetised, dopamine-intact rats. How chronic dopamine loss impacts on the electrophysiological properties of these and other types of striatal interneurons *in vivo* is unknown. During the course of this thesis research, I recorded, labelled and identified a few examples of four types of striatal interneuron (ChAT+, PV+, NOS+ and calretinin-expressing (CR+) interneurons, in 6-OHDA-lesioned rats (Table 4C and Figure 4.8 A-D). The ChAT+ interneuron was recorded during SWA and displayed a very low firing rate, with spike firing aligned to the peaks of cortical slow oscillations (Figure 4.8 A). Three PV+ were recorded during spontaneous activation (see Figure 4.8 B). These interneurons exhibited highly diverse firing rates, ranging from near quiescence to robust tonic firing (see Table 4C). The NOS+ interneuron, which also expressed neuropeptide Y (NPY), fired at comparatively low rates and with irregular firing patterns irrespective of the brain state (Figure 4.8 C).The CR+ interneuron was recorded during spontaneous activation and fired at a moderate rate and irregular manner, with some occasional bursting activity (Figure 4.8 D).

Because of the limited number of observations, it is not possible to draw any firm conclusions with respect to how dopamine loss impacts on the firing of these interneurons. However, these initial experiments are encouraging and suggest it should eventually be possible to define any alterations in the activity of one or more interneuron classes.

Interneurons in 6-OHDA-lesioned animals				
Cell ID	Cell type	Brain state	Rate (spike/s)	CV2
Fjxl006/cell i	ChAT+	SWA	0.35	2.6
Fjxl006/cell g	PV+	ACT	5.51	0.18
Kjxl128/cell g	PV+	ACT	17.39	0.05
Kjxl149/cell e	PV+	ACT	0.1	9.34
Fjxl022/cell n	PV+	SWA	9.52	0.09
Fjxl002/cell i	NOS+	ACT	0.55	1.78
Fjxl002/cell i	NOS+	SWA	1.36	0.73
Kjxl125/cell l	CR+	ACT	3.24	0.30

Table 4C **Firing rate and pattern of identified striatal interneurons recorded in 6-OHDA lesioned animals.** Analyses of the firing rate and regularities was performed in sample of different types of interneurons recorded during different brain state.

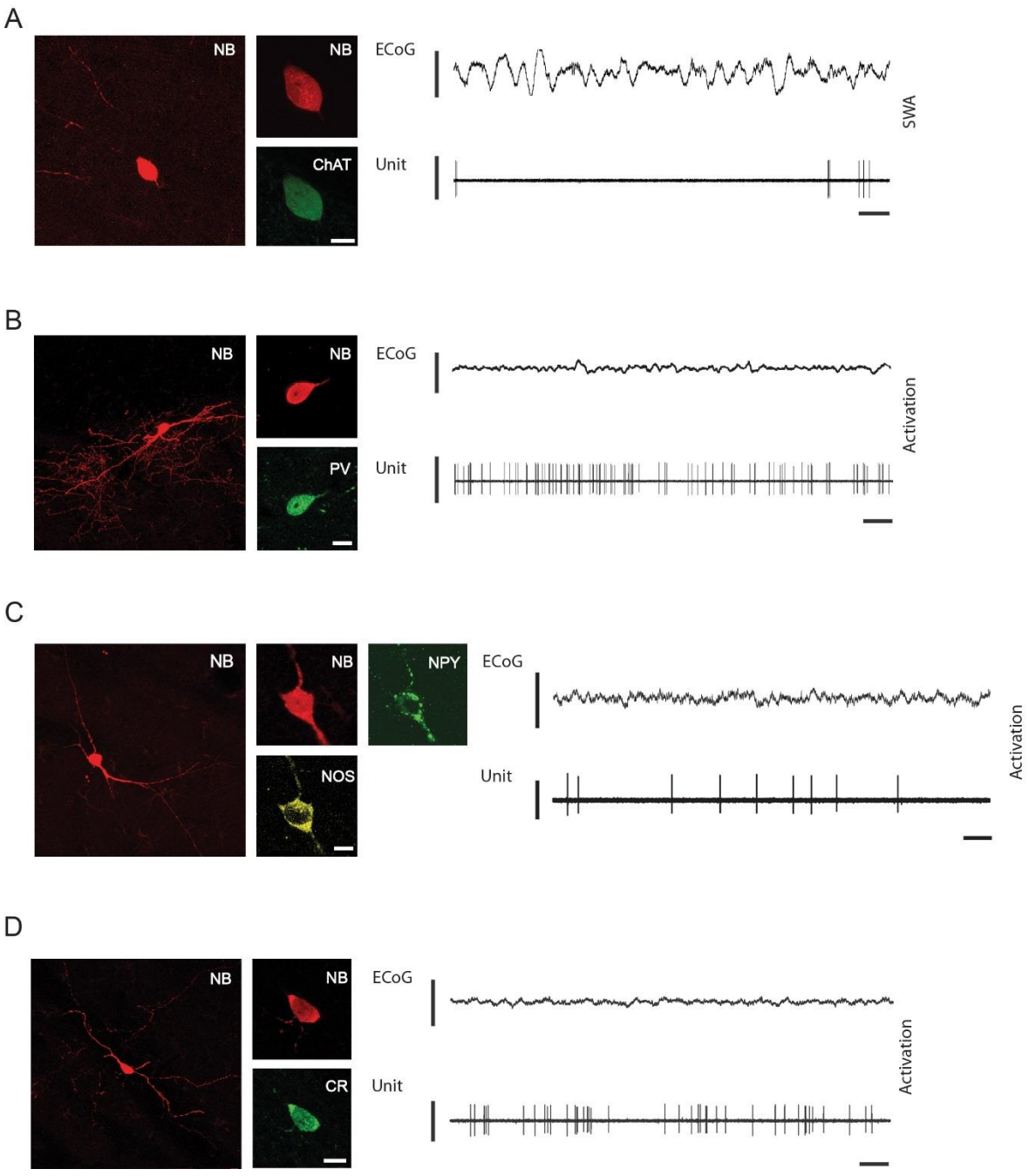
A
NB
NB
ChAT
ECoG
Unit
SWA
B
NB
NB
PV
ECoG
Unit
Activation
C
NB
NB
NPY
NOS
ECoG
Unit
Activation
D
NB
NB
CR
ECoG
Unit
Activation

Figure 4.8 **Spontaneous firing of identified striatal interneurons in 6-OHDA-lesioned rats.** ***A,*** Left side, confocal fluorescence micrographs of a neurobiotin (NB)-labelled cholinergic interneuron identified by its expression of choline acetyltransferase (ChAT). Right side, action potentials (unit activity) of the same neuron during cortical slow-wave activity, as recorded in the electrocorticogram (ECoG). ***B,*** Left side, micrographs of a NB-labelled GABAergic interneuron that expressed parvalbumin (PV). Right side, Spontaneous firing of the same PV+ interneuron during cortical activation. ***C,*** Left side, micrographs of a NB-labelled GABAergic interneuron that co-expressed nitric oxide synthase (NOS) and neuropeptide Y (NPY). Right side, Spontaneous firing of the same NOS+/NPY+ interneuron during cortical activation. ***D,*** Left side, micrographs of NB-labelled GABAergic interneuron that expressed calretinin (CR). Right side, spontaneous firing of the same CR+ neuron during cortical activation. Horizontal scale bars: micrographs, 20 µm; 1 second. Vertical scale bars: ECoG, 0.5 mV; Unit, 1mV

4.7 Spontaneous firing of identified MSNs located in ‘patches’ in dopamine-intact and 6-OHDA-lesioned animals

Striatum is organized in patch/striosome and matrix compartments (see section 1.2.2). The electrophysiological properties of neurochemically-identified MSNs in the patch compartments are unknown. The present study included recordings of 13 neurochemically-identified MSNs localized to patches, in both dopamine-intact and 6-OHDA-lesioned animals, during two well defined brain states (Figure 4.9 A-C and Table 4D for details). Patch compartments were defined as areas of striatal neuropil with intense immunoreactivity for mu opioid receptors (MOR), and include the subcallosal streak. During slow-wave activity patch MSNs present a low firing and irregular pattern with single group of units firing at the peak of the slow oscillations (Figure 4.9 A, B). During spontaneous activation, patch MSNs moderately increased their firing rate, displayed some bursting activity and presented an irregular pattern (Figure 4.9 C). As mentioned in section 2.6.1 of the methods chapter, to optimize immunolabelling for PPE, a heat pre-treatment was used as a means of antigen retrieval. It is possible that the enhanced fluorescence of the fibres crossing striosome (see Figure 4.9 C) are due to this treatment. Qualitative assessments of patch MSN firing rates and patterns indicated no apparent differences compared to MSNs located in the matrix (for this reason, patch and matrix MSNs were pooled in all previous analysis), although because of low number of observations, no statistical analysis was performed.

Dopamine-intact Group					
PPE+ SWA			PPE+ ACT		
Cell	Rate (spike/s)	CV2	Cell	Rate (spike/s)	CV2
Fjx037/cell c	0.17	5.72	Njx027/cell b	1.06	0.94
Njx027/cell b	0.55	1.36			
Fjx022/cell c	0.56	1.76			
PPE- SWA			PPE- ACT		
Cell	Rate (spike/s)	CV2	Cell	Rate (spike/s)	CV2
Fjx021/ cell d	0.20	4.68	Fjx026/ cell a	0.11	6.83
Fjx028/ cell f	0.09	10.90	Fjx028/ cell d	1.97	0.51

6-OHDA-lesioned Group					
PPE+ SWA			PPE+ ACT		
Cell	Rate (spike/s)	CV2	Cell	Rate (spike/s)	CV2
Fjxl012/ cell d	1.85	0.53	Fjxl012/ cell d	0.89	1.13
Fjxl022/ cell i	2.18	0.46	Fjxl012/ cell m	1.46	0.69
			Fjxl012/ cell e	2.78	0.36
PPE- SWA			PPE- ACT		
Cell	Rate (spike/s)	CV2	Cell	Rate (spike/s)	CV2
Fjxl019/ cell g	1.84	0.54	Fjxl028/ cell a	1.97	0.51
Fjxl028/ cell f	0.09	10.90			

Table 4D **Firing rates and patterns of identified MSNs located in striatal patches.** Identified MSNs located in patches are shown according to their expression of neuropeptide PPE, ongoing cortical activity and experimental group (dopamine-intact, 6-OHDA-lesioned).

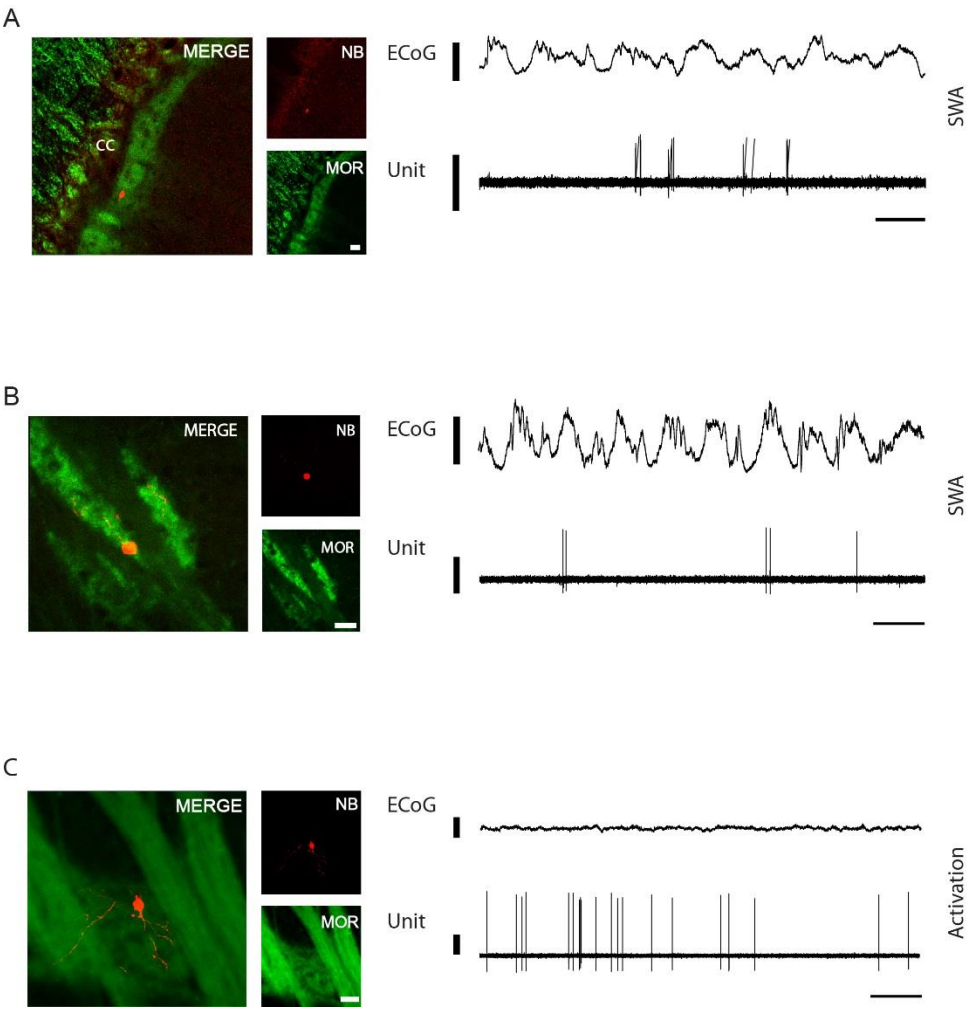

Figure 4.9 **Spontaneous firing of identified MSNs in 'patch' compartments in dopamine-intact rats.** ***A,*** Left side, confocal fluorescence micrographs of a neurobiotin (NB)-labelled MSN located in the subcallosal streak. These and others patch were identified by intense expression of immunoreactivity for mu opioid receptors (MOR). Right side, action potentials of the same MSN during spontaneous cortical slow-wave activity, as recorded in the electrocorticogram (ECoG). ***B,*** Left side, micrographs of a NB-labelled MSN in one of the central patches of striatum. Right side, spontaneous firing of the same neuron during slow-wave activity. ***C,*** Left side, micrographs of another NB-labelled MSN localized in a 'patch'. Right side, spontaneous firing of the same neuron during spontaneous activation. (Note the fibres of striatum enhanced due to the heat treatment of the section). All MSNs were further identified as PPE+ (micrographs not shown). Horizontal scale bars: micrographs, 20 µm; 1 second. Vertical scale bars: ECoG, 0.5 mV; Unit, 1mV. Cc, corpus callosum.

4.8 Discussion

The investigations described in this chapter allowed me to reach two key conclusions. First, that indirect pathway *(*PPE+) MSNs significantly enhance their firing rate (irrespective of brain state) and engage in aberrant beta oscillations after chronic dopamine loss. Although direct pathway (PPE-) MSNs also showed an enhanced firing rate during slow-wave activity, the firing of these neurons were rarely locked to beta oscillations. Second, that similar numbers of direct and indirect pathway MSNs are virtually quiescent after chronic dopamine loss. These data converge to suggest that increases in the firing rate and synchronization of a sub-population of indirect pathway MSNs is important for the generation and dissemination of excessive beta oscillations throughout the BG in Parkinsonism.

Dopamine depletion has a large impact on the firing of indirect pathway MSNs

The classical model for explaining the effects of chronic loss of dopamine on direct and indirect pathways predicts an imbalance in favour of the indirect pathway (Albin *et al.*, 1989; DeLong, 1990). As introduced in the previous chapter, several studies show that, on average, the discharge activity of unidentified striatal neurons is enhanced in 6-OHDA-lesioned rats (Schultz & Ungerstedt, 1978; Alloway & Rebec, 1984; Kish *et al.*, 1999; Chen *et al.*, 2001; Pang *et al.*, 2001; Tseng *et al.*, 2001; West & Grace, 2002). However, although these studies were informative about the overall electrophysiological differences of striatal cell populations under pathological conditions, they provided no direct insights into which types of striatal neuron were affected by dopamine loss, nor to what extent they were impaired, nor how different

brain states impacted on striatal neuron firing. Here, I show that, irrespective of the brain state, neurochemically-identified indirect pathway MSNs, significantly enhance their firing rates after chronic dopamine loss. This finding is in agreement with previous literature showing that, during SWA activity, a small sample of identified PPE+ MSNs were hyperactive in lesioned animals (Mallet *et al.*, 2006). By defining the electrophysiological properties of larger cohorts of identified PPE+ MSNs in dopamine-intact and 6-OHDA-lesioned animals across different brain states, I provide compelling evidence validating one key prediction of the classical model of BG dysfunction in Parkinson's disease. However, my data do not confirm a second key prediction, namely that direct pathway MSNs are hypoactive after dopamine loss. Indeed, during SWA, identified PPE- MSNs in the lesioned group tended to fire at significantly higher rates compared to neurons in the control group, and no differences in firing rates were observed during spontaneous activation. As mentioned before, accumulating evidence has challenged this classical view of imbalanced direct and indirect pathways in PD (see section 1.6.1). For instance, this model predicts that the main motor symptoms of PD (i.e. bradykinesia and akinesia) are the result of the elevated firing rate of BG output nuclei neurons. However, studies in both animal models and PD patients show only a small increase (or no increase) in GPi firing rate, which is likely not of sufficient strength to affect thalamic and cortical structures (Wichmann *et al.*, 1994b; Wichmann *et al.*, 1999; Raz *et al.*, 2000b; Levy *et al.*, 2001; Hutchison *et al.*, 2004; Rivlin-Etzion *et al.*, 2008). Other studies in a monkey model of PD, showed that the induced stimulation of STN which increases GPi neuron firing, is actually associated with motor improvement (Hashimoto *et al.*, 2003). My result showing that PPE- MSNs become hyperactive in SWA after chronic dopamine loss is in contrast with the results of another study

(Mallet *et al.*, 2006), which showed that direct pathway MSNs (detected by antidromic stimulation of SNr), present a markedly low firing rate in SWA in lesioned animals. The experimental approach of Mallet and colleagues (2006) mentioned above, distinguished direct and indirect pathway MSNs on the basis of their responsiveness to antidromic stimulation of the SNr only. Although this approach is compatible with anatomical evidence (PPE- neurons constitute the group of striatal projection neurons that monosynaptically innervate the SNr output nucleus of the BG), the local electrical stimulation of the SNr cannot guarantee an efficient stimulation of all MSNs (thus, neurons not responding to SNr stimulation could still be direct pathway MSNs). Moreover, direct pathway neurons are known to send collaterals to GPe. Additionally, for those few putative direct pathway MSNs recorded, no further histochemical identification was implemented and the identity of those neurons was investigated during SWA only. Hence, the research in this thesis provides the first unbiased recording and identification of direct and indirect pathway MSNs and evidence how their physiology is affected after dopamine loss. The number of PPE- MSNs recorded in 6-OHDA-lesioned animals was low compared to that recorded in controls. Future studies could work to increase the sample size of the PPE- neurons recorded in Parkinsonian animals to fortify the statistical reliability of this result of the firing rate. When results of this chapter were compared with the data obtained with the use of silicon probe, minor differences were noted. For instance, compared to identified MSNs, the firing rate of single units recorded with probes of both control and lesioned group was slightly higher, irrespective of the brain state. Because it was not possible to verify the identities of the cells recorded with silicon probes, s it is possible that some interneurons were taken into account and those, in turn, increased the average firing rate of the overall

population. Similarly, differences in the coefficient of variation were noted, and these, again, can be due to fact that interneurons, which are known to have varied firing patterns, were taken into account.

To investigate the relationship between the firing of identified PPE+ or PPE- MSNs and cortical brain states, I analysed the temporal dynamics between spike discharges and the simultaneously recorded ECoG oscillations. As for the investigation detailed in Chapter 3, all recordings in this chapter were conducted under general anaesthesia and thus the ECoG was either characterized by slow oscillations (~1 Hz) or by higher-frequency oscillations (Tseng *et al.*, 2001; Mallet *et al.*, 2005; Sharott *et al.*, 2012) (see section 2.2). In agreement with previous studies (Mallet *et al.,* 2006), I show that dopamine loss did not alter the temporal relationship between the firing of identified MSNs and cortical slow oscillations, with individual neurons, in every condition, presenting a preferred mean angle of firing at around the peak of slow oscillations. This is consistent, as for the analyses described in Chapter 3, that slow oscillations enable the firing of MSNs by oscillating between a hyperpolarized, quiescent state and a depolarized state that enables firing to occur.

During the activated state, the firing of PPE- neurons in both control and lesioned animals were only rarely phase-locked to the cortical beta oscillations. With respect to PPE+ MSNs, only a few neurons in the control group fired in phase with beta activity, but when the same cell-type was analysed after chronic dopamine loss, their tendency to phase-lock was much stronger, with ~50% of the population firing in phase with cortical beta activity. This is in agreement with a previous study of striatal LFPs in lesioned rats (Moran *et al.,* 2011), and computational investigations of the striatal microcircuit in Parkinsonism (McCarthy *et al.*, 2011; Damodaran *et al.*,

2015), which predict that the firing of striatal neurons is aberrantly synchronized at beta frequencies after chronic dopamine loss. Given that PPE+ MSNs are more likely to lock to cortical beta activity, it is possible that this specific population is more predisposed to engage in beta activity after dopamine loss. When analyses of the responses to cortical electrical were performed, I showed that direct and indirect pathway MSNs responded differently to electrical stimuli. Hence, it is possible that PPE+ and PPE- present distinct intrinsic mechanisms to respond to cortical inputs. If so, then it is possible that other intrinsic mechanism (e.g. conductances, excitability level, anatomical connection) could play a key role in favouring one population, over another, to become engaged in aberrant synchronization. Analysis of the phase angle of firing of PPE+ MSNs in the lesioned group shows that identified neurons preferentially fire at the trough of the oscillations. This is not only consistent with the finding described in Chapter 3 (see Figure 3.7 D), but also with the overall idea that indirect pathway neurons are in a leading position to propagate aberrant oscillations to the GPe, STN and then to the downstream BG network. As stated before, most GPe neurons in lesioned animals fire less at this phase of cortical beta oscillation (Mallet *et al.*, 2008a). Thus, it is tempting to speculate that the reduced firing of the GPe neurons results from the increased firing of PPE+ MSNs. To further investigate how PPE+ MSNs synchronize their activity during beta oscillations, I reanalysed unit activity data recorded from multi-electrode arrays. I decomposed the units into three functional groups: the first group contained pairs of neurons that displayed the firing characteristics of identified PPE+ neurons in lesioned animals (i.e. high firing rate and mean phase angle at around the trough of beta oscillations); the second consisted of neurons with opposite characteristics and were assumed to be PPE- MSNs; and the third group was composed of pairs of

putative PPE+ and PPE- MSNs. The results of this analysis indicated that dopamine loss leads to a selective increase in the synchronization of firing of PPE+ neurons. Additionally, this group of paired units was the only one showing a prominent peak in the power spectrum at beta frequencies. These data further support the idea that aberrantly synchronized output of indirect pathway MSNs underlie the phase preference of GPe neurons.

Finally, when analyses of firing rates was performed to understand whether and how brain state impacted on PPE+ MSNs, I found that during spontaneous activation their firing rates were significantly higher. This is in agreement with the view that cortical slow oscillations dictate a limited time-window in which MSNs can fire. In absence of slow oscillations, the firing of MSNs is not as limited and therefore they can fire more frequently. In conclusion, this study provides new insights into how the activity of identified striatal cell-types relates to aberrant synchronization and, in particular, how PPE+ neurons are positioned to spread the abnormal beta oscillations occurring in PD.

A subset of indirect pathway MSNs are quiescent after dopamine loss

Previous experiments/analyses in this thesis (see section 4.6) showed that a fraction of PPE+ MSNs, recorded during spontaneous activation, were virtually quiescent after chronic dopamine loss. To further investigate their firing properties, and to overcome the technical challenge of extracellularly-recording quiescent neurons, I decided to elicit action potential firing in striatal MSNs by electrically stimulating the motor cortex in 6-OHDA-lesioned animals. Because previous studies performed in dopamine-intact animals suggested that neurochemically-identified striatal MSNs

are more responsive to consecutive pairs of electrical stimuli (Mallet *et al.,* 2005), I used the same strategy to "detect" virtually quiescent neurons in lesioned rats. As a result of this investigation, I provide evidence that similar numbers of direct and indirect pathway MSNs are virtually quiescent after dopamine loss. Because my experimental procedures ensured a > 97% of dopamine loss (Schwarting & Huston, 1996a), it is unlikely lesions were not widely efficacious. Hence, I suggest the silent PPE+ neurons constitute a novel subclass of striatal projection neurons that are either not under strict control by dopamine or at least not controlled in a way predicted by the classical direct/indirect pathways model. When I analysed the responses of MSNs to cortical stimulation, I found that only PPE+ neurons had a significantly greater probability of firing on the second cortical stimulation. This is in agreement with Mallet and colleagues (2005) showing that the evoked responses of putative PV+ interneurons occurs earlier than those of MSNs, and therefore because of this "feed-forward inhibition", MSNs are more likely to respond to the second pulse. However, Mallet and colleagues did not probe cortical stimulation responses in 6-OHDA-lesioned rats, and therefore the lack of preference of the PPE- MSNs for the first or second cortical stimulation pulse could be related to chronic dopamine loss.

Firing of striatal interneurons after dopamine loss

The striatum contains several morphologically- and neurochemically-different cell types. In addition to the two main classes of spiny projection neurons, at least three types of GABAergic striatal interneuron (PV+, NOS+, CR+) and one type of cholinergic interneuron (ChAT+) interact within the striatal microcircuit. As

mentioned before, Sharott and colleagues (2012) have recently defined the firing of these striatal interneurons (with the exclusion of CR+ neurons), during two well defined brain states in dopamine-intact animals. These authors show that these different cell-types present several distinctive firing rates, patterns and relation to ongoing cortical activity useful for a qualitative discrimination. Whether and how the spontaneous firing properties of these four major classes of striatal interneuron are altered *in vivo* after chronic dopamine loss is still under investigation. However, my samples of interneurons allow for some useful early comparisons. For instance, in the 6-OHDA lesion model of PD, it is interesting to note that the firing rate of my ChAT+ interneuron is below the range reported for ChAT+ interneurons in the dopamine-intact brain (Sharott *et al.,* 2012). This thesis work provides the first insights into how CR+ interneurons fire *in vivo.*

Firing of MSNs located in patches before and after dopamine loss

The striatum is organized in compartments, the matrix and 'patches' (see Figure 1.1), that can be differentiated by a large number of molecules and input-output connections (Crittenden & Graybiel, 2011). A broad view is that the matrix contains direct and indirect pathway MSNs involved in sensory-motor and associative function, whereas patches contain MSNs involved in limbic functions. The importance of patch MSNs in relation to PD lies in their connections. In a recent single neuron tracing study, it has been shown that some MSNs located in patches project monosynaptically to the SNc, the area which contains dopamine-producing neurons that in turn project back to the entire striatum (Fujiyama *et al.*, 2011), but their electrophysiological properties are still unknown. Although patches account for

~10% of the striatal volume, their distribution within this nucleus is irregular, and this makes their *in vivo* detection and investigation a challenge. However, on a few occasions, I was able to record and identify patch MSNs in both control and lesioned animals. Preliminary analysis of their electrophysiological properties suggest that are very similar to those of MSNs located in the matrix, and it is also possible that they have a role in the pathophysiology of PD and/or other associative and cognitive disorders. Hence, future investigations should be focussed to these compartments in the striatum, and perhaps a genetically-modified mouse model combined with an optogenetic approach could clarify their role *in vivo.*

Concluding remarks

Synchronized neuronal activity is present at many levels in the basal ganglia. In the past decade attention has shifted to the rhythmic fluctuations in synchronized activity at 15-30 Hz that have been linked to attention, motor set, preparation or expectancy in these and other sensory motor circuits (Courtemanche *et al.*, 2003). As previously stated, synchronized oscillations occur at relatively low levels in the normal state (Nini *et al.*, 1995; Bergman *et al.*, 1998; Raz *et al.*, 2001) but it has been consistently shown that beta oscillations are exaggerated in the Parkinsonian state, in several nuclei of the basal ganglia (Brown *et al.*, 2001; Brown, 2003; Brittain & Brown, 2014). Further studies have advanced the investigation of these oscillations and described them as a causative reflection of the classical symptoms of PD (Brittain & Brown, 2014). With respect to striatum, previous studies have provided insights into the pathophysiological expression of oscillations in this nucleus, but they have not provided direct evidence of the presence of aberrant

synchronization at the level of firing of identified single cell types. Therefore, this thesis work provides new and important insights into the complex dysregulation of striatal neuron firing occurring after chronic dopamine loss. More specifically, my work suggests that the increased firing and synchronization of indirect pathway MSNs places them in a key position to influence aberrant oscillations in the BG network as a whole. This, in turn, raises several questions, for instance: how is the striatum capable of propagating beta oscillations? What are the intrinsic properties of PPE+ MSNs that facilitate their selective engagement with beta oscillations? What are the behavioural correlates of PPE+ MSN activity? In the past years, some are beginning to be answered. With the advent of optogenetics, a few studies have linked the activation of direct or indirect pathway MSNs to specific motor functions in awake behaving animals. The activation of direct and indirect pathway MSNs can be achieved through Cre-dependent virus-mediated expression of channelrhodopsin-2 in the striatum of bacterial artificial chromosome transgenic mice, expressing Cre recombinase under the control of the regulatory elements of D1R or D2R genes (Kravitz *et al.*, 2010). Thanks to this new approach, it has been shown that the excitation of presumably large numbers of indirect pathway MSNs elicits a Parkinsonian state (increased freezing, bradykinesia and decreased locomotor initiation). In contrast, the activation of (presumably large numbers) of direct pathway MSNs reduces freezing and increases locomotion (Kravitz *et al.*, 2010). Although this study did not probe the influence of aberrant neuronal synchronization in PD, or the relationship between firing rates and oscillations, and despite providing no direct evidence that decreasing activity along the indirect pathway can reverse 6-OHDA-induced movement deficits, it is still a valuable study for the comprehension of the striatal network dynamics occurring after chronic

dopamine loss. Studies in humans have been also of paramount importance (Brittain & Brown, 2014) but they are always restricted to the investigation of a pathological condition and lack, for ethical reasons, an ideal control group that can provide extra evidence of the pathophysiology of the striatal circuit.

The degeneration and death of dopaminergic neurons results in the major clinical motor symptoms of Parkinson's disease (Braak *et al.*, 2003b). Symptoms include bradykinesia, rigidity, postural instabilities and tremor. At later stage of the disease, however, additional cell types and neurotransmitter systems are involved, including those of the locus coeruleus, dorsal motor nucleus, substantia innominata, the autonomic nervous system and the cerebral cortex (Braak *et al.*, 2003b). For this reason, the treatment for PD is ideally not only restricted to restoring function to the dopaminergic system, but also to serotoninergic, cholinergic and noradrenergic systems (Schapira *et al.*, 2006). This thesis highlights the engagement of a specific, neurochemically-identified MSN population in Parkinsonism and it is reasonable to suggest that PPE+ MSNs are a promising therapeutic target for the treatment of PD. Indeed, an intervention that selectively reduces the firing and synchronization of PPE+ MSNs, in potential combination with antagonists of adenosine A2a receptors (A2AR) which are largely restricted to indirect pathway MSNs, would be an exciting candidate strategy for the treatment of the antikinetic symptoms of PD.

CHAPTER 5

General Discussion

5.1 Summary and concluding remarks

The striatum is the main input structure of the BG and it is mainly composed of GABAergic medium-sized densely-spiny projection neurons (MSNs). MSNs can be broadly segregated in two sub-classes according to their projection sites, neurochemical properties and receptor expression. The so-called direct pathway MSNs, innervate monosynaptically basal ganglia output nuclei and express type 1 dopamine receptor (D1R). In contrast, MSNs referred to as indirect pathway MSNs, exclusively innervate the GPe and express type 2 dopamine receptor (D2R) (Gerfen & Surmeier, 2011). Direct and indirect pathway MSNs provide the sole output to other basal ganglia nuclei (but see Somogyi *et al.,* 1981). This dichotomous organization of striatal MSNs and their outputs is a core component of "direct/indirect pathways model" which explains how both MSNs are differentially modulated by dopaminergic neurons of SNc. Specifically, the activation of D1Rs on direct pathway MSNs increases their output, whereas the activation of D2Rs on indirect pathways MSNs decreases their output (Albin *et al.*, 1989; DeLong, 1990). In Parkinson's disease, midbrain dopaminergic neurons selectively degenerate. According to the classic model, loss of dopaminergic innervation of the striatum in

PD imbalances the two striatal output systems (in favour of the indirect pathway), ultimately resulting in excessive inhibition of basal ganglia targets and hence, impaired movement (Albin et al., 1989). Although this scheme of basal ganglia function and dysfunction has advanced understanding of the pathophysiology of Parkinsonism, accumulating evidence challenges this classical view as, for example, there are indication that dopamine loss enhances the tendency of neurons in basal ganglia circuits to generate synchronized, oscillatory firing patterns, rather than simply altering the firing rate (Hammond et al., 2007). With respect to striatum, previous work provided insightful indications that striatum could have a major role in the pathophysiology of Parkinson's disease (Mallet *et al.,* 2006; Moran *et al.,* 2011), but taken together, these studies have not accounted for the complex intrinsic organization and cellular heterogeneity of striatum, nor the contribution of specific cell-types to aberrant oscillations. Hence, the overall objective of this thesis was to elucidate how the distinct structural, neurochemical and other intrinsic properties of striatal neurons are reflected in their firing properties *in vivo* as well as their possible cell-type-selective contributions to the aberrant oscillations arising in the Parkinsonian brain. To achieve this objective, *in vivo* electrophysiological and immunohistochemical approaches were taken. First, I used multi-electrode arrays to record the spontaneous firing of populations of neurons in dorsal striatum in both anaesthetised dopamine-intact and 6-OHDA-lesioned animals during SWA and spontaneous activation. I found an overall increase in the average firing rates of striatal neurons, irrespective of brain state, after chronic dopamine loss. Interestingly, many neurons in the Parkinsonian striatum still exhibited the low firing rates and irregular firing patterns typical of neurons in the dopamine-intact striatum. During SWA, the firing of striatal neurons in 6-OHDA-lesioned animals was more

strongly synchronized at low frequencies, in time with cortical slow (~1 Hz) oscillations. During spontaneous activation in 6-OHDA-lesioned animals, more striatal neurons engaged in synchronized firing in time with cortical beta oscillations. Second, I recorded the spontaneous firing of individual striatal neurons and juxtacellularly labelled the same neurons to verify cell type identity by means of their selective expression of PPE. After chronic dopamine loss, only indirect pathway (PPE+) MSNs significantly increased their firing rate across both brain states, and engaged in widespread, synchronized firing in the beta-frequency range. This did not hold true for *all* PPE+ MSNs. By means of electrical stimulation of corticostriatal neurons, I showed that striatum contained many MSNs that were virtually quiescent, which were just as likely to belong to the indirect pathway as the direct pathway. Finally, direct pathway (PPE-) MSNs increased their firing only during SWA, after chronic dopamine loss and rarely engaged in aberrant oscillations.

In conclusion, the findings reported in this thesis show how cortical inputs as well as midbrain dopaminergic inputs, are important for setting the firing rates and patterns of single neurons and populations of neurons in striatum. Furthermore, aberrant synchronization of firing of striatal neurons was shown to be cell-type selective. As such, these findings add further weight to the argument that the striatum should not be viewed as a passive relay station of information flow, but rather as an important circuit node from which excessively-synchronized rhythmic activity can be spread to the downstream BG network.

5.2 Technical considerations

The experimental observations and their resultant interpretations in this thesis should be considered in light of a number of technical issues arising from the methods employed. All *in vivo* electrophysiological recording were performed in animals that were deeply anaesthetised with urethane (with ketamine/xylazine supplements). Although general anaesthesia may interfere with a number of neurophysiological variables (Franks & Lieb, 1994; Mahon *et al.*, 2001), the impact of anaesthetics on subcortical structures is thought to be minimal (Sloan, 1998). The major benefits associated with general anaesthesia includes optimal stability for neuronal recording/labelling and surgical manipulations. Moreover, anaesthetized animals also have utility for establishing the impact extremes of cortical activity on striatal neurons, which are well stereotyped under urethane, and do not present rapid changes of activity associated with behaviour. Conversely, the limitation arising from using a model under general anaesthesia is that the findings do not contribute to the understanding of a firing rate/pattern associated with a specific behaviour.

To gain insight into the functions of striatal neurons in PD, the electrophysiological properties of MSNs were investigated using a well-established model of experimental PD, the unilateral 6-OHDA-lesioned rat. This model has been extensively used since its introduction as unilateral depletion is similar in many aspects to PD syndrome (Schwarting & Huston, 1996a). For instance, bradykinesia/akinesia and general postural rigidity are all “symptoms” that lesioned rats present. This model however, does not replicate the tremor seen in PD. The electrophysiological recordings performed in this research project were made ~4

weeks after the injection of 6-OHDA, so the time course does not replicate the slow and progressive nature of human Parkinsonism. However, although the 6-OHDA model does not parallel some of the pathological features of PD, it is still a useful model for understanding the neuronal basis of the excessive (beta) oscillations that arise in basal ganglia-thalamocortical circuits in PD and to study the consequences of the loss of dopamine.

5.3 Future work

There are several issues that have been brought to light by the data presented here and that need further examination. The heterogeneity of striatum is still not fully defined and thus, the specific contributions of different cell-types of striatum have not yet been fully investigated. For instance, for the second part of the thesis (Chapter 4) most of the MSNs examined were located in the matrix compartment of the striatum, so additional investigations to assess the (potentially) specialized contribution of MSNs located in patches needs to be carried out. Also, although the identification of MSNs of the indirect and direct pathways was extrapolated from the expression of PPE (or its absence), similar studies in the future, should seek to use complementary markers of direct pathway MSNs, such as preprotakykinin A (PPTA), the precursor of substance P. Further analyses should be made of that small fraction of neurons, located both in the matrix and patches, that express PPE, PPTA, or both markers or neither marker. Indeed the physiological properties and the anatomical connections of these diverse MSN types have not been fully described and they may well contribute to specific motor, associative or cognitive

functions. Finally the firing of striatal interneurons in dopamine-deprived animals has not been adequately explored yet, neither has their specific involvement in motor tasks. One way in which this could be addressed would be to use a similar recording/labelling approach to that used in Chapter 4 for direct and indirect pathway neurons, although, this would be extremely challenging given the relative scarcity of interneurons. If any of these suggested investigations could be performed in awake animals (freely moving/ head fixed), then differences in firing rate and pattern may be found that link to a specific behaviour. Additionally, with the use of the juxtacellular recording technique, it would be possible to verify the identity of recorded neurons. One way to identify synaptic connections of MSNs located in the patches is by the use of markers that allow highly-specific tracing of a neuron's presynaptic inputs, such as a modified rabies virus (Beier *et al.*, 2011; Choi & Callaway, 2011) or a DNA vector (Rancz *et al.*, 2011). By targeting these genetic manipulations to MSNs in patches, the entirety of their inputs could be examined as well as their electrophysiological properties.

A number of logical extensions to the analysis of aberrant synchronization in BG would be of great use in defining the mechanisms underlying PD. For instance, investigations designed to define the origins of abnormal beta activity have provided inconsistent data. Hence, understanding if there is an anatomical and a temporal starting point of aberrant beta activity, would increase the chance to clarify the pathophysiological mechanism of Parkinsonism *modus operandi*. Ideally, the utilisation of 'tetrodes' or other multi-electrode arrays to record the simultaneous activity of neurons in all BG nuclei and thalamo-cortical circuits, at different time points, after acute administration of dopaminergic receptor antagonists or toxins, can potentially lead to a better understanding of the evolution of beta activity in these

complex and interconnected circuits. As such, if a multi-electrode array would also allow the labelling of the recorded cells, the identification of specific single cell contribution could also being revealed. Alternatively, genetic targeting could also help (McNamara *et al.*, 2014).

References

Afsharpour, S. (1985a) Light microscopic analysis of Golgi-impregnated rat subthalamic neurons. *The Journal of comparative neurology*, **236**, 1-13.

Afsharpour, S. (1985b) Topographical projections of the cerebral cortex to the subthalamic nucleus. *The Journal of comparative neurology*, **236**, 14-28.

Agid, Y. (1991) Parkinson's disease: pathophysiology. *Lancet*, **337**, 1321-1324.

Aizman, O., Brismar, H., Uhlen, P., Zettergren, E., Levey, A.I., Forssberg, H., Greengard, P. & Aperia, A. (2000) Anatomical and physiological evidence for D1 and D2 dopamine receptor colocalization in neostriatal neurons. *Nature neuroscience*, **3**, 226-230.

Akins, P.T., Surmeier, D.J. & Kitai, S.T. (1990) M1 muscarinic acetylcholine receptor in cultured rat neostriatum regulates phosphoinositide hydrolysis. *Journal of neurochemistry*, **54**, 266-273.

Albin, R.L., Young, A.B. & Penney, J.B. (1989) The functional anatomy of basal ganglia disorders. *Trends in neurosciences*, **12**, 366-375.

Aldridge, J.W., Anderson, R.J. & Murphy, J.T. (1980) Sensory-motor processing in the caudate nucleus and globus pallidus: a single-unit study in behaving primates. *Canadian journal of physiology and pharmacology*, **58**, 1192-1201.

Alexander, G.E. & Crutcher, M.D. (1990) Functional architecture of basal ganglia circuits: neural substrates of parallel processing. *Trends in neurosciences*, **13**, 266-271.

Alexander, G.E., Crutcher, M.D. & DeLong, M.R. (1990) Basal ganglia-thalamocortical circuits: parallel substrates for motor, oculomotor, "prefrontal" and "limbic" functions. *Progress in brain research*, **85**, 119-146.

Alexander, G.E. & DeLong, M.R. (1985a) Microstimulation of the primate neostriatum. I. Physiological properties of striatal microexcitable zones. *Journal of neurophysiology*, **53**, 1401-1416.

Alexander, G.E. & DeLong, M.R. (1985b) Microstimulation of the primate neostriatum. II. Somatotopic organization of striatal microexcitable zones and their relation to neuronal response properties. *Journal of neurophysiology*, **53**, 1417-1430.

Alexander, G.E., DeLong, M.R. & Strick, P.L. (1986) Parallel organization of functionally segregated circuits linking basal ganglia and cortex. *Annual review of neuroscience*, **9**, 357-381.

Alloway, K.D. & Rebec, G.V. (1984) Apomorphine-induced inhibition of neostriatal activity is enhanced by lesions induced by 6-

hydroxydopamine but not by long-term administration of amphetamine. *Neuropharmacology*, **23**, 1033-1039.

Androulidakis, A.G., Doyle, L.M., Gilbertson, T.P. & Brown, P. (2006) Corrective movements in response to displacements in visual feedback are more effective during periods of 13-35 Hz oscillatory synchrony in the human corticospinal system. *The European journal of neuroscience*, **24**, 3299-3304.

Androulidakis, A.G., Doyle, L.M., Yarrow, K., Litvak, V., Gilbertson, T.P. & Brown, P. (2007) Anticipatory changes in beta synchrony in the human corticospinal system and associated improvements in task performance. *The European journal of neuroscience*, **25**, 3758-3765.

Aoki, C. & Pickel, V.M. (1990) Neuropeptide Y in cortex and striatum. Ultrastructural distribution and coexistence with classical neurotransmitters and neuropeptides. *Annals of the New York Academy of Sciences*, **611**, 186-205.

Aosaki, T., Graybiel, A.M. & Kimura, M. (1994) Effect of the nigrostriatal dopamine system on acquired neural responses in the striatum of behaving monkeys. *Science*, **265**, 412-415.

Aosaki, T., Kimura, M. & Graybiel, A.M. (1995) Temporal and spatial characteristics of tonically active neurons of the primate's striatum. *Journal of neurophysiology*, **73**, 1234-1252.

Aston-Jones, G. & Bloom, F.E. (1981) Activity of norepinephrine-containing locus coeruleus neurons in behaving rats anticipates fluctuations in the sleep-waking cycle. *The Journal of neuroscience : the official journal of the Society for Neuroscience*, **1**, 876-886.

Aziz, T.Z., Peggs, D., Sambrook, M.A. & Crossman, A.R. (1991) Lesion of the subthalamic nucleus for the alleviation of 1-methyl-4-phenyl-1,2,3,6-tetrahydropyridine (MPTP)-induced parkinsonism in the primate. *Movement disorders : official journal of the Movement Disorder Society*, **6**, 288-292.

Ballion, B., Mallet, N., Bezard, E., Lanciego, J.L. & Gonon, F. (2008) Intratelencephalic corticostriatal neurons equally excite striatonigral and striatopallidal neurons and their discharge activity is selectively reduced in experimental parkinsonism. *The European journal of neuroscience*, **27**, 2313-2321.

Bar-Gad, I. & Bergman, H. (2001) Stepping out of the box: information processing in the neural networks of the basal ganglia. *Current opinion in neurobiology*, **11**, 689-695.

Bar-Gad, I., Elias, S., Vaadia, E. & Bergman, H. (2004) Complex locking rather than complete cessation of neuronal activity in the globus pallidus of a 1-methyl-4-phenyl-1,2,3,6-tetrahydropyridine-treated primate in response to pallidal microstimulation. *The Journal of neuroscience : the official journal of the Society for Neuroscience*, **24**, 7410-7419.

Bargas, J., Ayala, G.X., Vilchis, C., Pineda, J.C. & Galarraga, E. (1999) Ca2+-activated outward currents in neostriatal neurons. *Neuroscience*, **88**, 479-488.

Bateup, H.S., Santini, E., Shen, W., Birnbaum, S., Valjent, E., Surmeier, D.J., Fisone, G., Nestler, E.J. & Greengard, P. (2010) Distinct subclasses of medium spiny neurons differentially regulate striatal motor behaviors. *Proceedings of the National Academy of Sciences of the United States of America*, **107**, 14845-14850.

Beckstead, R.M. (1978) Afferent connections of the entorhinal area in the rat as demonstrated by retrograde cell-labeling with horseradish peroxidase. *Brain research*, **152**, 249-264.

Beckstead, R.M., Edwards, S.B. & Frankfurter, A. (1981) A comparison of the intranigral distribution of nigrotectal neurons labeled with horseradish peroxidase in the monkey, cat, and rat. *The Journal of neuroscience : the official journal of the Society for Neuroscience*, **1**, 121-125.

Beier, K.T., Saunders, A., Oldenburg, I.A., Miyamichi, K., Akhtar, N., Luo, L., Whelan, S.P., Sabatini, B. & Cepko, C.L. (2011) Anterograde or retrograde transsynaptic labeling of CNS neurons with vesicular stomatitis virus vectors. *Proceedings of the National Academy of Sciences of the United States of America*, **108**, 15414-15419.

Benhamou, L. & Cohen, D. (2014) Electrophysiological characterization of entopeduncular nucleus neurons in anesthetized and freely moving rats. *Frontiers in systems neuroscience*, **8**, 7.

Beninato, M. & Spencer, R.F. (1988) The cholinergic innervation of the rat substantia nigra: a light and electron microscopic immunohistochemical study. *Experimental brain research*, **72**, 178-184.

Bennett, B.D. & Bolam, J.P. (1993) Characterization of calretinin-immunoreactive structures in the striatum of the rat. *Brain research*, **609**, 137-148.

Bennett, B.D. & Bolam, J.P. (1994) Synaptic input and output of parvalbumin-immunoreactive neurons in the neostriatum of the rat. *Neuroscience*, **62**, 707-719.

Bennett, B.D. & Wilson, C.J. (1998) Synaptic regulation of action potential timing in neostriatal cholinergic interneurons. *The Journal of neuroscience : the official journal of the Society for Neuroscience*, **18**, 8539-8549.

Bennett, B.D. & Wilson, C.J. (1999) Spontaneous activity of neostriatal cholinergic interneurons in vitro. *The Journal of neuroscience : the official journal of the Society for Neuroscience*, **19**, 5586-5596.

Bennett, M.R. (2000) Synaptic Transmission at Single Boutons in Sympathetic Ganglia. *News in physiological sciences : an international journal of physiology produced jointly by the International Union of Physiological Sciences and the American Physiological Society*, **15**, 98-101.

Bentivoglio, M., Kuypers, H.G., Catsman-Berrevoets, C.E. & Dann, O. (1979) Fuorescent retrograde neuronal labeling in rat by means of substances binding specifically to adenine-thymine rich DNA. *Neuroscience letters*, **12**, 235-240.

Bergman, H. & Deuschl, G. (2002) Pathophysiology of Parkinson's disease: from clinical neurology to basic neuroscience and back. *Movement disorders : official journal of the Movement Disorder Society*, **17 Suppl 3**, S28-40.

Bergman, H., Feingold, A., Nini, A., Raz, A., Slovin, H., Abeles, M. & Vaadia, E. (1998) Physiological aspects of information processing in the basal ganglia of normal and parkinsonian primates. *Trends in neurosciences*, **21**, 32-38.

Bergman, H., Wichmann, T. & DeLong, M.R. (1990) Reversal of experimental parkinsonism by lesions of the subthalamic nucleus. *Science*, **249**, 1436-1438.

Berke, J.D. (2009) Fast oscillations in cortical-striatal networks switch frequency following rewarding events and stimulant drugs. *The European journal of neuroscience*, **30**, 848-859.

Berke, J.D., Okatan, M., Skurski, J. & Eichenbaum, H.B. (2004) Oscillatory entrainment of striatal neurons in freely moving rats. *Neuron*, **43**, 883-896.

Berns, G.S. & Sejnowski, T.J. (1998) A computational model of how the basal ganglia produce sequences. *Journal of cognitive neuroscience*, **10**, 108-121.

Beurrier, C., Congar, P., Bioulac, B. & Hammond, C. (1999) Subthalamic nucleus neurons switch from single-spike activity to burst-firing mode. *The Journal of neuroscience : the official journal of the Society for Neuroscience*, **19**, 599-609.

Bevan, M.D., Bolam, J.P. & Crossman, A.R. (1994) Convergent synaptic input from the neostriatum and the subthalamus onto identified nigrothalamic neurons in the rat. *The European journal of neuroscience*, **6**, 320-334.

Bevan, M.D., Booth, P.A., Eaton, S.A. & Bolam, J.P. (1998) Selective innervation of neostriatal interneurons by a subclass of neuron in the globus pallidus of the rat. *The Journal of neuroscience : the official journal of the Society for Neuroscience*, **18**, 9438-9452.

Bevan, M.D., Magill, P.J., Terman, D., Bolam, J.P. & Wilson, C.J. (2002) Move to the rhythm: oscillations in the subthalamic nucleus-external globus pallidus network. *Trends in neurosciences*, **25**, 525-531.

Bevan, M.D., Smith, A.D. & Bolam, J.P. (1996) The substantia nigra as a site of synaptic integration of functionally diverse information arising from the ventral pallidum and the globus pallidus in the rat. *Neuroscience*, **75**, 5-12.

Bevan, M.D. & Wilson, C.J. (1999) Mechanisms underlying spontaneous oscillation and rhythmic firing in rat subthalamic

neurons. *The Journal of neuroscience : the official journal of the Society for Neuroscience*, **19**, 7617-7628.

Blanche, T.J., Spacek, M.A., Hetke, J.F. & Swindale, N.V. (2005) Polytrodes: high-density silicon electrode arrays for large-scale multiunit recording. *Journal of neurophysiology*, **93**, 2987-3000.

Blum, D., Torch, S., Lambeng, N., Nissou, M., Benabid, A.L., Sadoul, R. & Verna, J.M. (2001) Molecular pathways involved in the neurotoxicity of 6-OHDA, dopamine and MPTP: contribution to the apoptotic theory in Parkinson's disease. *Progress in neurobiology*, **65**, 135-172.

Bolam, J.P., Francis, C.M. & Henderson, Z. (1991) Cholinergic input to dopaminergic neurons in the substantia nigra: a double immunocytochemical study. *Neuroscience*, **41**, 483-494.

Bolam, J.P., Hanley, J.J., Booth, P.A. & Bevan, M.D. (2000) Synaptic organisation of the basal ganglia. *Journal of anatomy*, **196 (Pt 4)**, 527-542.

Bolam, J.P. & Izzo, P.N. (1988) The postsynaptic targets of substance P-immunoreactive terminals in the rat neostriatum with particular reference to identified spiny striatonigral neurons. *Experimental brain research*, **70**, 361-377.

Bolam, J.P., Smith, Y., Ingham, C.A., von Krosigk, M. & Smith, A.D. (1993) Convergence of synaptic terminals from the striatum and the globus pallidus onto single neurones in the substantia nigra and the entopeduncular nucleus. *Progress in brain research*, **99**, 73-88.

Boraud, T., Bezard, E., Bioulac, B. & Gross, C.E. (2002) From single extracellular unit recording in experimental and human Parkinsonism to the development of a functional concept of the role played by the basal ganglia in motor control. *Progress in neurobiology*, **66**, 265-283.

Braak, H. & Del Tredici, K. (2008) Invited Article: Nervous system pathology in sporadic Parkinson disease. *Neurology*, **70**, 1916-1925.

Braak, H., Del Tredici, K., Rub, U., de Vos, R.A., Jansen Steur, E.N. & Braak, E. (2003a) Staging of brain pathology related to sporadic Parkinson's disease. *Neurobiology of aging*, **24**, 197-211.

Braak, H., Rub, U. & Braak, E. (2000) [Neuroanatomy of Parkinson disease. Changes in the neuronal cytoskeleton of a few disease-susceptible types of neurons lead to progressive destruction of circumscribed areas in the limbic and motor systems]. *Der Nervenarzt*, **71**, 459-469.

Braak, H., Rub, U., Gai, W.P. & Del Tredici, K. (2003b) Idiopathic Parkinson's disease: possible routes by which vulnerable neuronal types may be subject to neuroinvasion by an unknown pathogen. *Journal of neural transmission*, **110**, 517-536.

Braak, H., Rub, U., Jansen Steur, E.N., Del Tredici, K. & de Vos, R.A. (2005) Cognitive status correlates with neuropathologic stage in Parkinson disease. *Neurology*, **64**, 1404-1410.

Breese, G.R. & Traylor, T.D. (1971) Depletion of brain noradrenaline and dopamine by 6-hydroxydopamine. *British journal of pharmacology*, **42**, 88-99.

Brittain, J.S. & Brown, P. (2014) Oscillations and the basal ganglia: motor control and beyond. *NeuroImage*, **85 Pt 2**, 637-647.

Brog, J.S., Salyapongse, A., Deutch, A.Y. & Zahm, D.S. (1993) The patterns of afferent innervation of the core and shell in the "accumbens" part of the rat ventral striatum: immunohistochemical detection of retrogradely transported fluoro-gold. *The Journal of comparative neurology*, **338**, 255-278.

Brown, M.T., Henny, P., Bolam, J.P. & Magill, P.J. (2009) Activity of neurochemically heterogeneous dopaminergic neurons in the substantia nigra during spontaneous and driven changes in brain state. *The Journal of neuroscience : the official journal of the Society for Neuroscience*, **29**, 2915-2925.

Brown, P. (2003) Oscillatory nature of human basal ganglia activity: relationship to the pathophysiology of Parkinson's disease. *Movement disorders : official journal of the Movement Disorder Society*, **18**, 357-363.

Brown, P. (2006) Bad oscillations in Parkinson's disease. *Journal of neural transmission. Supplementum*, 27-30.

Brown, P., Mazzone, P., Oliviero, A., Altibrandi, M.G., Pilato, F., Tonali, P.A. & Di Lazzaro, V. (2004) Effects of stimulation of the subthalamic area on oscillatory pallidal activity in Parkinson's disease. *Experimental neurology*, **188**, 480-490.

Brown, P., Oliviero, A., Mazzone, P., Insola, A., Tonali, P. & Di Lazzaro, V. (2001) Dopamine dependency of oscillations between subthalamic nucleus and pallidum in Parkinson's disease. *The Journal of neuroscience : the official journal of the Society for Neuroscience*, **21**, 1033-1038.

Bullock, T.H. (1997) Signals and signs in the nervous system: the dynamic anatomy of electrical activity is probably information-rich. *Proceedings of the National Academy of Sciences of the United States of America*, **94**, 1-6.

Bunney, B.S. & Aghajanian, G.K. (1976) The precise localization of nigral afferents in the rat as determined by a retrograde tracing technique. *Brain research*, **117**, 423-435.

Buonamici, M., Maj, R., Pagani, F., Rossi, A.C. & Khazan, N. (1986) Tremor at rest episodes in unilaterally 6-OHDA-induced substantia nigra lesioned rats: EEG-EMG and behavior. *Neuropharmacology*, **25**, 323-325.

Burbaud, P., Gross, C., Benazzouz, A., Coussemacq, M. & Bioulac, B. (1995) Reduction of apomorphine-induced rotational behaviour by subthalamic lesion in 6-OHDA lesioned rats is associated with a normalization of firing rate and discharge pattern of pars reticulata neurons. *Experimental brain research*, **105**, 48-58.

Buzsaki, G. (2002) Theta oscillations in the hippocampus. *Neuron*, **33**, 325-340.

Buzsaki, G. & Draguhn, A. (2004) Neuronal oscillations in cortical networks. *Science*, **304**, 1926-1929.

Buzsaki, G., Laszlovszky, I., Lajtha, A. & Vadasz, C. (1990) Spike-and-wave neocortical patterns in rats: genetic and aminergic control. *Neuroscience*, **38**, 323-333.

Calabresi, P., Centonze, D., Pisani, A., Sancesario, G., Gubellini, P., Marfia, G.A. & Bernardi, G. (1998) Striatal spiny neurons and cholinergic interneurons express differential ionotropic glutamatergic responses and vulnerability: implications for ischemia and Huntington's disease. *Annals of neurology*, **43**, 586-597.

Calabresi, P., Picconi, B., Tozzi, A., Ghiglieri, V. & Di Filippo, M. (2014) Direct and indirect pathways of basal ganglia: a critical reappraisal. *Nature neuroscience*, **17**, 1022-1030.

Carlson, J.D., Cleary, D.R., Cetas, J.S., Heinricher, M.M. & Burchiel, K.J. (2010) Deep brain stimulation does not silence neurons in subthalamic nucleus in Parkinson's patients. *Journal of neurophysiology*, **103**, 962-967.

Carrillo-Reid, L., Tecuapetla, F., Tapia, D., Hernandez-Cruz, A., Galarraga, E., Drucker-Colin, R. & Bargas, J. (2008) Encoding network states by striatal cell assemblies. *Journal of neurophysiology*, **99**, 1435-1450.

Cassidy, M. & Brown, P. (2001) Task-related EEG-EEG coherence depends on dopaminergic activity in Parkinson's disease. *Neuroreport*, **12**, 703-707.

Cassidy, M., Mazzone, P., Oliviero, A., Insola, A., Tonali, P., Di Lazzaro, V. & Brown, P. (2002) Movement-related changes in synchronization in the human basal ganglia. *Brain : a journal of neurology*, **125**, 1235-1246.

Centonze, D., Grande, C., Saulle, E., Martin, A.B., Gubellini, P., Pavon, N., Pisani, A., Bernardi, G., Moratalla, R. & Calabresi, P. (2003a) Distinct roles of D1 and D5 dopamine receptors in motor activity and striatal synaptic plasticity. *The Journal of neuroscience : the official journal of the Society for Neuroscience*, **23**, 8506-8512.

Centonze, D., Gubellini, P., Pisani, A., Bernardi, G. & Calabresi, P. (2003b) Dopamine, acetylcholine and nitric oxide systems interact to induce corticostriatal synaptic plasticity. *Reviews in the neurosciences*, **14**, 207-216.

Chakravarthy, V.S., Joseph, D. & Bapi, R.S. (2010) What do the basal ganglia do? A modeling perspective. *Biological cybernetics*, **103**, 237-253.

Chandler, W.F. & Crosby, E.C. (1975) Motor effects of stimulation and ablation of the caudate nucleus of the monkey. *Neurology*, **25**, 1160-1163.

Chang, H.T., Kita, H. & Kitai, S.T. (1983) The fine structure of the rat subthalamic nucleus: an electron microscopic study. *The Journal of comparative neurology*, **221**, 113-123.

Chang, H.T., Wilson, C.J. & Kitai, S.T. (1981) Single neostriatal efferent axons in the globus pallidus: a light and electron microscopic study. *Science*, **213**, 915-918.

Charara, A. & Parent, A. (1994) Brainstem dopaminergic, cholinergic and serotoninergic afferents to the pallidum in the squirrel monkey. *Brain research*, **640**, 155-170.

Chen, C.C., Litvak, V., Gilbertson, T., Kuhn, A., Lu, C.S., Lee, S.T., Tsai, C.H., Tisch, S., Limousin, P., Hariz, M. & Brown, P. (2007) Excessive synchronization of basal ganglia neurons at 20 Hz slows movement in Parkinson's disease. *Experimental neurology*, **205**, 214-221.

Chen, M.T., Morales, M., Woodward, D.J., Hoffer, B.J. & Janak, P.H. (2001) In vivo extracellular recording of striatal neurons in the awake rat following unilateral 6-hydroxydopamine lesions. *Experimental neurology*, **171**, 72-83.

Chevalier, G., Thierry, A.M., Shibazaki, T. & Feger, J. (1981) Evidence for a GABAergic inhibitory nigrotectal pathway in the rat. *Neuroscience letters*, **21**, 67-70.

Chevalier, G., Vacher, S., Deniau, J.M. & Desban, M. (1985) Disinhibition as a basic process in the expression of striatal functions. I. The striato-nigral influence on tecto-spinal/tecto-diencephalic neurons. *Brain research*, **334**, 215-226.

Choi, J. & Callaway, E.M. (2011) Monosynaptic inputs to ErbB4-expressing inhibitory neurons in mouse primary somatosensory cortex. *The Journal of comparative neurology*, **519**, 3402-3414.

Chung, J.W., Hassler, R. & Wagner, A. (1977) Degeneration of two of nine types of synapses in the putamen after center median coagulation in the cat. *Experimental brain research*, **28**, 345-361.

Cools, A.R. (1973) Chemical and electrical stimulation of the caudate nucleus in freely moving cats: the role of dopamine. *Brain research*, **58**, 437-451.

Corvaja, N., Doucet, G. & Bolam, J.P. (1993) Ultrastructure and synaptic targets of the raphe-nigral projection in the rat. *Neuroscience*, **55**, 417-427.

Courtemanche, R., Fujii, N. & Graybiel, A.M. (2003) Synchronous, focally modulated beta-band oscillations characterize local field potential activity in the striatum of awake behaving monkeys. *The Journal of neuroscience : the official journal of the Society for Neuroscience*, **23**, 11741-11752.

Cowan, R.L., Wilson, C.J., Emson, P.C. & Heizmann, C.W. (1990) Parvalbumin-containing GABAergic interneurons in the rat neostriatum. *The Journal of comparative neurology*, **302**, 197-205.

Crittenden, J.R. & Graybiel, A.M. (2011) Basal Ganglia disorders associated with imbalances in the striatal striosome and matrix compartments. *Frontiers in neuroanatomy*, **5**, 59.

Crutcher, M.D. & DeLong, M.R. (1984) Single cell studies of the primate putamen.

II. Relations to direction of movement and pattern of muscular activity. *Experimental brain research*, **53**, 244-258.

Damodaran, S., Cressman, J.R., Jedrzejewski-Szmek, Z. & Blackwell, K.T. (2015) Desynchronization of Fast-Spiking Interneurons Reduces beta-Band Oscillations and Imbalance in Firing in the Dopamine-Depleted Striatum. *The Journal of neuroscience : the official journal of the Society for Neuroscience*, **35**, 1149-1159.

Dauer, W. & Przedborski, S. (2003) Parkinson's disease: mechanisms and models. *Neuron*, **39**, 889-909.

Dautan, D., Huerta-Ocampo, I., Witten, I.B., Deisseroth, K., Bolam, J.P., Gerdjikov, T. & Mena-Segovia, J. (2014) A major external source of cholinergic innervation of the striatum and nucleus accumbens originates in the brainstem. *The Journal of neuroscience : the official journal of the Society for Neuroscience*, **34**, 4509-4518.

DeCoteau, W.E., Hoang, L., Huff, L., Stone, A. & Kesner, R.P. (2004) Effects of hippocampus and medial caudate nucleus lesions on memory for direction information in rats. *Behavioral neuroscience*, **118**, 540-545.

Degos, B., Deniau, J.M., Chavez, M. & Maurice, N. (2009) Chronic but not acute dopaminergic transmission interruption promotes a progressive increase in cortical beta frequency synchronization: relationships to vigilance state and akinesia. *Cerebral cortex*, **19**, 1616-1630.

DeLong, M.R. (1971) Activity of pallidal neurons during movement. *Journal of neurophysiology*, **34**, 414-427.

DeLong, M.R. (1983) The neurophysiologic basis of abnormal movements in basal ganglia disorders. *Neurobehavioral toxicology and teratology*, **5**, 611-616.

DeLong, M.R. (1990) Primate models of movement disorders of basal ganglia origin. *Trends in neurosciences*, **13**, 281-285.

DeLong, M.R., Crutcher, M.D. & Georgopoulos, A.P. (1985) Primate globus pallidus and subthalamic nucleus: functional organization. *Journal of neurophysiology*, **53**, 530-543.

Deniau, J.M. & Chevalier, G. (1992) The lamellar organization of the rat substantia nigra pars reticulata: distribution of projection neurons. *Neuroscience*, **46**, 361-377.

Deniau, J.M., Degos, B., Bosch, C. & Maurice, N. (2010) Deep brain stimulation mechanisms: beyond the concept of local functional inhibition. *The European journal of neuroscience*, **32**, 1080-1091.

Deniau, J.M., Hammond, C., Chevalier, G. & Feger, J. (1978) Evidence for branched subthalamic nucleus projections to substantia nigra, entopeduncular nucleus and globus pallidus. *Neuroscience letters*, **9**, 117-121.

Deniau, J.M., Kitai, S.T., Donoghue, J.P. & Grofova, I. (1982) Neuronal interactions in the substantia nigra

pars reticulata through axon collaterals of the projection neurons. An electrophysiological and morphological study. *Experimental brain research*, **47**, 105-113.

Deumens, R., Blokland, A. & Prickaerts, J. (2002) Modeling Parkinson's disease in rats: an evaluation of 6-OHDA lesions of the nigrostriatal pathway. *Experimental neurology*, **175**, 303-317.

Di Chiara, G., Morelli, M. & Consolo, S. (1994) Modulatory functions of neurotransmitters in the striatum: ACh/dopamine/NMDA interactions. *Trends in neurosciences*, **17**, 228-233.

Doig, N.M., Moss, J. & Bolam, J.P. (2010) Cortical and thalamic innervation of direct and indirect pathway medium-sized spiny neurons in mouse striatum. *The Journal of neuroscience : the official journal of the Society for Neuroscience*, **30**, 14610-14618.

Dostrovsky, J.O. & Lozano, A.M. (2002) Mechanisms of deep brain stimulation. *Movement disorders : official journal of the Movement Disorder Society*, **17 Suppl 3**, S63-68.

Dray, A., Gonye, T.J., Oakley, N.R. & Tanner, T. (1976) Proceedings: A raphe-substantia nigra projection in the rat. *The Journal of physiology*, **257**, 29P-30P.

Dube, L., Smith, A.D. & Bolam, J.P. (1988) Identification of synaptic terminals of thalamic or cortical origin in contact with distinct medium-size spiny neurons in the rat neostriatum. *The Journal of comparative neurology*, **267**, 455-471.

Durieux, P.F., Bearzatto, B., Guiducci, S., Buch, T., Waisman, A., Zoli, M., Schiffmann, S.N. & de Kerchove d'Exaerde, A. (2009) D2R striatopallidal neurons inhibit both locomotor and drug reward processes. *Nature neuroscience*, **12**, 393-395.

Eccles, J.C. (1951) Interpretation of action potentials evoked in the cerebral cortex. *Electroencephalography and clinical neurophysiology*, **3**, 449-464.

Ellender, T.J., Huerta-Ocampo, I., Deisseroth, K., Capogna, M. & Bolam, J.P. (2011) Differential modulation of excitatory and inhibitory striatal synaptic transmission by histamine. *The Journal of neuroscience : the official journal of the Society for Neuroscience*, **31**, 15340-15351.

Engel, A.K. & Fries, P. (2010) Beta-band oscillations--signalling the status quo? *Current opinion in neurobiology*, **20**, 156-165.

Eusebio, A., Chen, C.C., Lu, C.S., Lee, S.T., Tsai, C.H., Limousin, P., Hariz, M. & Brown, P. (2008) Effects of low-frequency stimulation of the subthalamic nucleus on movement in Parkinson's disease. *Experimental neurology*, **209**, 125-130.

Eusebio, A., Thevathasan, W., Doyle Gaynor, L., Pogosyan, A., Bye, E., Foltynie, T., Zrinzo, L., Ashkan, K., Aziz, T. & Brown, P. (2011) Deep brain stimulation can suppress pathological synchronisation in parkinsonian patients. *Journal of*

neurology, neurosurgery, and psychiatry, **82**, 569-573.

Fallon, J.H. & Moore, R.Y. (1978) Catecholamine innervation of the basal forebrain. IV. Topography of the dopamine projection to the basal forebrain and neostriatum. *The Journal of comparative neurology*, **180**, 545-580.

Faull, R.L. & Mehler, W.R. (1978) The cells of origin of nigrotectal, nigrothalamic and nigrostriatal projections in the rat. *Neuroscience*, **3**, 989-1002.

Feger, J. & Robledo, P. (1991) The Effects of Activation or Inhibition of the Subthalamic Nucleus on the Metabolic and Electrophysiological Activities Within the Pallidal Complex and Substantia Nigra in the Rat. *The European journal of neuroscience*, **3**, 947-952.

Ferguson, S.M., Eskenazi, D., Ishikawa, M., Wanat, M.J., Phillips, P.E., Dong, Y., Roth, B.L. & Neumaier, J.F. (2011) Transient neuronal inhibition reveals opposing roles of indirect and direct pathways in sensitization. *Nature neuroscience*, **14**, 22-24.

Fields, H.L., Hjelmstad, G.O., Margolis, E.B. & Nicola, S.M. (2007) Ventral tegmental area neurons in learned appetitive behavior and positive reinforcement. *Annual review of neuroscience*, **30**, 289-316.

Filion, M. & Harnois, C. (1978) A comparison of projections of entopeduncular neurons to the thalamus, the midbrain and the habenula in the cat. *The Journal of comparative neurology*, **181**, 763-780.

Fogelson, N., Kuhn, A.A., Silberstein, P., Limousin, P.D., Hariz, M., Trottenberg, T., Kupsch, A. & Brown, P. (2005) Frequency dependent effects of subthalamic nucleus stimulation in Parkinson's disease. *Neuroscience letters*, **382**, 5-9.

Franks, N.P. & Lieb, W.R. (1994) Molecular and cellular mechanisms of general anaesthesia. *Nature*, **367**, 607-614.

Freund, T.F., Powell, J.F. & Smith, A.D. (1984) Tyrosine hydroxylase-immunoreactive boutons in synaptic contact with identified striatonigral neurons, with particular reference to dendritic spines. *Neuroscience*, **13**, 1189-1215.

Frotscher, M., Rinne, U., Hassler, R. & Wagner, A. (1981) Termination of cortical afferents on identified neurons in the caudate nucleus of the cat. A combined Golgi-EM degeneration study. *Experimental brain research*, **41**, 329-337.

Fujimoto, K. & Kita, H. (1992) Responses of rat substantia nigra pars reticulata units to cortical stimulation. *Neuroscience letters*, **142**, 105-109.

Fujiyama, F., Sohn, J., Nakano, T., Furuta, T., Nakamura, K.C., Matsuda, W. & Kaneko, T. (2011) Exclusive and common targets of neostriatofugal projections of rat striosome neurons: a single neuron-tracing study using a viral vector. *The European journal of neuroscience*, **33**, 668-677.

Fujiyama, F., Unzai, T., Nakamura, K., Nomura, S. & Kaneko, T. (2006) Difference in organization of

corticostriatal and thalamostriatal synapses between patch and matrix compartments of rat neostriatum. *The European journal of neuroscience*, **24**, 2813-2824.

Furuta, T. & Kaneko, T. (2006) Third pathway in the cortico-basal ganglia loop: Neurokinin B-producing striatal neurons modulate cortical activity via striato-innominato-cortical projection. *Neuroscience research*, **54**, 1-10.

Gabel, L.A. & Nisenbaum, E.S. (1999) Muscarinic receptors differentially modulate the persistent potassium current in striatal spiny projection neurons. *Journal of neurophysiology*, **81**, 1418-1423.

Gardiner, T.W. & Kitai, S.T. (1992) Single-unit activity in the globus pallidus and neostriatum of the rat during performance of a trained head movement. *Experimental brain research*, **88**, 517-530.

Gardiner, T.W. & Nelson, R.J. (1992) Striatal neuronal activity during the initiation and execution of hand movements made in response to visual and vibratory cues. *Experimental brain research*, **92**, 15-26.

Gatev, P., Darbin, O. & Wichmann, T. (2006) Oscillations in the basal ganglia under normal conditions and in movement disorders. *Movement disorders : official journal of the Movement Disorder Society*, **21**, 1566-1577.

Gauthier, J., Parent, M., Levesque, M. & Parent, A. (1999) The axonal arborization of single nigrostriatal neurons in rats. *Brain research*, **834**, 228-232.

Georgopoulos, A.P., DeLong, M.R. & Crutcher, M.D. (1983) Relations between parameters of step-tracking movements and single cell discharge in the globus pallidus and subthalamic nucleus of the behaving monkey. *The Journal of neuroscience : the official journal of the Society for Neuroscience*, **3**, 1586-1598.

Gerfen, C.R. (1984) The neostriatal mosaic: compartmentalization of corticostriatal input and striatonigral output systems. *Nature*, **311**, 461-464.

Gerfen, C.R. (1985) The neostriatal mosaic. I. Compartmental organization of projections from the striatum to the substantia nigra in the rat. *The Journal of comparative neurology*, **236**, 454-476.

Gerfen, C.R. (1992) The neostriatal mosaic: multiple levels of compartmental organization in the basal ganglia. *Annu Rev Neurosci*, **15**, 285-320.

Gerfen, C.R., Baimbridge, K.G. & Thibault, J. (1987a) The neostriatal mosaic: III. Biochemical and developmental dissociation of patch-matrix mesostriatal systems. *The Journal of neuroscience : the official journal of the Society for Neuroscience*, **7**, 3935-3944.

Gerfen, C.R., Herkenham, M. & Thibault, J. (1987b) The neostriatal mosaic: II. Patch- and matrix-directed mesostriatal dopaminergic and non-dopaminergic systems. *The Journal of neuroscience : the official journal*

of the Society for Neuroscience, **7**, 3915-3934.

Gerfen, C.R. & Surmeier, D.J. (2011) Modulation of striatal projection systems by dopamine. *Annual review of neuroscience*, **34**, 441-466.

Gertler, T.S., Chan, C.S. & Surmeier, D.J. (2008) Dichotomous anatomical properties of adult striatal medium spiny neurons. *The Journal of neuroscience : the official journal of the Society for Neuroscience*, **28**, 10814-10824.

Gervasoni, D., Lin, S.C., Ribeiro, S., Soares, E.S., Pantoja, J. & Nicolelis, M.A. (2004) Global forebrain dynamics predict rat behavioral states and their transitions. *The Journal of neuroscience : the official journal of the Society for Neuroscience*, **24**, 11137-11147.

Giachetti, A., Said, S.I., Reynolds, R.C. & Koniges, F.C. (1977) Vasoactive intestinal polypeptide in brain: localization in and release from isolated nerve terminals. *Proceedings of the National Academy of Sciences of the United States of America*, **74**, 3424-3428.

Gibb, W.R. & Lees, A.J. (1991) Anatomy, pigmentation, ventral and dorsal subpopulations of the substantia nigra, and differential cell death in Parkinson's disease. *Journal of neurology, neurosurgery, and psychiatry*, **54**, 388-396.

Gilbertson, T., Lalo, E., Doyle, L., Di Lazzaro, V., Cioni, B. & Brown, P. (2005) Existing motor state is favored at the expense of new movement during 13-35 Hz oscillatory synchrony in the human corticospinal system. *The Journal of neuroscience : the official journal of the Society for Neuroscience*, **25**, 7771-7779.

Gimenez-Amaya, J.M., McFarland, N.R., de las Heras, S. & Haber, S.N. (1995) Organization of thalamic projections to the ventral striatum in the primate. *The Journal of comparative neurology*, **354**, 127-149.

Gittis, A.H., Nelson, A.B., Thwin, M.T., Palop, J.J. & Kreitzer, A.C. (2010) Distinct roles of GABAergic interneurons in the regulation of striatal output pathways. *The Journal of neuroscience : the official journal of the Society for Neuroscience*, **30**, 2223-2234.

Goldman, P.S. & Nauta, W.J. (1977) An intricately patterned prefronto-caudate projection in the rhesus monkey. *The Journal of comparative neurology*, **72**, 369-386.

Gonya-Magee, T. & Anderson, M.E. (1983) An electrophysiological characterization of projections from the pedunculopontine area to entopeduncular nucleus and globus pallidus in the cat. *Experimental brain research*, **49**, 269-279.

Goto, Y. & O'Donnell, P. (2001) Network synchrony in the nucleus accumbens in vivo. *The Journal of neuroscience : the official journal of the Society for Neuroscience*, **21**, 4498-4504.

Gradinaru, V., Mogri, M., Thompson, K.R., Henderson, J.M. & Deisseroth, K. (2009) Optical deconstruction of parkinsonian neural circuitry. *Science*, **324**, 354-359.

Graybiel, A.M. (2000) The basal ganglia. *Current biology : CB*, **10**, R509-511.

Graybiel, A.M., Baughman, R.W. & Eckenstein, F. (1986) Cholinergic neuropil of the striatum observes striosomal boundaries. *Nature*, **323**, 625-627.

Graybiel, A.M. & Ragsdale, C.W., Jr. (1978) Histochemically distinct compartments in the striatum of human, monkeys, and cat demonstrated by acetylthiocholinesterase staining. *Proceedings of the National Academy of Sciences of the United States of America*, **75**, 5723-5726.

Grillner, S. (2006) Biological pattern generation: the cellular and computational logic of networks in motion. *Neuron*, **52**, 751-766.

Grillner, S., Markram, H., De Schutter, E., Silberberg, G. & LeBeau, F.E. (2005) Microcircuits in action--from CPGs to neocortex. *Trends in neurosciences*, **28**, 525-533.

Grofova, I., Deniau, J.M. & Kitai, S.T. (1982) Morphology of the substantia nigra pars reticulata projection neurons intracellularly labeled with HRP. *The Journal of comparative neurology*, **208**, 352-368.

Haber, S.N., Lynd, E., Klein, C. & Groenewegen, H.J. (1990) Topographic organization of the ventral striatal efferent projections in the rhesus monkey: an anterograde tracing study. *The Journal of comparative neurology*, **293**, 282-298.

Hammond, C., Bergman, H. & Brown, P. (2007) Pathological synchronization in Parkinson's disease: networks, models and treatments. *Trends in neurosciences*, **30**, 357-364.

Hammond, C., Deniau, J.M., Rouzaire-Dubois, B. & Feger, J. (1978) Pepipheral input to the rat subthalamic nucleus, an electrophysiological study. *Neuroscience letters*, **9**, 171-176.

Hammond, C. & Yelnik, J. (1983) Intracellular labelling of rat subthalamic neurones with horseradish peroxidase: computer analysis of dendrites and characterization of axon arborization. *Neuroscience*, **8**, 781-790.

Haracz, J.L., Tschanz, J.T., Wang, Z., White, I.M. & Rebec, G.V. (1993) Striatal single-unit responses to amphetamine and neuroleptics in freely moving rats. *Neuroscience and biobehavioral reviews*, **17**, 1-12.

Hashimoto, T., Elder, C.M., Okun, M.S., Patrick, S.K. & Vitek, J.L. (2003) Stimulation of the subthalamic nucleus changes the firing pattern of pallidal neurons. *The Journal of neuroscience : the official journal of the Society for Neuroscience*, **23**, 1916-1923.

Hassler, R., Chung, J.W., Rinne, U. & Wagner, A. (1978) Selective degeneration of two out of the nine types of synapses in cat caudate nucleus after cortical lesions. *Experimental brain research*, **31**, 67-80.

Hassler, R., Usunoff, K.G., Romansky, K.V. & Christ, J.F. (1982) Electron

microscopy of the subthalamic nucleus in the baboon. I. Synaptic organization of the subthalamic nucleus in the baboon. *Journal fur Hirnforschung*, **23**, 597-611.

Hedreen, J.C. (1999) Tyrosine hydroxylase-immunoreactive elements in the human globus pallidus and subthalamic nucleus. *The Journal of comparative neurology*, **409**, 400-410.

Herkenham, M. & Pert, C.B. (1981) Mosaic distribution of opiate receptors, parafascicular projections and acetylcholinesterase in rat striatum. *Nature*, **291**, 415-418.

Hikida, T., Kimura, K., Wada, N., Funabiki, K. & Nakanishi, S. (2010) Distinct roles of synaptic transmission in direct and indirect striatal pathways to reward and aversive behavior. *Neuron*, **66**, 896-907.

Hikosaka, O., Sakamoto, M. & Usui, S. (1989) Functional properties of monkey caudate neurons. III. Activities related to expectation of target and reward. *Journal of neurophysiology*, **61**, 814-832.

Holgado, A.J., Terry, J.R. & Bogacz, R. (2010) Conditions for the generation of beta oscillations in the subthalamic nucleus-globus pallidus network. *The Journal of neuroscience : the official journal of the Society for Neuroscience*, **30**, 12340-12352.

Holt, G.R., Softky, W.R., Koch, C. & Douglas, R.J. (1996) Comparison of discharge variability in vitro and in vivo in cat visual cortex neurons. *Journal of neurophysiology*, **75**, 1806-1814.

Horak, F.B. & Anderson, M.E. (1984a) Influence of globus pallidus on arm movements in monkeys. I. Effects of kainic acid-induced lesions. *Journal of neurophysiology*, **52**, 290-304.

Horak, F.B. & Anderson, M.E. (1984b) Influence of globus pallidus on arm movements in monkeys. II. Effects of stimulation. *Journal of neurophysiology*, **52**, 305-322.

Hornykiewicz, O. (1988) The pathochemical perspectives of Parkinson's disease. An attempt at a neurochemical definition. *Functional neurology*, **3**, 379-391.

Hudson, J.L., van Horne, C.G., Stromberg, I., Brock, S., Clayton, J., Masserano, J., Hoffer, B.J. & Gerhardt, G.A. (1993) Correlation of apomorphine- and amphetamine-induced turning with nigrostriatal dopamine content in unilateral 6-hydroxydopamine lesioned rats. *Brain research*, **626**, 167-174.

Huerta-Ocampo, I., Mena-Segovia, J. & Bolam, J.P. (2014) Convergence of cortical and thalamic input to direct and indirect pathway medium spiny neurons in the striatum. *Brain structure & function*, **219**, 1787-1800.

Hutchison, W.D., Dostrovsky, J.O., Walters, J.R., Courtemanche, R., Boraud, T., Goldberg, J. & Brown, P. (2004) Neuronal oscillations in the basal ganglia and movement disorders: evidence from whole animal and human recordings. *The Journal of neuroscience : the official journal of the Society for Neuroscience*, **24**, 9240-9243.

Hutchison, W.D., Lang, A.E., Dostrovsky, J.O. & Lozano, A.M. (2003) Pallidal neuronal activity: implications for models of dystonia. *Annals of neurology*, **53**, 480-488.

Ibanez-Sandoval, O., Tecuapetla, F., Unal, B., Shah, F., Koos, T. & Tepper, J.M. (2011) A novel functionally distinct subtype of striatal neuropeptide Y interneuron. *The Journal of neuroscience : the official journal of the Society for Neuroscience*, **31**, 16757-16769.

Ince, E., Ciliax, B.J. & Levey, A.I. (1997) Differential expression of D1 and D2 dopamine and m4 muscarinic acetylcholine receptor proteins in identified striatonigral neurons. *Synapse*, **27**, 357-366.

Iwahori, N. (1978) A Golgi study on the subthalamic nucleus of the cat. *The Journal of comparative neurology*, **182**, 383-397.

Jackson, A. & Crossman, A.R. (1981a) Subthalamic nucleus efferent projection to the cerebral cortex. *Neuroscience*, **6**, 2367-2377.

Jackson, A. & Crossman, A.R. (1981b) Subthalamic projection to nucleus tegmenti pedunculopontinus in the rat. *Neuroscience letters*, **22**, 17-22.

Jackson, A. & Crossman, A.R. (1983) Nucleus tegmenti pedunculopontinus: efferent connections with special reference to the basal ganglia, studied in the rat by anterograde and retrograde transport of horseradish peroxidase. *Neuroscience*, **10**, 725-765.

Jacobowitz, D.M. & Winsky, L. (1991) Immunocytochemical localization of calretinin in the forebrain of the rat. *The Journal of comparative neurology*, **304**, 198-218.

Jaeger, D., Gilman, S. & Aldridge, J.W. (1995) Neuronal activity in the striatum and pallidum of primates related to the execution of externally cued reaching movements. *Brain research*, **694**, 111-127.

Jan, C., Francois, C., Tande, D., Yelnik, J., Tremblay, L., Agid, Y. & Hirsch, E. (2000) Dopaminergic innervation of the pallidum in the normal state, in MPTP-treated monkeys and in parkinsonian patients. *The European journal of neuroscience*, **12**, 4525-4535.

Jenkinson, N. & Brown, P. (2011) New insights into the relationship between dopamine, beta oscillations and motor function. *Trends in neurosciences*, **34**, 611-618.

Jiao, Y., Sun, Z., Lee, T., Fusco, F.R., Kimble, T.D., Meade, C.A., Cuthbertson, S. & Reiner, A. (1999) A simple and sensitive antigen retrieval method for free-floating and slide-mounted tissue sections. *Journal of neuroscience methods*, **93**, 149-162.

Jimenez-Castellanos, J. & Graybiel, A.M. (1989) Compartmental origins of striatal efferent projections in the cat. *Neuroscience*, **32**, 297-321.

Joel, D. & Weiner, I. (1997) The connections of the primate subthalamic nucleus: indirect pathways and the open-interconnected scheme of basal ganglia-thalamocortical circuitry.

Brain research. Brain research reviews, **23**, 62-78.

Kawaguchi, Y. (1993) Physiological, morphological, and histochemical characterization of three classes of interneurons in rat neostriatum. *The Journal of neuroscience : the official journal of the Society for Neuroscience*, **13**, 4908-4923.

Kawaguchi, Y., Wilson, C.J., Augood, S.J. & Emson, P.C. (1995) Striatal interneurones: chemical, physiological and morphological characterization. *Trends in neurosciences*, **18**, 527-535.

Kawaguchi, Y., Wilson, C.J. & Emson, P.C. (1989) Intracellular recording of identified neostriatal patch and matrix spiny cells in a slice preparation preserving cortical inputs. *Journal of neurophysiology*, **62**, 1052-1068.

Kawaguchi, Y., Wilson, C.J. & Emson, P.C. (1990) Projection subtypes of rat neostriatal matrix cells revealed by intracellular injection of biocytin. *The Journal of neuroscience : the official journal of the Society for Neuroscience*, **10**, 3421-3438.

Kelly, R.M. & Strick, P.L. (2004) Macro-architecture of basal ganglia loops with the cerebral cortex: use of rabies virus to reveal multisynaptic circuits. *Progress in brain research*, **143**, 449-459.

Kemp, J.M. & Powell, T.P. (1970) The cortico-striate projection in the monkey. *Brain : a journal of neurology*, **93**, 525-546.

Kimchi, E.Y. & Laubach, M. (2009) Dynamic encoding of action selection by the medial striatum. *The Journal of neuroscience : the official journal of the Society for Neuroscience*, **29**, 3148-3159.

Kimura, M. (1992) Behavioral modulation of sensory responses of primate putamen neurons. *Brain research*, **578**, 204-214.

Kimura, M., Aosaki, T., Hu, Y., Ishida, A. & Watanabe, K. (1992) Activity of primate putamen neurons is selective to the mode of voluntary movement: visually guided, self-initiated or memory-guided. *Experimental brain research*, **89**, 473-477.

Kimura, M., Rajkowski, J. & Evarts, E. (1984) Tonically discharging putamen neurons exhibit set-dependent responses. *Proceedings of the National Academy of Sciences of the United States of America*, **81**, 4998-5001.

Kincaid, A.E., Penney, J.B., Jr., Young, A.B. & Newman, S.W. (1991) The globus pallidus receives a projection from the parafascicular nucleus in the rat. *Brain research*, **553**, 18-26.

Kincaid, A.E. & Wilson, C.J. (1996) Corticostriatal innervation of the patch and matrix in the rat neostriatum. *The Journal of comparative neurology*, **374**, 578-592.

Kish, L.J., Palmer, M.R. & Gerhardt, G.A. (1999) Multiple single-unit recordings in the striatum of freely moving animals: effects of apomorphine and D-amphetamine in

normal and unilateral 6-hydroxydopamine-lesioned rats. *Brain research*, **833**, 58-70.

Kita, H. & Armstrong, W. (1991) A biotin-containing compound N-(2-aminoethyl)biotinamide for intracellular labeling and neuronal tracing studies: comparison with biocytin. *Journal of neuroscience methods*, **37**, 141-150.

Kita, H., Chang, H.T. & Kitai, S.T. (1983a) The morphology of intracellularly labeled rat subthalamic neurons: a light microscopic analysis. *The Journal of comparative neurology*, **215**, 245-257.

Kita, H., Chang, H.T. & Kitai, S.T. (1983b) Pallidal inputs to subthalamus: intracellular analysis. *Brain research*, **264**, 255-265.

Kita, H. & Kitai, S.T. (1987) Efferent projections of the subthalamic nucleus in the rat: light and electron microscopic analysis with the PHA-L method. *The Journal of comparative neurology*, **260**, 435-452.

Kita, H. & Kitai, S.T. (1991) Intracellular study of rat globus pallidus neurons: membrane properties and responses to neostriatal, subthalamic and nigral stimulation. *Brain research*, **564**, 296-305.

Kita, H., Kosaka, T. & Heizmann, C.W. (1990) Parvalbumin-immunoreactive neurons in the rat neostriatum: a light and electron microscopic study. *Brain research*, **536**, 1-15.

Kita, H., Tokuno, H. & Nambu, A. (1999) Monkey globus pallidus external segment neurons projecting to the neostriatum. *Neuroreport*, **10**, 1467-1472.

Kita, T., Kita, H. & Kitai, S.T. (1984) Passive electrical membrane properties of rat neostriatal neurons in an in vitro slice preparation. *Brain research*, **300**, 129-139.

Kiyatkin, E.A. & Rebec, G.V. (1999a) Modulation of striatal neuronal activity by glutamate and GABA: iontophoresis in awake, unrestrained rats. *Brain research*, **822**, 88-106.

Kiyatkin, E.A. & Rebec, G.V. (1999b) Striatal neuronal activity and responsiveness to dopamine and glutamate after selective blockade of D1 and D2 dopamine receptors in freely moving rats. *The Journal of neuroscience : the official journal of the Society for Neuroscience*, **19**, 3594-3609.

Klemm, W.R. (2001) Behavioral arrest: in search of the neural control system. *Progress in neurobiology*, **65**, 453-471.

Kondo, T. (2008) Dopamine dysregulation syndrome. Hypothetical application of reward system stimulation for the treatment of anhedonia in Parkinson's disease patients. *Journal of neurology*, **255 Suppl 4**, 14-18.

Koos, T. & Tepper, J.M. (1999) Inhibitory control of neostriatal projection neurons by GABAergic interneurons. *Nature neuroscience*, **2**, 467-472.

Kornhuber, J., Kim, J.S., Kornhuber, M.E. & Kornhuber, H.H. (1984) The cortico-nigral projection: reduced glutamate

content in the substantia nigra following frontal cortex ablation in the rat. *Brain research*, **322**, 124-126.

Kravitz, A.V., Freeze, B.S., Parker, P.R., Kay, K., Thwin, M.T., Deisseroth, K. & Kreitzer, A.C. (2010) Regulation of parkinsonian motor behaviours by optogenetic control of basal ganglia circuitry. *Nature*, **466**, 622-626.

Kravitz, A.V. & Kreitzer, A.C. (2012) Striatal mechanisms underlying movement, reinforcement, and punishment. *Physiology*, **27**, 167-177.

Kreiss, D.S., Anderson, L.A. & Walters, J.R. (1996) Apomorphine and dopamine D(1) receptor agonists increase the firing rates of subthalamic nucleus neurons. *Neuroscience*, **72**, 863-876.

Kreitzer, A.C. (2009) Physiology and pharmacology of striatal neurons. *Annual review of neuroscience*, **32**, 127-147.

Kubota, Y., Mikawa, S. & Kawaguchi, Y. (1993) Neostriatal GABAergic interneurones contain NOS, calretinin or parvalbumin. *Neuroreport*, **5**, 205-208.

Kuhn, A.A., Kupsch, A., Schneider, G.H. & Brown, P. (2006) Reduction in subthalamic 8-35 Hz oscillatory activity correlates with clinical improvement in Parkinson's disease. *The European journal of neuroscience*, **23**, 1956-1960.

Kuhn, A.A., Tsui, A., Aziz, T., Ray, N., Brucke, C., Kupsch, A., Schneider, G.H. & Brown, P. (2009) Pathological synchronisation in the subthalamic nucleus of patients with Parkinson's disease relates to both bradykinesia and rigidity. *Experimental neurology*, **215**, 380-387.

Kuhn, A.A., Williams, D., Kupsch, A., Limousin, P., Hariz, M., Schneider, G.H., Yarrow, K. & Brown, P. (2004) Event-related beta desynchronization in human subthalamic nucleus correlates with motor performance. *Brain : a journal of neurology*, **127**, 735-746.

Kunzle, H. (1975) Bilateral projections from precentral motor cortex to the putamen and other parts of the basal ganglia. An autoradiographic study in Macaca fascicularis. *Brain research*, **88**, 195-209.

Kwak, R., Sakamoto, T. & Suzuki, J. (1979) Arrest reaction in man: motor arrest response by electrical stimulation of the deep structure of the cerebrum. *The Tohoku journal of experimental medicine*, **127**, 237-246.

Lacey, C.J., Bolam, J.P. & Magill, P.J. (2007) Novel and distinct operational principles of intralaminar thalamic neurons and their striatal projections. *The Journal of neuroscience : the official journal of the Society for Neuroscience*, **27**, 4374-4384.

Lachaux, J.P., Rodriguez, E., Martinerie, J. & Varela, F.J. (1999) Measuring phase synchrony in brain signals. *Human brain mapping*, **8**, 194-208.

Lang, A.E. & Lozano, A.M. (1998) Parkinson's disease. First of two parts. *The New England journal of medicine*, **339**, 1044-1053.

Lapper, S.R. & Bolam, J.P. (1992) Input from the frontal cortex and the parafascicular nucleus to cholinergic interneurons in the dorsal striatum of the rat. *Neuroscience*, **51**, 533-545.

Lavoie, B. & Parent, A. (1990) Immunohistochemical study of the serotoninergic innervation of the basal ganglia in the squirrel monkey. *The Journal of comparative neurology*, **299**, 1-16.

Lavoie, B., Smith, Y. & Parent, A. (1989) Dopaminergic innervation of the basal ganglia in the squirrel monkey as revealed by tyrosine hydroxylase immunohistochemistry. *The Journal of comparative neurology*, **289**, 36-52.

Lebedev, M.A. & Nelson, R.J. (1999) Rhythmically firing neostriatal neurons in monkey: activity patterns during reaction-time hand movements. *Journal of neurophysiology*, **82**, 1832-1842.

Lee, H.J., Rye, D.B., Hallanger, A.E., Levey, A.I. & Wainer, B.H. (1988) Cholinergic vs. noncholinergic efferents from the mesopontine tegmentum to the extrapyramidal motor system nuclei. *The Journal of comparative neurology*, **275**, 469-492.

Lee, I.H. & Assad, J.A. (2003) Putaminal activity for simple reactions or self-timed movements. *Journal of neurophysiology*, **89**, 2528-2537.

Levesque, M., Charara, A., Gagnon, S., Parent, A. & Deschenes, M. (1996) Corticostriatal projections from layer V cells in rat are collaterals of long-range corticofugal axons. *Brain research*, **709**, 311-315.

Levesque, M. & Parent, A. (1998) Axonal arborization of corticostriatal and corticothalamic fibers arising from prelimbic cortex in the rat. *Cerebral cortex*, **8**, 602-613.

Levine, M.S., Hull, C.D. & Buchwald, N.A. (1974) Pallidal and entopeduncular intracellular responses to striatal, cortical, thalamic, and sensory inputs. *Experimental neurology*, **44**, 448-460.

Levy, R., Dostrovsky, J.O., Lang, A.E., Sime, E., Hutchison, W.D. & Lozano, A.M. (2001) Effects of apomorphine on subthalamic nucleus and globus pallidus internus neurons in patients with Parkinson's disease. *Journal of neurophysiology*, **86**, 249-260.

Liang, L., DeLong, M.R. & Papa, S.M. (2008) Inversion of dopamine responses in striatal medium spiny neurons and involuntary movements. *The Journal of neuroscience : the official journal of the Society for Neuroscience*, **28**, 7537-7547.

Lidsky, T.I. (1975) Pallidal and entopeduncular single unit activity in cats during drinking. *Electroencephalography and clinical neurophysiology*, **39**, 79-84.

Liles, S.L. & Updyke, B.V. (1985) Projection of the digit and wrist area of precentral gyrus to the putamen: relation between topography and physiological properties of neurons in the putamen. *Brain research*, **339**, 245-255.

Lindvall, O. & Bjorklund, A. (1979) Dopaminergic innervation of the globus pallidus by collaterals from the nigrostriatal pathway. *Brain research*, **172**, 169-173.

Litvak, V., Jha, A., Eusebio, A., Oostenveld, R., Foltynie, T., Limousin, P., Zrinzo, L., Hariz, M.I., Friston, K. & Brown, P. (2011) Resting oscillatory cortico-subthalamic connectivity in patients with Parkinson's disease. *Brain : a journal of neurology*, **134**, 359-374.

Lobo, M.K., Covington, H.E., 3rd, Chaudhury, D., Friedman, A.K., Sun, H., Damez-Werno, D., Dietz, D.M., Zaman, S., Koo, J.W., Kennedy, P.J., Mouzon, E., Mogri, M., Neve, R.L., Deisseroth, K., Han, M.H. & Nestler, E.J. (2010) Cell type-specific loss of BDNF signaling mimics optogenetic control of cocaine reward. *Science*, **330**, 385-390.

Loucif, K.C., Wilson, C.L., Baig, R., Lacey, M.G. & Stanford, I.M. (2005) Functional interconnectivity between the globus pallidus and the subthalamic nucleus in the mouse brain slice. *The Journal of physiology*, **567**, 977-987.

Lozano, A.M., Dostrovsky, J., Chen, R. & Ashby, P. (2002) Deep brain stimulation for Parkinson's disease: disrupting the disruption. *Lancet neurology*, **1**, 225-231.

MacLeod, N.K., Ryman, A. & Arbuthnott, G.W. (1990) Electrophysiological properties of nigrothalamic neurons after 6-hydroxydopamine lesions in the rat. *Neuroscience*, **38**, 447-456.

Magill, P.J., Bolam, J.P. & Bevan, M.D. (2000) Relationship of activity in the subthalamic nucleus-globus pallidus network to cortical electroencephalogram. *The Journal of neuroscience : the official journal of the Society for Neuroscience*, **20**, 820-833.

Magill, P.J., Bolam, J.P. & Bevan, M.D. (2001) Dopamine regulates the impact of the cerebral cortex on the subthalamic nucleus-globus pallidus network. *Neuroscience*, **106**, 313-330.

Magill, P.J., Pogosyan, A., Sharott, A., Csicsvari, J., Bolam, J.P. & Brown, P. (2006a) Changes in functional connectivity within the rat striatopallidal axis during global brain activation in vivo. *The Journal of neuroscience : the official journal of the Society for Neuroscience*, **26**, 6318-6329.

Magill, P.J., Sharott, A., Bevan, M.D., Brown, P. & Bolam, J.P. (2004) Synchronous unit activity and local field potentials evoked in the subthalamic nucleus by cortical stimulation. *Journal of neurophysiology*, **92**, 700-714.

Magill, P.J., Sharott, A., Bolam, J.P. & Brown, P. (2006b) Delayed synchronization of activity in cortex and subthalamic nucleus following cortical stimulation in the rat. *The Journal of physiology*, **574**, 929-946.

Mahon, S., Deniau, J.M. & Charpier, S. (2001) Relationship between EEG potentials and intracellular activity of striatal and cortico-striatal neurons: an in vivo study under different anesthetics. *Cerebral cortex*, **11**, 360-373.

Mahon, S., Vautrelle, N., Pezard, L., Slaght, S.J., Deniau, J.M., Chouvet, G. & Charpier, S. (2006) Distinct patterns of striatal medium spiny neuron activity during the natural sleep-wake cycle. *The Journal of neuroscience : the official journal of the Society for Neuroscience*, **26**, 12587-12595.

Mailly, P., Charpier, S., Menetrey, A. & Deniau, J.M. (2003) Three-dimensional organization of the recurrent axon collateral network of the substantia nigra pars reticulata neurons in the rat. *The Journal of neuroscience : the official journal of the Society for Neuroscience*, **23**, 5247-5257.

Mallet, N., Ballion, B., Le Moine, C. & Gonon, F. (2006) Cortical inputs and GABA interneurons imbalance projection neurons in the striatum of parkinsonian rats. *The Journal of neuroscience : the official journal of the Society for Neuroscience*, **26**, 3875-3884.

Mallet, N., Le Moine, C., Charpier, S. & Gonon, F. (2005) Feedforward inhibition of projection neurons by fast-spiking GABA interneurons in the rat striatum in vivo. *The Journal of neuroscience : the official journal of the Society for Neuroscience*, **25**, 3857-3869.

Mallet, N., Micklem, B.R., Henny, P., Brown, M.T., Williams, C., Bolam, J.P., Nakamura, K.C. & Magill, P.J. (2012) Dichotomous organization of the external globus pallidus. *Neuron*, **74**, 1075-1086.

Mallet, N., Pogosyan, A., Marton, L.F., Bolam, J.P., Brown, P. & Magill, P.J. (2008a) Parkinsonian beta oscillations in the external globus pallidus and their relationship with subthalamic nucleus activity. *The Journal of neuroscience : the official journal of the Society for Neuroscience*, **28**, 14245-14258.

Mallet, N., Pogosyan, A., Sharott, A., Csicsvari, J., Bolam, J.P., Brown, P. & Magill, P.J. (2008b) Disrupted dopamine transmission and the emergence of exaggerated beta oscillations in subthalamic nucleus and cerebral cortex. *The Journal of neuroscience : the official journal of the Society for Neuroscience*, **28**, 4795-4806.

Marceglia, S., Foffani, G., Bianchi, A.M., Baselli, G., Tamma, F., Egidi, M. & Priori, A. (2006) Dopamine-dependent non-linear correlation between subthalamic rhythms in Parkinson's disease. *The Journal of physiology*, **571**, 579-591.

Marsden, C.D. & Obeso, J.A. (1994) The functions of the basal ganglia and the paradox of stereotaxic surgery in Parkinson's disease. *Brain : a journal of neurology*, **117 (Pt 4)**, 877-897.

Masterman, D.L. & Cummings, J.L. (1997) Frontal-subcortical circuits: the anatomic basis of executive, social and motivated behaviors. *Journal of psychopharmacology*, **11**, 107-114.

Maurice, N., Deniau, J.M., Menetrey, A., Glowinski, J. & Thierry, A.M. (1998) Prefrontal cortex-basal ganglia circuits in the rat: involvement of ventral pallidum and subthalamic nucleus. *Synapse*, **29**, 363-370.

McCarthy, M.M., Moore-Kochlacs, C., Gu, X., Boyden, E.S., Han, X. & Kopell, N. (2011) Striatal origin of the pathologic beta oscillations in Parkinson's disease. *Proceedings of the National Academy of Sciences of the United States of America*, **108**, 11620-11625.

McGeorge, A.J. & Faull, R.L. (1989) The organization of the projection from the cerebral cortex to the striatum in the rat. *Neuroscience*, **29**, 503-537.

McNamara, C.G., Tejero-Cantero, A., Trouche, S., Campo-Urriza, N. & Dupret, D. (2014) Dopaminergic neurons promote hippocampal reactivation and spatial memory persistence. *Nature neuroscience*, **17**, 1658-1660.

Mena-Segovia, J., Winn, P. & Bolam, J.P. (2008) Cholinergic modulation of midbrain dopaminergic systems. *Brain research reviews*, **58**, 265-271.

Mermelstein, P.G., Song, W.J., Tkatch, T., Yan, Z. & Surmeier, D.J. (1998) Inwardly rectifying potassium (IRK) currents are correlated with IRK subunit expression in rat nucleus accumbens medium spiny neurons. *The Journal of neuroscience : the official journal of the Society for Neuroscience*, **18**, 6650-6661.

Mink, J.W. (1996) The basal ganglia: focused selection and inhibition of competing motor programs. *Progress in neurobiology*, **50**, 381-425.

Mink, J.W. & Thach, W.T. (1991) Basal ganglia motor control. I. Nonexclusive relation of pallidal discharge to five movement modes. *Journal of neurophysiology*, **65**, 273-300.

Moran, A. & Bar-Gad, I. (2010) Revealing neuronal functional organization through the relation between multi-scale oscillatory extracellular signals. *Journal of neuroscience methods*, **186**, 116-129.

Moran, R.J., Mallet, N., Litvak, V., Dolan, R.J., Magill, P.J., Friston, K.J. & Brown, P. (2011) Alterations in brain connectivity underlying beta oscillations in Parkinsonism. *PLoS computational biology*, **7**, e1002124.

Morello, M., Reiner, A., Sancesario, G., Karle, E.J. & Bernardi, G. (1997) Ultrastructural study of nitric oxide synthase-containing striatal neurons and their relationship with parvalbumin-containing neurons in rats. *Brain research*, **776**, 30-39.

Morgane, P.J., Galler, J.R. & Mokler, D.J. (2005) A review of systems and networks of the limbic forebrain/limbic midbrain. *Progress in neurobiology*, **75**, 143-160.

Moss, J. & Bolam, J.P. (2008) A dopaminergic axon lattice in the striatum and its relationship with cortical and thalamic terminals. *The Journal of neuroscience : the official journal of the Society for Neuroscience*, **28**, 11221-11230.

Mouroux, M., Hassani, O.K. & Feger, J. (1997) Electrophysiological and Fos immunohistochemical evidence for the excitatory nature of the parafascicular projection to the globus pallidus. *Neuroscience*, **81**, 387-397.

Murer, M.G. & Pazo, J.H. (1993) Circling behaviour induced by activation of GABAA receptors in the subthalamic nucleus. *Neuroreport*, **4**, 1219-1222.

Murer, M.G., Riquelme, L.A., Tseng, K.Y. & Pazo, J.H. (1997) Substantia nigra pars reticulata single unit activity in normal and 60HDA-lesioned rats: effects of intrastriatal apomorphine and subthalamic lesions. *Synapse*, **27**, 278-293.

Murthy, V.N. & Fetz, E.E. (1992) Coherent 25- to 35-Hz oscillations in the sensorimotor cortex of awake behaving monkeys. *Proceedings of the National Academy of Sciences of the United States of America*, **89**, 5670-5674.

Naito, A. & Kita, H. (1994a) The cortico-nigral projection in the rat: an anterograde tracing study with biotinylated dextran amine. *Brain research*, **637**, 317-322.

Naito, A. & Kita, H. (1994b) The cortico-pallidal projection in the rat: an anterograde tracing study with biotinylated dextran amine. *Brain research*, **653**, 251-257.

Nakanishi, H., Hori, N. & Kastuda, N. (1985) Neostriatal evoked inhibition and effects of dopamine on globus pallidal neurons in rat slice preparations. *Brain research*, **358**, 282-286.

Nakanishi, H., Kita, H. & Kitai, S.T. (1987a) Electrical membrane properties of rat subthalamic neurons in an in vitro slice preparation. *Brain research*, **437**, 35-44.

Nakanishi, H., Kita, H. & Kitai, S.T. (1987b) Intracellular study of rat substantia nigra pars reticulata neurons in an in vitro slice preparation: electrical membrane properties and response characteristics to subthalamic stimulation. *Brain research*, **437**, 45-55.

Nakanishi, H., Kita, H. & Kitai, S.T. (1990) Intracellular study of rat entopeduncular nucleus neurons in an in vitro slice preparation: electrical membrane properties. *Brain research*, **527**, 81-88.

Nambu, A. & Tachibana, Y. (2014) Mechanism of parkinsonian neuronal oscillations in the primate basal ganglia: some considerations based on our recent work. *Frontiers in systems neuroscience*, **8**, 74.

Nambu, A., Tokuno, H. & Takada, M. (2002) Functional significance of the cortico-subthalamo-pallidal 'hyperdirect' pathway. *Neuroscience research*, **43**, 111-117.

Nauta, H.J. (1974) Evidence of a pallidohabenular pathway in the cat. *The Journal of comparative neurology*, **156**, 19-27.

Nevado-Holgado, A.J., Mallet, N., Magill, P.J. & Bogacz, R. (2014) Effective connectivity of the subthalamic nucleus-globus pallidus network during Parkinsonian oscillations. *The Journal of physiology*, **592**, 1429-1455.

Nicola, S.M., Surmeier, J. & Malenka, R.C. (2000) Dopaminergic modulation of neuronal excitability in the striatum

and nucleus accumbens. *Annual review of neuroscience*, **23**, 185-215.

Nini, A., Feingold, A., Slovin, H. & Bergman, H. (1995) Neurons in the globus pallidus do not show correlated activity in the normal monkey, but phase-locked oscillations appear in the MPTP model of parkinsonism. *Journal of neurophysiology*, **74**, 1800-1805.

Nisenbaum, E.S. & Wilson, C.J. (1995) Potassium currents responsible for inward and outward rectification in rat neostriatal spiny projection neurons. *The Journal of neuroscience : the official journal of the Society for Neuroscience*, **15**, 4449-4463.

Nisenbaum, E.S., Xu, Z.C. & Wilson, C.J. (1994) Contribution of a slowly inactivating potassium current to the transition to firing of neostriatal spiny projection neurons. *Journal of neurophysiology*, **71**, 1174-1189.

Noda, H., Manohar, S. & Adey, W.R. (1968) Responses of cat pallidal neurons to cortical and subcortical stimuli. *Experimental neurology*, **20**, 585-610.

Nowak, L.G. & Bullier, J. (1998) Axons, but not cell bodies, are activated by electrical stimulation in cortical gray matter. I. Evidence from chronaxie measurements. *Experimental brain research*, **118**, 477-488.

Obeso, J.A., Jahanshahi, M., Alvarez, L., Macias, R., Pedroso, I., Wilkinson, L., Pavon, N., Day, B., Pinto, S., Rodriguez-Oroz, M.C., Tejeiro, J., Artieda, J., Talelli, P., Swayne, O., Rodriguez, R., Bhatia, K., Rodriguez-Diaz, M., Lopez, G., Guridi, J. & Rothwell, J.C. (2009) What can man do without basal ganglia motor output? The effect of combined unilateral subthalamotomy and pallidotomy in a patient with Parkinson's disease. *Experimental neurology*, **220**, 283-292.

Obeso, J.A., Rodriguez-Oroz, M.C., Rodriguez, M., DeLong, M.R. & Olanow, C.W. (2000) Pathophysiology of levodopa-induced dyskinesias in Parkinson's disease: problems with the current model. *Annals of neurology*, **47**, S22-32; discussion S32-24.

Oertel, W.H. & Mugnaini, E. (1984) Immunocytochemical studies of GABAergic neurons in rat basal ganglia and their relations to other neuronal systems. *Neuroscience letters*, **47**, 233-238.

Ohye, C., Le Gayader, C. & Feger, J. (1976) Responses of subthalamic and pallidal neurons to striatal stimulation: an extracellular study on awake monkeys. *Brain research*, **111**, 241-252.

Oorschot, D.E. (1996) Total number of neurons in the neostriatal, pallidal, subthalamic, and substantia nigral nuclei of the rat basal ganglia: a stereological study using the cavalieri and optical disector methods. *The Journal of comparative neurology*, **366**, 580-599.

Overton, P.G. & Greenfield, S.A. (1995) Determinants of neuronal firing pattern in the guinea-pig subthalamic nucleus: an in vivo and in vitro comparison. *Journal of neural transmission. Parkinson's*

disease and dementia section, **10**, 41-54.

Pahapill, P.A. & Lozano, A.M. (2000) The pedunculopontine nucleus and Parkinson's disease. *Brain : a journal of neurology*, **123 (Pt 9)**, 1767-1783.

Pang, Z., Ling, G.Y., Gajendiran, M. & Xu, Z.C. (2001) Enhanced excitatory synaptic transmission in spiny neurons of rat striatum after unilateral dopamine denervation. *Neuroscience letters*, **308**, 201-205.

Parent, A. & Hazrati, L.N. (1995a) Functional anatomy of the basal ganglia. I. The cortico-basal ganglia-thalamo-cortical loop. *Brain research. Brain research reviews*, **20**, 91-127.

Parent, A. & Hazrati, L.N. (1995b) Functional anatomy of the basal ganglia. II. The place of subthalamic nucleus and external pallidum in basal ganglia circuitry. *Brain research. Brain research reviews*, **20**, 128-154.

Parent, M., Levesque, M. & Parent, A. (2001) Two types of projection neurons in the internal pallidum of primates: single-axon tracing and three-dimensional reconstruction. *The Journal of comparative neurology*, **439**, 162-175.

Parent, M., Wallman, M.J., Gagnon, D. & Parent, A. (2011) Serotonin innervation of basal ganglia in monkeys and humans. *Journal of chemical neuroanatomy*, **41**, 256-265.

Park, M.R., Falls, W.M. & Kitai, S.T. (1982) An intracellular HRP study of the rat globus pallidus. I. Responses and light microscopic analysis. *The Journal of comparative neurology*, **211**, 284-294.

Parthasarathy, H.B. & Graybiel, A.M. (1997) Cortically driven immediate-early gene expression reflects modular influence of sensorimotor cortex on identified striatal neurons in the squirrel monkey. *The Journal of neuroscience : the official journal of the Society for Neuroscience*, **17**, 2477-2491.

Partridge, J.G., Janssen, M.J., Chou, D.Y., Abe, K., Zukowska, Z. & Vicini, S. (2009) Excitatory and inhibitory synapses in neuropeptide Y-expressing striatal interneurons. *Journal of neurophysiology*, **102**, 3038-3045.

Paulus, W. & Jellinger, K. (1991) The neuropathologic basis of different clinical subgroups of Parkinson's disease. *Journal of neuropathology and experimental neurology*, **50**, 743-755.

Perkins, M.N. & Stone, T.W. (1980) Subthalamic projections to the globus pallidus: an electrophysiological study in the rat. *Experimental neurology*, **68**, 500-511.

Perreault, M.L., Hasbi, A., O'Dowd, B.F. & George, S.R. (2011) The dopamine d1-d2 receptor heteromer in striatal medium spiny neurons: evidence for a third distinct neuronal pathway in Basal Ganglia. *Frontiers in neuroanatomy*, **5**, 31.

Pfurtscheller, G., Stancak, A., Jr. & Neuper, C. (1996) Post-movement beta synchronization. A correlate of an

idling motor area? *Electroencephalography and clinical neurophysiology*, **98**, 281-293.

Pinault, D. (1996) A novel single-cell staining procedure performed in vivo under electrophysiological control: morpho-functional features of juxtacellularly labeled thalamic cells and other central neurons with biocytin or Neurobiotin. *Journal of neuroscience methods*, **65**, 113-136.

Planert, H., Szydlowski, S.N., Hjorth, J.J., Grillner, S. & Silberberg, G. (2010) Dynamics of synaptic transmission between fast-spiking interneurons and striatal projection neurons of the direct and indirect pathways. *The Journal of neuroscience : the official journal of the Society for Neuroscience*, **30**, 3499-3507.

Plenz, D. & Aertsen, A. (1996) Neural dynamics in cortex-striatum co-cultures--II. Spatiotemporal characteristics of neuronal activity. *Neuroscience*, **70**, 893-924.

Plenz, D. & Kital, S.T. (1999) A basal ganglia pacemaker formed by the subthalamic nucleus and external globus pallidus. *Nature*, **400**, 677-682.

Pogosyan, A., Gaynor, L.D., Eusebio, A. & Brown, P. (2009) Boosting cortical activity at Beta-band frequencies slows movement in humans. *Current biology : CB*, **19**, 1637-1641.

Precht, W. & Yoshida, M. (1971) Blockage of caudate-evoked inhibition of neurons in the substantia nigra by picrotoxin. *Brain research*, **32**, 229-233.

Priori, A., Foffani, G., Pesenti, A., Tamma, F., Bianchi, A.M., Pellegrini, M., Locatelli, M., Moxon, K.A. & Villani, R.M. (2004) Rhythm-specific pharmacological modulation of subthalamic activity in Parkinson's disease. *Experimental neurology*, **189**, 369-379.

Rafols, J.A. & Fox, C.A. (1976) The neurons in the primate subthalamic nucleus: a Golgi and electron microscopic study. *The Journal of comparative neurology*, **168**, 75-111.

Ragsdale, C.W., Jr. & Graybiel, A.M. (1981) The fronto-striatal projection in the cat and monkey and its relationship to inhomogeneities established by acetylcholinesterase histochemistry. *Brain research*, **208**, 259-266.

Ragsdale, C.W., Jr. & Graybiel, A.M. (1988) Fibers from the basolateral nucleus of the amygdala selectively innervate striosomes in the caudate nucleus of the cat. *The Journal of comparative neurology*, **269**, 506-522.

Ramanathan, S., Hanley, J.J., Deniau, J.M. & Bolam, J.P. (2002) Synaptic convergence of motor and somatosensory cortical afferents onto GABAergic interneurons in the rat striatum. *The Journal of neuroscience : the official journal of the Society for Neuroscience*, **22**, 8158-8169.

Rancz, E.A., Franks, K.M., Schwarz, M.K., Pichler, B., Schaefer, A.T. & Margrie, T.W. (2011) Transfection via whole-cell recording in vivo: bridging single-cell physiology, genetics and

connectomics. *Nature neuroscience*, **14**, 527-532.

Ray, N.J., Jenkinson, N., Wang, S., Holland, P., Brittain, J.S., Joint, C., Stein, J.F. & Aziz, T. (2008) Local field potential beta activity in the subthalamic nucleus of patients with Parkinson's disease is associated with improvements in bradykinesia after dopamine and deep brain stimulation. *Experimental neurology*, **213**, 108-113.

Raz, A., Frechter-Mazar, V., Feingold, A., Abeles, M., Vaadia, E. & Bergman, H. (2001) Activity of pallidal and striatal tonically active neurons is correlated in mptp-treated monkeys but not in normal monkeys. *The Journal of neuroscience : the official journal of the Society for Neuroscience*, **21**, RC128.

Raz, A., Vaadia, E. & Bergman, H. (2000a) Firing patterns and correlations of spontaneous discharge of pallidal neurons in the normal and the tremulous 1-methyl-4-phenyl-1,2,3,6-tetrahydropyridine vervet model of parkinsonism. *The Journal of neuroscience : the official journal of the Society for Neuroscience*, **20**, 8559-8571.

Raz, N., Williamson, A., Gunning-Dixon, F., Head, D. & Acker, J.D. (2000b) Neuroanatomical and cognitive correlates of adult age differences in acquisition of a perceptual-motor skill. *Microscopy research and technique*, **51**, 85-93.

Redgrave, P., Prescott, T.J. & Gurney, K. (1999) The basal ganglia: a vertebrate solution to the selection problem? *Neuroscience*, **89**, 1009-1023.

Reiner, A., Medina, L. & Haber, S.N. (1999) The distribution of dynorphinergic terminals in striatal target regions in comparison to the distribution of substance P-containing and enkephalinergic terminals in monkeys and humans. *Neuroscience*, **88**, 775-793.

Reynolds, J.N. & Wickens, J.R. (2000) Substantia nigra dopamine regulates synaptic plasticity and membrane potential fluctuations in the rat neostriatum, in vivo. *Neuroscience*, **99**, 199-203.

Ricardo, J.A. (1980) Efferent connections of the subthalamic region in the rat. I. The subthalamic nucleus of Luys. *Brain research*, **202**, 257-271.

Rinvik, E. & Ottersen, O.P. (1993) Terminals of subthalamonigral fibres are enriched with glutamate-like immunoreactivity: an electron microscopic, immunogold analysis in the cat. *Journal of chemical neuroanatomy*, **6**, 19-30.

Rivlin-Etzion, M., Marmor, O., Saban, G., Rosin, B., Haber, S.N., Vaadia, E., Prut, Y. & Bergman, H. (2008) Low-pass filter properties of basal ganglia cortical muscle loops in the normal and MPTP primate model of parkinsonism. *The Journal of neuroscience : the official journal of the Society for Neuroscience*, **28**, 633-649.

Robledo, P. & Feger, J. (1990) Excitatory influence of rat subthalamic nucleus to substantia nigra pars reticulata and the pallidal complex:

electrophysiological data. *Brain research*, **518**, 47-54.

Robledo, P. & Feger, J. (1991) Acute monoaminergic depletion in the rat potentiates the excitatory effect of the subthalamic nucleus in the substantia nigra pars reticulata but not in the pallidal complex. *Journal of neural transmission. General section*, **86**, 115-126.

Rodriguez, M. & Gonzalez-Hernandez, T. (1999) Electrophysiological and morphological evidence for a GABAergic nigrostriatal pathway. *The Journal of neuroscience : the official journal of the Society for Neuroscience*, **19**, 4682-4694.

Rolls, E.T., Thorpe, S.J. & Maddison, S.P. (1983) Responses of striatal neurons in the behaving monkey. 1. Head of the caudate nucleus. *Behavioural brain research*, **7**, 179-210.

Romo, R., Scarnati, E. & Schultz, W. (1992) Role of primate basal ganglia and frontal cortex in the internal generation of movements. II. Movement-related activity in the anterior striatum. *Experimental brain research*, **91**, 385-395.

Rouzaire-dubois, B., Hammond, C., Hamon, B. & Feger, J. (1980) Pharmacological blockade of the globus palidus-induced inhibitory response of subthalamic cells in the rat. *Brain research*, **200**, 321-329.

Rymar, V.V., Sasseville, R., Luk, K.C. & Sadikot, A.F. (2004) Neurogenesis and stereological morphometry of calretinin-immunoreactive GABAergic interneurons of the neostriatum. *The Journal of comparative neurology*, **469**, 325-339.

Sadikot, A.F., Parent, A., Smith, Y. & Bolam, J.P. (1992) Efferent connections of the centromedian and parafascicular thalamic nuclei in the squirrel monkey: a light and electron microscopic study of the thalamostriatal projection in relation to striatal heterogeneity. *The Journal of comparative neurology*, **320**, 228-242.

Salinas, E. & Sejnowski, T.J. (2001) Gain modulation in the central nervous system: where behavior, neurophysiology, and computation meet. *The Neuroscientist : a review journal bringing neurobiology, neurology and psychiatry*, **7**, 430-440.

Saper, C.B. & Loewy, A.D. (1982) Projections of the pedunculopontine tegmental nucleus in the rat: evidence for additional extrapyramidal circuitry. *Brain research*, **252**, 367-372.

Schapira, A.H., Bezard, E., Brotchie, J., Calon, F., Collingridge, G.L., Ferger, B., Hengerer, B., Hirsch, E., Jenner, P., Le Novere, N., Obeso, J.A., Schwarzschild, M.A., Spampinato, U. & Davidai, G. (2006) Novel pharmacological targets for the treatment of Parkinson's disease. *Nature reviews. Drug discovery*, **5**, 845-854.

Schultz, W. (1998) Predictive reward signal of dopamine neurons. *Journal of neurophysiology*, **80**, 1-27.

Schultz, W. & Ungerstedt, U. (1978) Short-term increase and long-term reversion of striatal cell activity after

degeneration of the nigrostriatal dopamine system. *Experimental brain research*, **33**, 159-171.

Schulz, J.M., Oswald, M.J. & Reynolds, J.N. (2011) Visual-induced excitation leads to firing pauses in striatal cholinergic interneurons. *The Journal of neuroscience : the official journal of the Society for Neuroscience*, **31**, 11133-11143.

Schwarting, R.K. & Huston, J.P. (1996a) The unilateral 6-hydroxydopamine lesion model in behavioral brain research. Analysis of functional deficits, recovery and treatments. *Progress in neurobiology*, **50**, 275-331.

Schwarting, R.K. & Huston, J.P. (1996b) Unilateral 6-hydroxydopamine lesions of meso-striatal dopamine neurons and their physiological sequelae. *Progress in neurobiology*, **49**, 215-266.

Sharott, A., Doig, N.M., Mallet, N. & Magill, P.J. (2012) Relationships between the firing of identified striatal interneurons and spontaneous and driven cortical activities in vivo. *The Journal of neuroscience : the official journal of the Society for Neuroscience*, **32**, 13221-13236.

Sharott, A., Gulberti, A., Zittel, S., Tudor Jones, A.A., Fickel, U., Munchau, A., Koppen, J.A., Gerloff, C., Westphal, M., Buhmann, C., Hamel, W., Engel, A.K. & Moll, C.K. (2014) Activity parameters of subthalamic nucleus neurons selectively predict motor symptom severity in Parkinson's disease. *The Journal of neuroscience : the official journal of the Society for Neuroscience*, **34**, 6273-6285.

Sharott, A., Magill, P.J., Bolam, J.P. & Brown, P. (2005a) Directional analysis of coherent oscillatory field potentials in the cerebral cortex and basal ganglia of the rat. *The Journal of physiology*, **562**, 951-963.

Sharott, A., Magill, P.J., Harnack, D., Kupsch, A., Meissner, W. & Brown, P. (2005b) Dopamine depletion increases the power and coherence of beta-oscillations in the cerebral cortex and subthalamic nucleus of the awake rat. *The European journal of neuroscience*, **21**, 1413-1422.

Shen, W., Hamilton, S.E., Nathanson, N.M. & Surmeier, D.J. (2005) Cholinergic suppression of KCNQ channel currents enhances excitability of striatal medium spiny neurons. *The Journal of neuroscience : the official journal of the Society for Neuroscience*, **25**, 7449-7458.

Shink, E., Bevan, M.D., Bolam, J.P. & Smith, Y. (1996) The subthalamic nucleus and the external pallidum: two tightly interconnected structures that control the output of the basal ganglia in the monkey. *Neuroscience*, **73**, 335-357.

Shink, E. & Smith, Y. (1995) Differential synaptic innervation of neurons in the internal and external segments of the globus pallidus by the GABA- and glutamate-containing terminals in the squirrel monkey. *The Journal of comparative neurology*, **358**, 119-141.

Silberstein, P., Pogosyan, A., Kuhn, A.A., Hotton, G., Tisch, S., Kupsch, A., Dowsey-Limousin, P., Hariz, M.I. & Brown, P. (2005) Cortico-cortical coupling in Parkinson's disease and

its modulation by therapy. *Brain : a journal of neurology*, **128**, 1277-1291.

Singer, W. (1999a) Neuronal synchrony: a versatile code for the definition of relations? *Neuron*, **24**, 49-65, 111-125.

Singer, W. (1999b) Time as coding space? *Current opinion in neurobiology*, **9**, 189-194.

Sloan, T.B. (1998) Anesthetic effects on electrophysiologic recordings. *Journal of clinical neurophysiology : official publication of the American Electroencephalographic Society*, **15**, 217-226.

Smith, Y., Bevan, M.D., Shink, E. & Bolam, J.P. (1998a) Microcircuitry of the direct and indirect pathways of the basal ganglia. *Neuroscience*, **86**, 353-387.

Smith, Y. & Bolam, J.P. (1989) Neurons of the substantia nigra reticulata receive a dense GABA-containing input from the globus pallidus in the rat. *Brain research*, **493**, 160-167.

Smith, Y. & Bolam, J.P. (1990) The output neurones and the dopaminergic neurones of the substantia nigra receive a GABA-containing input from the globus pallidus in the rat. *The Journal of comparative neurology*, **296**, 47-64.

Smith, Y. & Kieval, J.Z. (2000) Anatomy of the dopamine system in the basal ganglia. *Trends in neurosciences*, **23**, S28-33.

Smith, Y. & Parent, A. (1988) Neurons of the subthalamic nucleus in primates display glutamate but not GABA immunoreactivity. *Brain research*, **453**, 353-356.

Smith, Y., Shink, E. & Sidibe, M. (1998b) Neuronal circuitry and synaptic connectivity of the basal ganglia. *Neurosurgery clinics of North America*, **9**, 203-222.

Soltis, R.P., Anderson, L.A., Walters, J.R. & Kelland, M.D. (1994) A role for non-NMDA excitatory amino acid receptors in regulating the basal activity of rat globus pallidus neurons and their activation by the subthalamic nucleus. *Brain research*, **666**, 21-30.

Somogyi, P., Bolam, J.P. & Smith, A.D. (1981) Monosynaptic cortical input and local axon collaterals of identified striatonigral neurons. A light and electron microscopic study using the Golgi-peroxidase transport-degeneration procedure. *The Journal of comparative neurology*, **195**, 567-584.

Sporns, O., Tononi, G. & Edelman, G.M. (2002) Theoretical neuroanatomy and the connectivity of the cerebral cortex. *Behavioural brain research*, **135**, 69-74.

Steriade, M. (2000) Corticothalamic resonance, states of vigilance and mentation. *Neuroscience*, **101**, 243-276.

Stern, E.A., Jaeger, D. & Wilson, C.J. (1998) Membrane potential synchrony of simultaneously recorded striatal spiny neurons in vivo. *Nature*, **394**, 475-478.

Stern, E.A., Kincaid, A.E. & Wilson, C.J. (1997) Spontaneous subthreshold membrane potential fluctuations and action potential variability of rat corticostriatal and striatal neurons in vivo. *Journal of neurophysiology*, **77**, 1697-1715.

Stoffers, D., Bosboom, J.L., Deijen, J.B., Wolters, E., Stam, C.J. & Berendse, H.W. (2008a) Increased cortico-cortical functional connectivity in early-stage Parkinson's disease: an MEG study. *NeuroImage*, **41**, 212-222.

Stoffers, D., Bosboom, J.L., Wolters, E., Stam, C.J. & Berendse, H.W. (2008b) Dopaminergic modulation of cortico-cortical functional connectivity in Parkinson's disease: an MEG study. *Experimental neurology*, **213**, 191-195.

Surmeier, D.J., Ding, J., Day, M., Wang, Z. & Shen, W. (2007) D1 and D2 dopamine-receptor modulation of striatal glutamatergic signaling in striatal medium spiny neurons. *Trends in neurosciences*, **30**, 228-235.

Surmeier, D.J., Song, W.J. & Yan, Z. (1996) Coordinated expression of dopamine receptors in neostriatal medium spiny neurons. *The Journal of neuroscience : the official journal of the Society for Neuroscience*, **16**, 6579-6591.

Temel, Y., Blokland, A., Steinbusch, H.W. & Visser-Vandewalle, V. (2005) The functional role of the subthalamic nucleus in cognitive and limbic circuits. *Progress in neurobiology*, **76**, 393-413.

Tepper, J.M. & Bolam, J.P. (2004) Functional diversity and specificity of neostriatal interneurons. *Current opinion in neurobiology*, **14**, 685-692.

Tepper, J.M., Tecuapetla, F., Koos, T. & Ibanez-Sandoval, O. (2010) Heterogeneity and diversity of striatal GABAergic interneurons. *Frontiers in neuroanatomy*, **4**, 150.

Threlfell, S., Lalic, T., Platt, N.J., Jennings, K.A., Deisseroth, K. & Cragg, S.J. (2012) Striatal dopamine release is triggered by synchronized activity in cholinergic interneurons. *Neuron*, **75**, 58-64.

Timmermann, L., Gross, J., Butz, M., Kircheis, G., Haussinger, D. & Schnitzler, A. (2004) Pathological oscillatory coupling within the human motor system in different tremor syndromes as revealed by magnetoencephalography. *Neurology & clinical neurophysiology : NCN*, **2004**, 26.

Tokuno, H., Chiken, S., Kametani, K. & Moriizumi, T. (2002) Efferent projections from the striatal patch compartment: anterograde degeneration after selective ablation of neurons expressing mu-opioid receptor in rats. *Neuroscience letters*, **332**, 5-8.

Tokuno, H., Moriizumi, T., Kudo, M. & Nakamura, Y. (1988) A morphological evidence for monosynaptic projections from the nucleus tegmenti pedunculopontinus pars compacta (TPC) to nigrostriatal projection

neurons. *Neuroscience letters*, **85**, 1-4.

Totterdell, S., Bolam, J.P. & Smith, A.D. (1984) Characterization of pallidonigral neurons in the rat by a combination of Golgi impregnation and retrograde transport of horseradish peroxidase: their monosynaptic input from the neostriatum. *Journal of neurocytology*, **13**, 593-616.

Treisman, A. (1996) The binding problem. *Current opinion in neurobiology*, **6**, 171-178.

Tseng, K.Y., Kasanetz, F., Kargieman, L., Riquelme, L.A. & Murer, M.G. (2001) Cortical slow oscillatory activity is reflected in the membrane potential and spike trains of striatal neurons in rats with chronic nigrostriatal lesions. *The Journal of neuroscience : the official journal of the Society for Neuroscience*, **21**, 6430-6439.

Tsubokawa, T. & Sutin, J. (1972) Pallidal and tegmental inhibition of oscillatory slow waves and unit activity in the subthalamic nucleus. *Brain research*, **41**, 101-118.

Turner, R.S. & Anderson, M.E. (1997) Pallidal discharge related to the kinematics of reaching movements in two dimensions. *Journal of neurophysiology*, **77**, 1051-1074.

Turner, R.S. & Anderson, M.E. (2005) Context-dependent modulation of movement-related discharge in the primate globus pallidus. *The Journal of neuroscience : the official journal of the Society for Neuroscience*, **25**, 2965-2976.

Turner, R.S. & Desmurget, M. (2010) Basal ganglia contributions to motor control: a vigorous tutor. *Current opinion in neurobiology*, **20**, 704-716.

Uhlhaas, P.J. & Singer, W. (2006) Neural synchrony in brain disorders: relevance for cognitive dysfunctions and pathophysiology. *Neuron*, **52**, 155-168.

Unal, B., Shah, F., Kothari, J. & Tepper, J.M. (2013) Anatomical and electrophysiological changes in striatal TH interneurons after loss of the nigrostriatal dopaminergic pathway. *Brain structure & function*.

Ungerstedt, U. (1968) 6-Hydroxy-dopamine induced degeneration of central monoamine neurons. *European journal of pharmacology*, **5**, 107-110.

Ungerstedt, U. (1971) Striatal dopamine release after amphetamine or nerve degeneration revealed by rotational behaviour. *Acta physiologica Scandinavica. Supplementum*, **367**, 49-68.

Urbain, N., Gervasoni, D., Souliere, F., Lobo, L., Rentero, N., Windels, F., Astier, B., Savasta, M., Fort, P., Renaud, B., Luppi, P.H. & Chouvet, G. (2000) Unrelated course of subthalamic nucleus and globus pallidus neuronal activities across vigilance states in the rat. *The European journal of neuroscience*, **12**, 3361-3374.

Urbain, N., Rentero, N., Gervasoni, D., Renaud, B. & Chouvet, G. (2002) The switch of subthalamic neurons from an irregular to a bursting pattern does not solely depend on their

GABAergic inputs in the anesthetic-free rat. *The Journal of neuroscience : the official journal of the Society for Neuroscience*, **22**, 8665-8675.

van der Kooy, D. & Carter, D.A. (1981) The organization of the efferent projections and striatal afferents of the entopeduncular nucleus and adjacent areas in the rat. *Brain research*, **211**, 15-36.

Venance, L. & Glowinski, J. (2003) Heterogeneity of spike frequency adaptation among medium spiny neurones from the rat striatum. *Neuroscience*, **122**, 77-92.

Vila, M., Perier, C., Feger, J., Yelnik, J., Faucheux, B., Ruberg, M., Raisman-Vozari, R., Agid, Y. & Hirsch, E.C. (2000) Evolution of changes in neuronal activity in the subthalamic nucleus of rats with unilateral lesion of the substantia nigra assessed by metabolic and electrophysiological measurements. *The European journal of neuroscience*, **12**, 337-344.

Vincent, S.R., Staines, W.A. & Fibiger, H.C. (1983) Histochemical demonstration of separate populations of somatostatin and cholinergic neurons in the rat striatum. *Neuroscience letters*, **35**, 111-114.

von Krosigk, M., Smith, Y., Bolam, J.P. & Smith, A.D. (1992) Synaptic organization of GABAergic inputs from the striatum and the globus pallidus onto neurons in the substantia nigra and retrorubral field which project to the medullary reticular formation. *Neuroscience*, **50**, 531-549.

Vuillet, J., Dimova, R., Nieoullon, A. & Kerkerian-Le Goff, L. (1992) Ultrastructural relationships between choline acetyltransferase- and neuropeptide γ-containing neurons in the rat striatum. *Neuroscience*, **46**, 351-360.

Weinberger, M., Mahant, N., Hutchison, W.D., Lozano, A.M., Moro, E., Hodaie, M., Lang, A.E. & Dostrovsky, J.O. (2006) Beta oscillatory activity in the subthalamic nucleus and its relation to dopaminergic response in Parkinson's disease. *Journal of neurophysiology*, **96**, 3248-3256.

West, A.R. & Grace, A.A. (2002) Opposite influences of endogenous dopamine D1 and D2 receptor activation on activity states and electrophysiological properties of striatal neurons: studies combining in vivo intracellular recordings and reverse microdialysis. *The Journal of neuroscience : the official journal of the Society for Neuroscience*, **22**, 294-304.

Wichmann, T., Bergman, H. & DeLong, M.R. (1994a) The primate subthalamic nucleus. I. Functional properties in intact animals. *Journal of neurophysiology*, **72**, 494-506.

Wichmann, T., Bergman, H. & DeLong, M.R. (1994b) The primate subthalamic nucleus. III. Changes in motor behavior and neuronal activity in the internal pallidum induced by subthalamic inactivation in the MPTP model of parkinsonism. *Journal of neurophysiology*, **72**, 521-530.

Wichmann, T., Bergman, H., Starr, P.A., Subramanian, T., Watts, R.L. &

DeLong, M.R. (1999) Comparison of MPTP-induced changes in spontaneous neuronal discharge in the internal pallidal segment and in the substantia nigra pars reticulata in primates. *Experimental brain research*, **125**, 397-409.

Wichmann, T. & DeLong, M.R. (1996) Functional and pathophysiological models of the basal ganglia. *Current opinion in neurobiology*, **6**, 751-758.

Wictorin, K., Clarke, D.J., Bolam, J.P. & Bjorklund, A. (1989) Host Corticostriatal Fibres Establish Synaptic Connections with Grafted Striatal Neurons in the Ibotenic Acid Lesioned Striatum. *The European journal of neuroscience*, **1**, 189-195.

Wigmore, M.A. & Lacey, M.G. (2000) A Kv3-like persistent, outwardly rectifying, Cs+-permeable, K+ current in rat subthalamic nucleus neurones. *The Journal of physiology*, **527 Pt 3**, 493-506.

Williams, D., Tijssen, M., Van Bruggen, G., Bosch, A., Insola, A., Di Lazzaro, V., Mazzone, P., Oliviero, A., Quartarone, A., Speelman, H. & Brown, P. (2002) Dopamine-dependent changes in the functional connectivity between basal ganglia and cerebral cortex in humans. *Brain : a journal of neurology*, **125**, 1558-1569.

Williams, S.M. & Goldman-Rakic, P.S. (1998) Widespread origin of the primate mesofrontal dopamine system. *Cerebral cortex*, **8**, 321-345.

Wilson, C.J. (2005) The mechanism of intrinsic amplification of hyperpolarizations and spontaneous bursting in striatal cholinergic interneurons. *Neuron*, **45**, 575-585.

Wilson, C.J. & Kawaguchi, Y. (1996) The origins of two-state spontaneous membrane potential fluctuations of neostriatal spiny neurons. *The Journal of neuroscience : the official journal of the Society for Neuroscience*, **16**, 2397-2410.

Wilson, C.J. & Phelan, K.D. (1982) Dual topographic representation of neostriatum in the globus pallidus of rats. *Brain research*, **243**, 354-359.

Wilson, C.J., Young, S.J. & Groves, P.M. (1977) Statistical properties of neuronal spike trains in the substantia nigra: cell types and their interactions. *Brain research*, **136**, 243-260.

Woolf, N.J. & Butcher, L.L. (1986) Cholinergic systems in the rat brain: III. Projections from the pontomesencephalic tegmentum to the thalamus, tectum, basal ganglia, and basal forebrain. *Brain research bulletin*, **16**, 603-637.

Wu, Y., Richard, S. & Parent, A. (2000) The organization of the striatal output system: a single-cell juxtacellular labeling study in the rat. *Neuroscience research*, **38**, 49-62.

Xu, Z.C., Wilson, C.J. & Emson, P.C. (1989) Restoration of the corticostriatal projection in rat neostriatal grafts: electron microscopic analysis. *Neuroscience*, **29**, 539-550.

Xu, Z.C., Wilson, C.J. & Emson, P.C. (1991) Restoration of thalamostriatal projections in rat neostriatal grafts:

an electron microscopic analysis. *The Journal of comparative neurology*, **303**, 22-34.

Yan, Z., Flores-Hernandez, J. & Surmeier, D.J. (2001) Coordinated expression of muscarinic receptor messenger RNAs in striatal medium spiny neurons. *Neuroscience*, **103**, 1017-1024.

Yan, Z. & Surmeier, D.J. (1997) D5 dopamine receptors enhance Zn2+-sensitive GABA(A) currents in striatal cholinergic interneurons through a PKA/PP1 cascade. *Neuron*, **19**, 1115-1126.

Yelnik, J. & Percheron, G. (1979) Subthalamic neurons in primates: a quantitative and comparative analysis. *Neuroscience*, **4**, 1717-1743.

Yoshida, S., Nambu, A. & Jinnai, K. (1993) The distribution of the globus pallidus neurons with input from various cortical areas in the monkeys. *Brain research*, **611**, 170-174.

Zaborszky, L., Alheid, G.F., Beinfeld, M.C., Eiden, L.E., Heimer, L. & Palkovits, M. (1985) Cholecystokinin innervation of the ventral striatum: a morphological and radioimmunological study. *Neuroscience*, **14**, 427-453.

Zhou, F.M., Liang, Y. & Dani, J.A. (2001) Endogenous nicotinic cholinergic activity regulates dopamine release in the striatum. *Nature neuroscience*, **4**, 1224-1229.

Zold, C.L., Kasanetz, F., Pomata, P.E., Belluscio, M.A., Escande, M.V., Galinanes, G.L., Riquelme, L.A. & Murer, M.G. (2012) Striatal gating through up states and oscillations in the basal ganglia: Implications for Parkinson's disease. *Journal of physiology, Paris*, **106**, 40-46.